GL04006

REPORT DOCUMENTATION PAGE

1a. REPORT SECURITY CLASSIFICATION	1b. RESTRICTIVE MARKINGS
UNCLASSIFIED	

2a. SECURITY CLASSIFICATION AUTHORITY	3. DISTRIBUTION / AVAILABILITY OF REPORT
UNCLASSIFIED	Approved for public release; distribution
2b. DECLASSIFICATION / DOWNGRADING SCHEDULE	is unlimited

4. PERFORMING ORGANIZATION REPORT NUMBER(S)	5. MONITORING ORGANIZATION REPORT NUMBER(S)
	USAFSAM-TR-87

6a. NAME OF PERFORMING ORGANIZATION	6b. OFFICE SYMBOL (If applicable)	7a. NAME OF MONITORING ORGANIZATION
University of Utah Research Institute		USAF School of Aerospace Medicine (RZP)

6c. ADDRESS (City, State, and ZIP Code)	7b. ADDRESS (City, State, and ZIP Code)
391 Chipeta Way, Suite C Salt Lake City, UT 84108-1295	Aerospace Medical Division (AFSC) Brooks Air Force Base, TX 78235-5301

8a. NAME OF FUNDING/SPONSORING ORGANIZATION	8b. OFFICE SYMBOL (If applicable)	9. PROCUREMENT INSTRUMENT IDENTIFICATION NUMBER

8c. ADDRESS (City, State, and ZIP Code)	10. SOURCE OF FUNDING NUMBERS			
	PROGRAM ELEMENT NO.	PROJECT NO.	TASK NO.	WORK UNIT ACCESSION NO.

11. TITLE (Include Security Classification)

BASIS FOR RFR-SAFETY STANDARDS IN THE 10 KHz - 50 MHz Region

12. PERSONAL AUTHOR(S)
O.P. Gandhi

13a. TYPE OF REPORT	13b. TIME COVERED	14. DATE OF REPORT (Year, Month, Day)	15. PAGE COUNT
Final Report	FROM 8-1-85 TO 6-30-87	July 15, 1987	

16. SUPPLEMENTARY NOTATION

17.	COSATI CODES		18. SUBJECT TERMS (Continue on reverse if necessary and identify by block number)
FIELD	GROUP	SUB-GROUP	Induced RF Currents, Contact Hazards, High Current densities, High SARs for Body Extremities Occupational, general population, RF Safety guidelines

19. ABSTRACT (Continue on reverse if necessary and identify by block number)

The report gives the data on radiofrequency (RF) currents induced in a human being for plane-wave exposure conditions 0-50 MHz. Also studied is the effect of shoes and floors on the induced RF currents. Since high RF currents may occur for the body extremities such as ankle and wrist regions, surface temperature elevations were measured for these regions for a healthy human subject for a variety of RF currents for the frequency band 1-50 MHz.

To obtain rates of energy deposition (specific absorption rates or SARs) due to RF magnetic fields, we have developed a 36,776 - cell, anatomically-based, inhomogeneous model of man and have used the previously formulated impedance method. Even though, detailed calculations have been made only for an irradiation frequency of 30 MHz, electromagnetic scaling concepts have been used to estimate whole-body-averaged and peak SARs due to RF magnetic fields at other frequencies as well as in the band 0.1-100 MHz. (See back)

20. DISTRIBUTION/AVAILABILITY OF ABSTRACT	21. ABSTRACT SECURITY CLASSIFICATION
☒ UNCLASSIFIED/UNLIMITED ☐ SAME AS RPT. ☐ DTIC USERS	UNCLASSIFIED

22a. NAME OF RESPONSIBLE INDIVIDUAL	22b. TELEPHONE (Include Area Code)	22c. OFFICE SYMBOL
William D. Hurt	(512)536-3582	USAFSAM/RZP

DD FORM 1473, 84 MAR — 83 APR edition may be used until exhausted. — SECURITY CLASSIFICATION OF THIS PAGE
All other editions are obsolete.

TABLE OF CONTENTS

FIGURE CAPTIONS

Figure 1.   RF foot currents for a grounded subject exposed to a vertically-polarized plane wave.

Figure 2.   Current reduction factor (R_1) as a function of frequency, for band 0.7-50 MHz. R_1 is the ratio of the foot currents with and without shoes.

Figure 3.   Experimental arrangement for the measurement of human body impedance.

Figure 4.   Ratio of foot to hand currents (I_F/I_H).

Figure 5.   Current reduction factor (R_2) plotted against frequency for various styrofoam thicknesses. R_2 is the ratio of foot current with styrofoam separating subject from ground to current when subject is barefoot on ground.

Figure 6.   Current reduction factor (R_3) plotted as a function of styrofoam floor thickness at f = 27.12 MHz. The subject wore rubber-soled shoes. R_3 is the ratio of foot current with styrofoam separating subject from ground to current when subject is directly on ground.

Figure 7.   Foot current reduction factor with the metallic bypass straps to reduce high SARs in the ankle region. d is the width of the metallic strap.

Figure 8.   Current for perception without gloves and with conducting gloves. The sections where the perceptions occur are also indicated.

Figure 9.   Foot current induced in an adult male (h = 1.75 m) subjected to fields recommended in the ANSI-1982 RF safety guide.

Figure 10.   Ankle-section high-water-content tissue SAR for adult male (h = 1.75 m) for electric fields recommended in the ANSI-1982 RF safety guide.

Figure 11.   Average body impedance of adult males (N = 197), adult females (N = 170), and ten-year-old children (dashed line) for grasping contact with a brass rod of diameter 1.5 cm and length 14 cm.

Figure 12.   Average body impedance of adult males (N = 197), adult females (N = 170), and ten-year-old children (dashed line) for finger contact (plate of area 144 mm^2).

Figure 13.   Average threshold current for perception, finger contact for adult males (N = 197), adult females (N = 170), and ten-year-old children. Contact area = 25 mm^2.

TABLE CAPTIONS

Table 1.   Average measured impedance Z of adult males (N=2) for grasping contact.

Table 2.   Open circuit electrode reactance X_c, and computed value of body impedance Z_b as a function of frequency.

Table 3.   Average value of threshold currents for two subjects.

Table 4.   Induced currents and ankle-section wet-tissue SARs for the ANSI C95.1-1982 recommended E-field of 61.4 V/m [1].

Table 5.   Capacitance-to-ground, effective area, and effective height of various vehicles in quasi-static (low frequency) status.

Table 6.   Tissue dielectric properties at 30 MHz.

Table 7.   Whole-body-averaged and peak SARs scaled from the values calculated at 30 MHz for an anatomically-realistic model of a human being. A magnetic field of 1 A/m oriented from front to back of the body is assumed to obtain highest possible SARs.

Table 8.   Occupational exposure radio-frequency protection guides.

Table 9.   Whole-body-averaged and peak SARs for an anatomically-realistic model of a human being for RF magnetic fields given by Eq. 20. A magnetic field orientation from front to back of the body is assumed to obtain highest possible SARs.

Table 10.   Radio-frequency protection guides for general population.

Table 11.   Induced currents and ankle-section SARs for an incident E-field of 8 V/m (scaled from Table 4).

BASIS FOR RFR-SAFETY STANDARDS

IN THE 10 kHz - 50 MHz REGION

I. INTRODUCTION

The radio-frequency radiation (RFR) standards presently suggested by the American National Standards Institute (ANSI) [1], the American Conference of Governmental Industrial Hygienists (ACGIH) [2], and more recently by standards-setting groups elsewhere (Canada, IRPA, Australia, etc.) [3], have relied on the knowledge of whole-body-average specific absorption rate (SAR). This knowledge has led to recommendations that the allowed power density can be increased in proportion to the square of the frequency from 1 mW/cm^2 (E = 61.4 V/m) for frequencies below 30 MHz. Recognizing that if the exposure limits were allowed to increase without limit at lower frequencies, potential hazards could exist for shock and burn, an upper bound of 100 mW/cm^2 (E = 614 V/m) has been recommended for the region 10 kHz - 3 MHz. Even though the present project did not call for studies above 3 MHz, because of the similarity of engineering analysis, we have examined the entire region 10 kHz - 50 MHz.

This report gives the data on RF currents induced in a human being for plane-wave exposure conditions 0-50 MHz [4]. Using electromagnetic scaling concepts, projections have been made for individuals of different heights, as well as for 10- and 5-year-old children. Also studied is the effect of shoes on the induced RF currents. We had previously conducted a study where the body impedance and threshold currents needed to produce sensations of perception and pain had been measured for 367 human subjects for the frequency range 10 kHz to 3 MHz [5]. As a part of the present project, we have obtained data on body impedance and threshold currents for perception at higher frequencies to 50 MHz. We have also studied the role of false floors in the workplace to reduce RF currents induced in a human operator as well as some safety equipment to mitigate RF hazards. Toward the latter objective we have

characterized the use of current-bypass metallic straps to reduce the high SARs in the ankle region and metal-coated insulating gloves to reduce contact hazards.

A great deal of effort was expended to study the thermal implications of high SARs in the body extremities (wrist and ankle sections) at the ANSI recommended VLF-VHF safety levels. The data generated as a result of these studies have been written up as a paper (attached here as Appendix A) that has been submitted for possible publication to IEEE Transactions on Biomedical Engineering. Surface temperature elevations of the wrist and ankle sections were measured for a healthy human subject at room temperature (22-25° C) for a variety of RF currents and SARs for the frequency band 1-50 MHz.

To obtain the SARs due to RF magnetic fields, we have developed a three-dimensional, 36,776-cell inhomogeneous model of man. This model is based on the anatomic cross sections of the human body [6] where one of 14 tissue types are used to describe a grid of dimensions 0.635 x 0.635 cms. The data are then combined to obtain percentages of the various tissues in cubical cells of dimensions 1.31 cm for each of the sides. Using the previously described impedance method [7], SARs are calculated for the model exposed to a uniform RF magnetic field at 30 MHz polarized from front to back of the body, which is the highest coupling orientation for the magnetic field component of electro-magnetic waves. Electromagnetic scaling concepts are used to estimate whole-body-averaged and peak SARs due to RF magnetic fields at other frequencies in the band 0.1-100 MHz.

The available data are used to recommend occupational as well as general population safety guidelines for RFR. An important feature of the recommended guideline for frequencies higher than or equal to 100 kHz is a limit of 100 mA on the RF current induced in the human body for no contact with metallic objects in RF fields. At lower frequencies, the limiting currents are reduced in proportion to the frequency. Radio-frequency current meters are presently being developed in our laboratory that should allow these measurements in the frequency band 10 kHz - 50 MHz. In the absence of knowledge of coupling of spatially-inhomogeneous RF fields to the human body, averaging of the E- and H-fields over the volume of the human body is recommended to use the proposed guidelines. Some initial work in estimating the SARs for spatially-variable

VHF fields has previously been done in our laboratory [4,8]. Further work is, however, needed to define the absorption for spatially-variable RF fields.

II. RF CURRENTS INDUCED IN A HUMAN BEING
FOR PLANE-WAVE EXPOSURE CONDITIONS

We have previously shown [9] that vertically-polarized incident plane waves are capable of inducing fairly significant RF currents in a free-standing, grounded human being. The foot current I_h flowing under this situation has been measured for a number of human subjects and found to satisfy the following empirical relationship

$$\frac{I_h}{E} = 0.108 \ h_m^2 \ f_{MHz} \qquad \frac{mA}{(V/m)} \qquad (1)$$

where E is the plane-wave incident electric field (assumed vertical) in V/m, h_m is the height of the individual in meters and f_{MHz} is the frequency in MHz. Equation 1 is very similar though about 20 percent higher than the expression empirically obtained by Deno [10] for 50/60 Hz currents induced in a human. Fairly similar results have also been reported by a number of authors, most notably Hill and Walsh [11, to 10 MHz], Tell et al. [12, to 1.47 MHz], Guy and Chou [13, 0.146 MHz], and by Gronhaug and Busmundrud [14, to 27.0 MHz]. In our previous work [9], we had found Eq. 1 to be valid to 27.4 MHz. To obtain the upper frequency limit for Eq. 1, we conducted a set of experiments to determine the foot currents flowing through a free-standing, grounded human being in the frequency range of 27 to 50 MHz.

The RF radiator consisted of a quarter-wave monopole antenna excited by means of a Kenwood model TS 4305 transceiver (for f = 27 MHz) or MCL power generator model 15122 (for f in range 30 to 50 MHz). The electric field intensity E at the position of the subject was measured via a Holaday H3003 probe (for f = 27 MHz) or an Instruments for Industry, Inc. model EFS-1 field meter. The currents were measured by having the subject stand barefoot or with rubber-soled shoes on a 6 mm thick 21 x 32 cm polyethylene sheet clad on both sides with copper. The current from the upper copper sheet passed to the

lower plate through a relatively noninductive carbon resistor (nominal value = 5 Ω) placed at the center of the sensor across which the RF voltage V was measured using a Fluke model 8060A digital multimeter. The impedance Z of this resistor was measured at each of the experimental frequencies using Hewlett Packard (HP) model 4815A vector impedance meter (frequency range of this instrument is 0.5 to 108 MHz). The current I_h was then obtained as $|V|/|Z|$. For all of the experiments the subjects were at a distance of 5 meters or more from the radiator. This was to satisfy the distance needed for far-field irradiation: $d \geqslant 2 D^2/\lambda = \lambda/2$ for quarter-wave monopole antennas. In order to ground the lower plate of the current sensor, it was placed on a sheet of aluminum screening (approximately 2.5 m x 2.5 m). This screening was not earthed, recognizing that there would be sufficient capacitance and hence a fairly small reactance between it and the ground under the asphalt. At least three subjects were used and the individual measurements scaled to the average adult male height of 1.75 m through the scaling relationship from Eq. 1 that $I_h \approx h^2$. Figure 1 shows the average values of I_h/E as a function of frequency. For frequencies in excess of 27 MHz, the experimentally observed currents are found to be in good agreement with the following empirical expression:

$$\frac{I_h}{E} = 11.0 \ \frac{f_{MHz}}{f_r} \ \sin\left(\frac{\pi}{2} \ \frac{f_{MHz}}{f_r}\right) \ \frac{mA}{(V/m)} \tag{2}$$

which is also plotted for comparison in Figure 1. The expression in Eq. 2 uses a factor similar to the current reduction factor $\sin\left(\frac{\pi}{2} \cdot f_{MHz}/f_r\right)$ at the base of a rod monopole antenna of a length somewhat in excess of a quarter wavelength. Noting that a resonance frequency of about 32-35 MHz was previously observed for a 1.75 m-tall human being under grounded conditions [15], an f_r = 32 MHz has been used to calculate the numbers from Eq. 2 that are plotted for comparison in Figure 1. A multiplier term of 11.0 is used in Eq. 2 to obtain an agreement with Eq. 1 at 27.4 MHz. It should be recalled that Eq. 1 was previously tested at lower frequencies 0.63-27.4 MHz. In formulating Eq. 2 we have made use of an experimental observation [4] that the distribution of induced current in a standing human being is fairly similar to

- 4 -

● Experimental data

○ From Eq. 2, $\dfrac{I_h}{E} = 11.0\left(\dfrac{f_{MHz}}{32}\right)\sin\left[\dfrac{\pi}{2}\left(\dfrac{f_{MHz}}{32}\right)\right]$

$\dfrac{I_h}{E}$

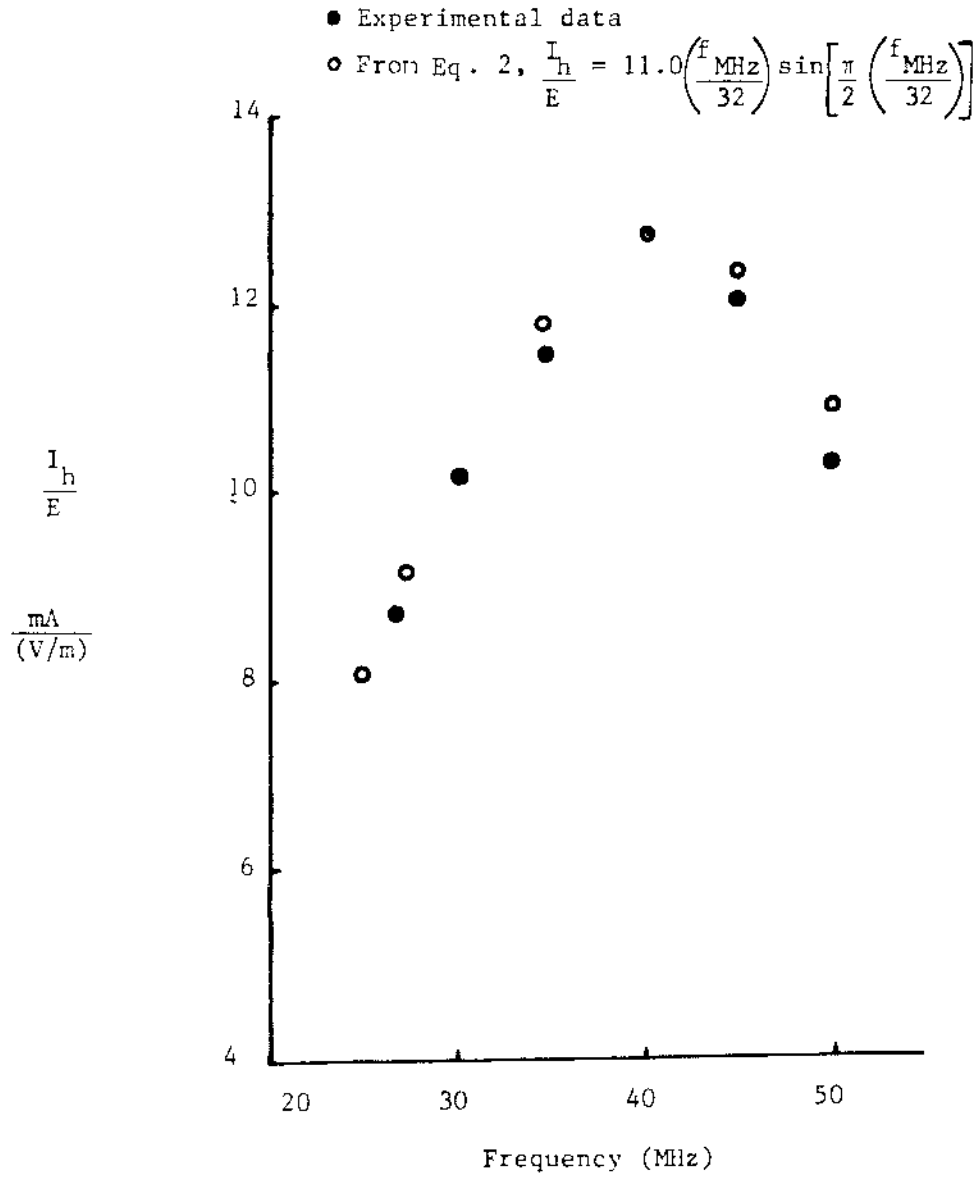$\dfrac{mA}{(V/m)}$

Frequency (MHz)

Figure 1. RF foot currents for a grounded subject exposed to a vertically-polarized plane wave.

the current distribution on a metallic monopole antenna — the current variation may be approximated by a fraction of a sine wave with the maximum value at the base or feet, provided the frequency is less than or equal to f_r. For f larger than f_r, as anticipated from the current variation on a monopole antenna, the current would no longer be maximum at its base, but rather at a point increasing higher up on the monopole. The factor f_{MHz}/f_r is included in Eq. 2 in recognition of the fact (also seen in Eq. 1) that the magnitude of the induced RF current increases with increasing frequency.

III. EFFECT OF SHOES ON THE INDUCED RF CURRENTS

We had determined earlier [9] that the currents measured for subjects wearing rubber-soled shoes were lower than those for barefoot conditions. As a part of this project we have extended the measurements to higher frequencies. The measured reduction in current as a function of frequency is plotted in Figure 2. Whereas a current reduction factor on the order of 0.62-0.64 was observed for lower frequencies of about 1 MHz, the current may be as high as 0.8-0.82 times the barefoot current at higher frequencies. Consequently, rubber-soled shoes were found to be incapable of reducing the RF-induced currents except by fairly small amounts. The electrical "safety shoes" (Size 11, Vibram Manufacturing Company; rubber sole thickness = 1.75 cm) were previously observed [4] to be even worse in this regard and gave currents that were somewhat higher than those with street-type rubber-soled shoes. This may be due to a somewhat larger sole area leading to a higher capacitance and hence lower reactance to ground at RF frequencies.

IV. CONTACT HAZARDS IN THE VLF TO VHF BAND

We have previously evaluated the threshold incident electric fields for the frequency band 10 kHz - 3 MHz for perception and pain for conditions of contact with commonly encountered metallic objects such as car, van, school bus, etc. [5]. To extend the data to 50 MHz we have carried out additional experiments for the body impedance and threshold currents for perception.

The averages of the data obtained for two volunteers are given in Tables 1 and 2. For impedance measurements, the arrangement of Figure 3 was used
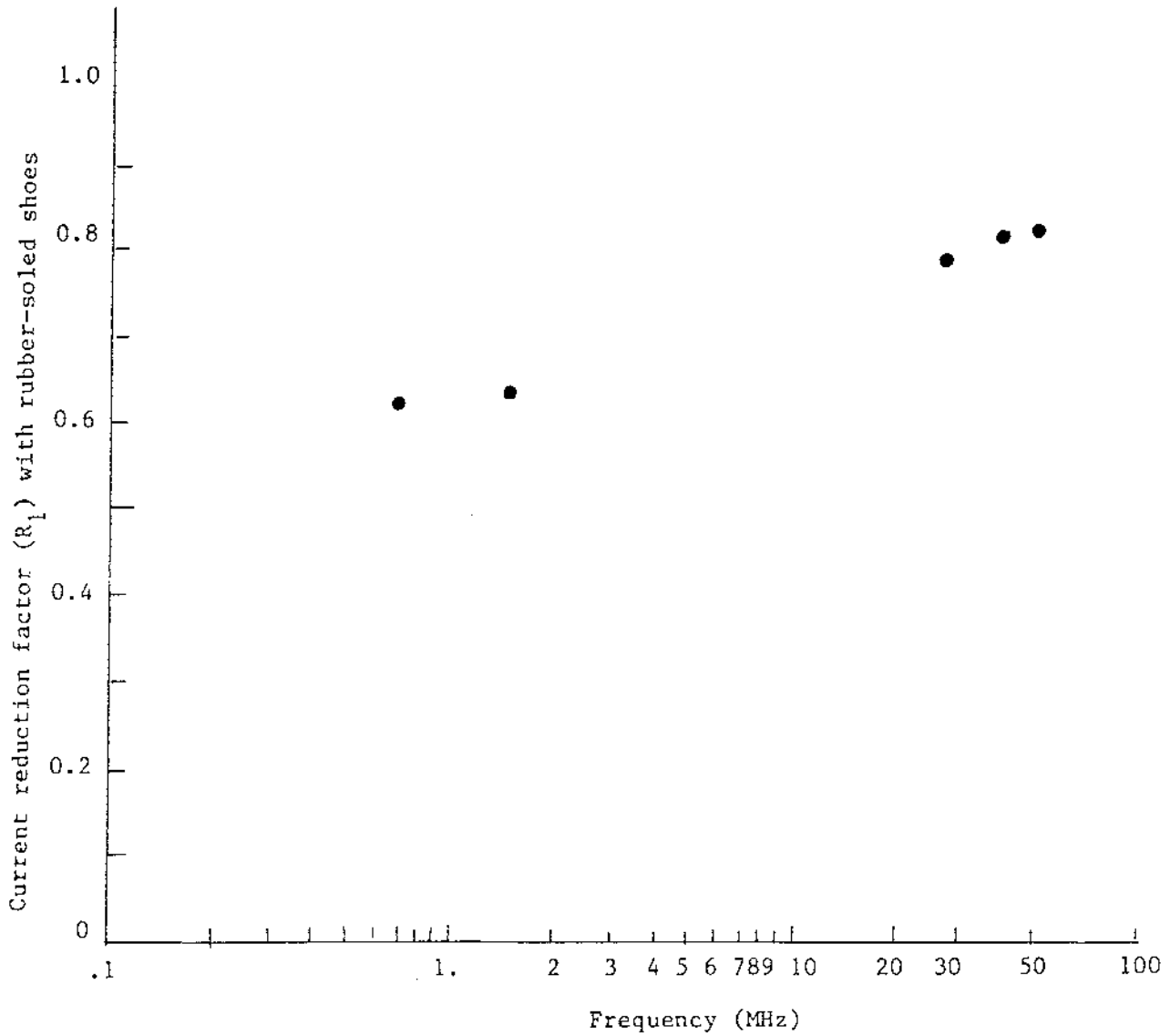
Figure 2. Current reduction factor (R_1) as a function of
frequency, for band 0.7-50 MHz. R_1 is the ratio
of the foot currents with and without shoes.

TABLE 1. AVERAGE MEASURED IMPEDANCE Z OF ADULT MALES (N=2) FOR GRASPING CONTACT

F_{MHz}	Z magnitude and phase Ohms (subjects barefoot)	Z magnitude and phase Ohms subjects with rubber-soled shoes
1	416.0 $\angle$ -9.7°	1006.0 $\angle$ -72°
3	385.0 $\angle$ -15.2°	460.0 $\angle$ -55.4°
9.5	316.4 $\angle$ -30.2°	280.0 $\angle$ -42.8°
16	216.4 $\angle$ -39.8°	231.6 $\angle$ -43°
22.5	213.6 $\angle$ -46.2°	194.0 $\angle$ -46°
27	192.0 $\angle$ -48.8°	179.0 $\angle$ -48°
40.68	137.4 $\angle$ -50.4°	135.8 $\angle$ -49.2°
46	132.4 $\angle$ -50.5°	133.0 $\angle$ -49.4°
50	126.0 $\angle$ -51.3°	124.8 $\angle$ -49.9°

TABLE 2. OPEN CIRCUIT ELECTRODE REACTANCE X_c, AND COMPUTED VALUE OF BODY IMPEDANCE Z_b AS A FUNCTION OF FREQUENCY

| F_{MHz}	Open Circuit Electrode Reactance X_c Ohms	Computed Body Impedance Z_b (subject barefoot) Ohms	Computed Body Impedance Z_b (with shoes) Ohms
1	13.5 K $\angle$ -90°	418.0 $\angle$ -8.0°	1082.4 $\angle$ -70.6°
3	4.5 K $\angle$ -90°	392.4 $\angle$ -10.4°	501.3 $\angle$ -51.8°
9.5	1.4 K $\angle$ -90°	348.6 $\angle$ -17.8°	413.0 $\angle$ -33.2°
16	850 $\angle$ -90°	251.8 $\angle$ -26.7°	276.3 $\angle$ -29.3°
22.5	600 $\angle$ -90°	272.9 $\angle$ -27.9°	242.7 $\angle$ -29.7°
27	495 $\angle$ -90°	256.6 $\angle$ -28.3°	232.4 $\angle$ -29.7°
40.68	330 $\angle$ -89°	186.8 $\angle$ -28.8°	183.7 $\angle$ -27.9°
46	290 $\angle$ -90°	186.5 $\angle$ -26.4°	185.5 $\angle$ -24.8°
50	267 $\angle$ -90°	180.7 $\angle$ -26.3°	175.9 $\angle$ -24.8°
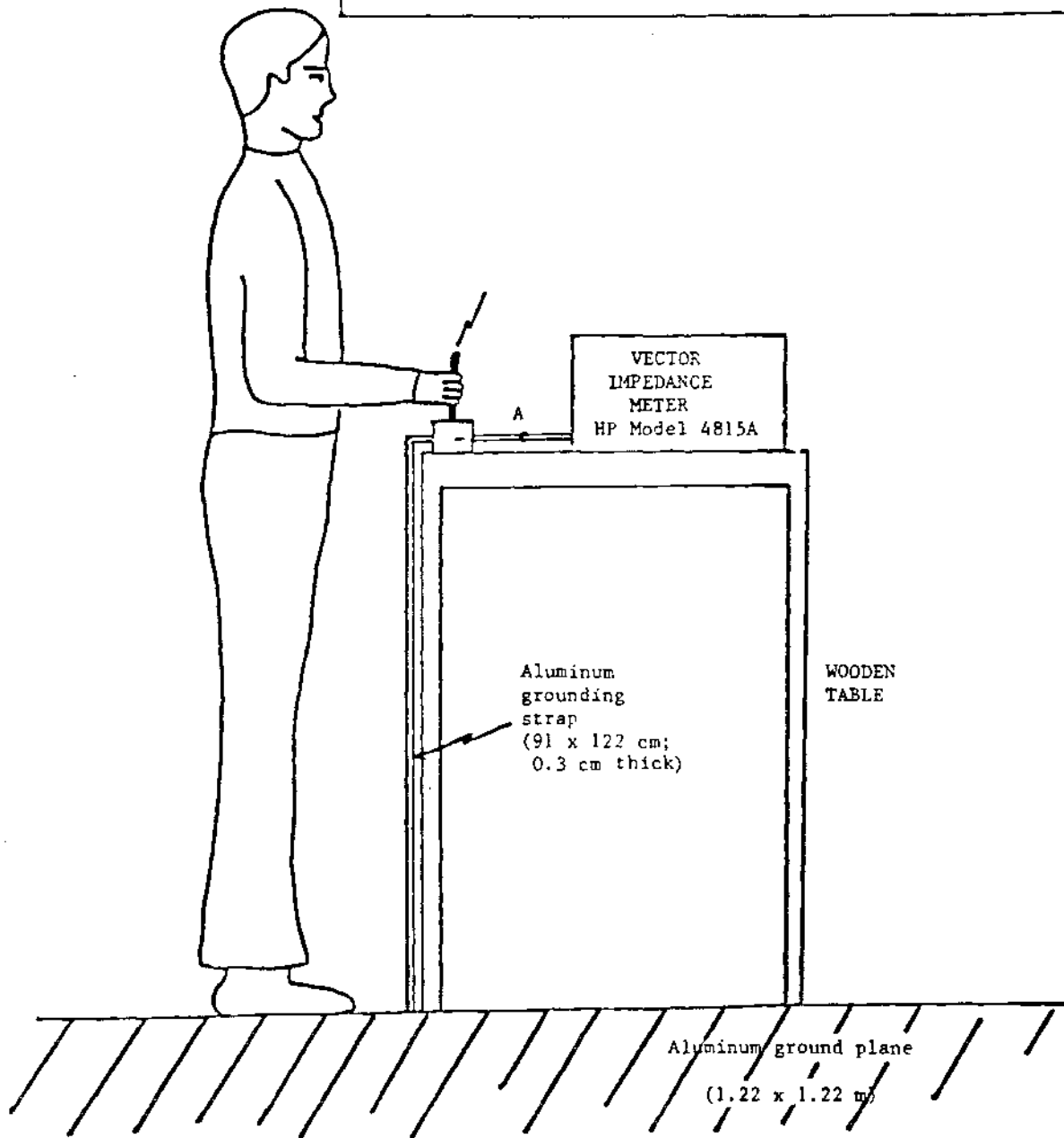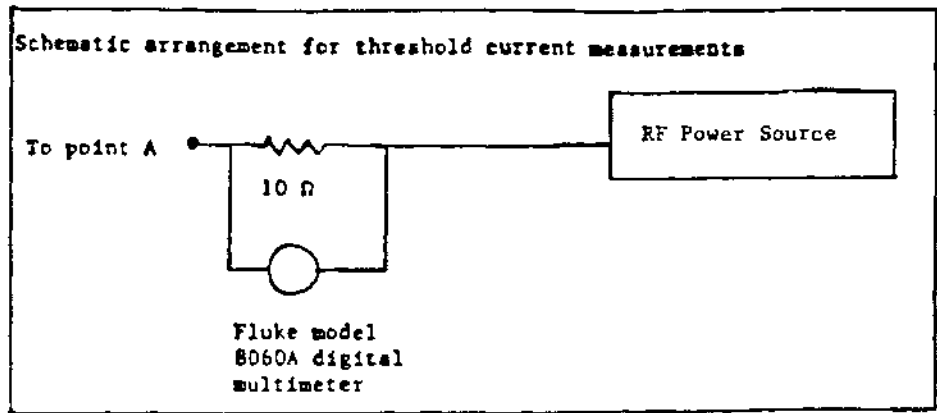
Figure 3. Experimental arrangement for the measurement of human body impedance.

which is similar to that of reference 5, except that the width of the vertical aluminum plate has been widened to 122 cm to reduce its inductance and hence its effective impedance at higher frequencies. It was argued that a wider plate is also more simulant of the actual conditions of contact of a human with large metallic objects and in that sense the measurements will be more representative of the effective impedance of the human body. The subject stood barefoot or with rubber-soled street shoes on a large (1.22 x 1.22 m) aluminum sheet which served as the ground plane and held a cylindrical brass rod electrode (diameter 1.5 cm, length = 14 cm) in the palm of his hand. The impedance between the rod electrode and ground was measured using a vector impedance meter, Hewlett Packard model 4815A (frequency range 0.5-108 MHz). The data are given in Table 1. Recognizing that the open-circuit capacitance of the rod electrode to ground may be substantial and that this will modify the measured values, the open-circuit reactance X_c was measured as a function of frequency. The data on X_c are given in Table 2. Since impedance Z of Table 1 may be considered as a parallel combination of X_c and the actual body impedance Z_b of the subject, this allows the calculation of Z_b. The values thus calculated are given in Table 2. It is interesting to note that there is very little difference in the human body impedance with and without shoes for higher frequencies. This, of course, is on account of substantial capacitance between feet and ground for a subject wearing shoes, which is equivalent to a fairly low series reactance, particularly at higher RF frequencies.

V. CURRENTS FOR THRESHOLD OF PERCEPTION

The schematic arrangement for threshold currents of perception is shown in the insert of Figure 3. Measurements were made with the subject grasping the rod electrode while the second grounding electrode was provided by a flexible copper armband around his forearm just below the elbow. The power sources used were: General Radio type 1330-A bridge oscillator and Kron-Hite model BR 7500 power amplifier for measurements at 1 MHz; 100 W Kenwood model TS 4305 transveceiver for the frequency band 3-30 MHz; and MCL power generator model 15122 for frequencies higher than 30 MHz.

To determine the current entering the hand of the subject at f = 1 MHz, a Fluke model 8060A digital multimeter (with model 85 RF high frequency probe)

was used to measure the voltage across a 10 ohm low-inductance resistor in series with the rod electrode. For frequencies 3-50 MHz a bidirectional power meter (Philco Model 164B) was used to determine the forward and reflected powers. It was found necessary to use impedance matching networks at the various experimental frequencies to reduce the reflected power. The same were therefore designed and fabricated for each of the frequencies using three reactances in the T-network configuration. Knowing the forward and reflected powers, P_F and P_R, respectively, and the measured resistance R between the two terminals (with subject holding the rod electrode and the armband around his forearm), it is possible to determine the hand current I_h from the relationship,

$$I_h = \left[\frac{P_F - P_R}{R} \right]^{1/2} \tag{3}$$

The average of the currents for threshold of perception for two subjects is given in Table 3. Note that the current for threshold of perception is rela-

TABLE 3. AVERAGE VALUE OF THRESHOLD CURRENTS FOR TWO SUBJECTS

F_{MHz}	Threshold Current mA
1	280.0
3	287.5
9.5	297.0
16	303.9
22.5	303.9
27	301.0
33	266.0
40.68	267.7
46	298.7
50	289.2

tively independent of frequency for the frequency band 1-50 MHz. A similar result was previously obtained for a 367-subject study, albeit for a narrower frequency band 0.1-3.0 MHz [5]. As previously noted for lower frequencies 0.1-3.0 MHz, the sensation of current, for the newly-studied higher frequencies to 50 MHz, is also one of heating felt mostly in the region of the wrist. For this cross section the current density and hence the SAR is the highest. The relative constancy of the threshold current of perception in the frequency region 3-50 MHz may be due to the relative constancy of the tissue conductivity σ in this frequency region and a relatively frequency-independent SAR on the order of 80-90 W/kg needed in the wrist cross section for perception of warmth.

VI. RATIO OF FOOT TO HAND CURRENT FOR
CONDITIONS OF GRASPING CONTACT

As discussed in reference 5, substantial hand currents have been estimated for a human being holding the handle of vehicles parked in the E-fields suggested in the ANSI guideline. A set of experiments were performed to determine the fraction of the hand current that would pass through the subject's feet. A purpose of these experiments also was to be able to estimate the SAR at the other extremity of the human body of relatively small cross section; i.e., the ankle section. The experimental setup was similar to the one used for determining the threshold currents in the last section (Figure 3). However, in these experiments no armband was used. The current flowing through the feet was measured by means of the bilayer current sensor described in detail in Section II. The ratio of the foot to hand currents is plotted in Figure 4 as a function of frequency. While the use of footwear reduces substantially the flow of currents at lower frequencies, at higher frequencies there is little difference with or without shoes. Also, over a third of the current entering the hand will pass through the feet at higher frequencies with or without shoes.

VII. USE OF FALSE FLOORS IN THE WORKPLACE

We have evaluated a possible use of false floors in reducing the RF currents induced in a human operator. Reduced RF currents should reduce the
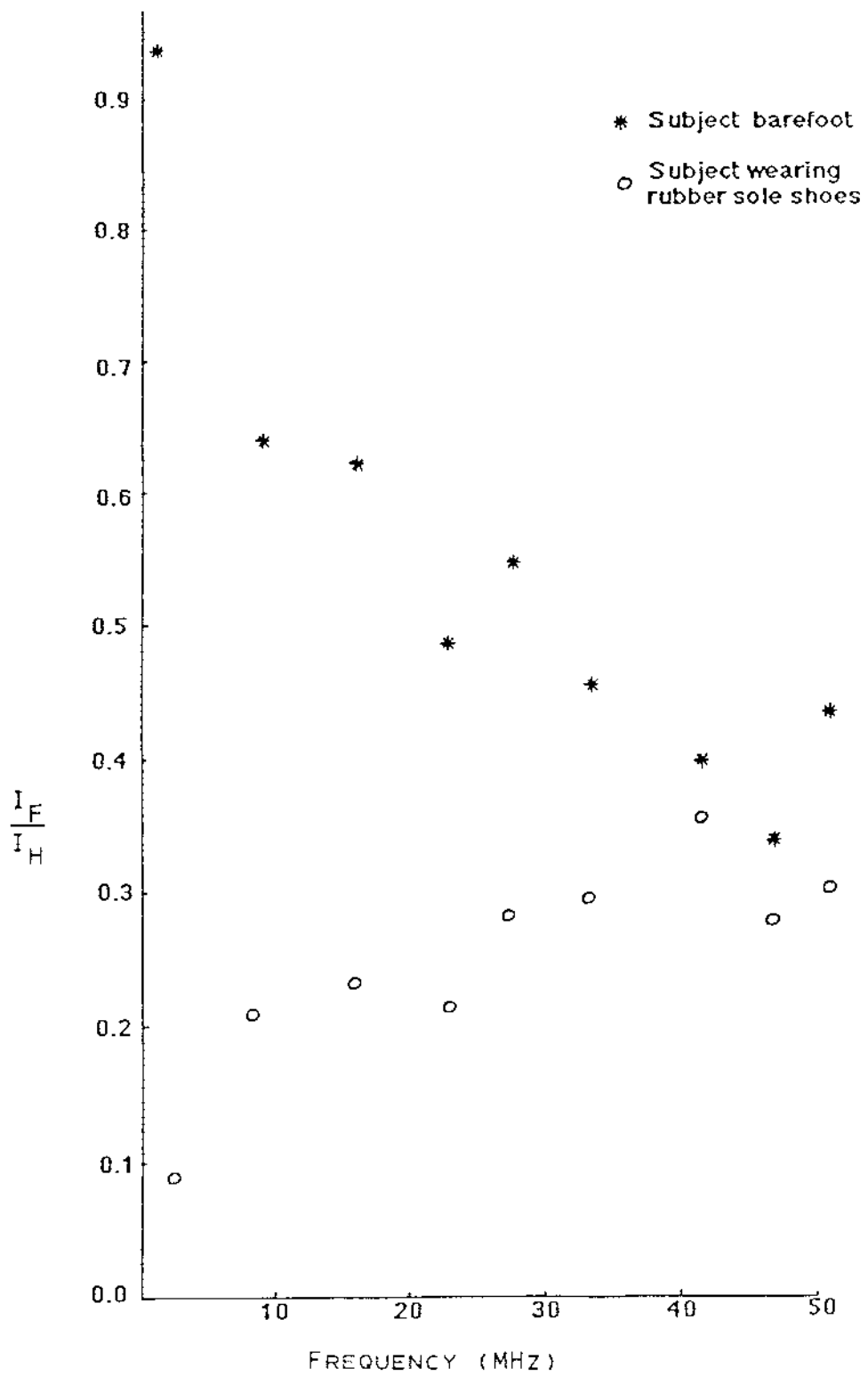
Figure 4. Ratio of foot to hand currents $\left(I_F / I_H \right)$.

ankle-section SAR since the latter is proportional to I_h^2. We have used sytrofoam sheets to separate the subjects from the ground. The reduction in current for various thicknesses of styrofoam is given in Figure 5 as a function of frequency. It should be noted that a styrofoam platform 15-20 cm thick under the feet resulted in an induced current that was substantially less at lower frequencies (< 27 MHz) than if this platform had not been used. The efficacy of these dielectric platforms diminished, however, with increasing frequencies. At 50 MHz, for example, even with a 30 cm thick platform the RF current passing through the feet of an operator was almost two-thirds as much as for grounded conditions.

A similar result was obtained for a subject wearing rubber-soled shoes. The corresponding reduction in the foot current at the irradiation frequency of 27.12 MHz is shown in Figure 6 for various thicknesses of the styrofoam platforms.

The data of Figures 5 and 6 indicate that use of insulating floors to separate the operator from ground can provide an effective technique to diminish the RF-induced currents in the workplace environment, particularly at lower RF frequencies. Similiar techniques cannot, unfortunately, be used for the general population.

VIII. EFFORTS TO MITIGATE RF HAZARDS IN THE WORKPLACE

A. Use of Current-Bypass Metallic Straps to Reduce the High SARs in the Ankle Region

We have investigated the use of grounding metallic straps to bypass the current from the ankle cross section reducing thereby the otherwise high SARs in this region. We have measured the current reduction factors when copper grounding straps of a couple of widths (3 and 6 cm) were used for both of the legs. The grounding straps were wrapped around the legs approximately 20 cm above the bottom of the feet and connected to the lower ground plate of the bilayer current sensor. For experiments at frequencies higher than or equal to 27 MHz, quarter-wavelength monopole antennas, described in Section II, were used as sources of radiation and the currents were measured through the subject's feet with and without the use of the grounding straps. Since the quarter-wavelength antennas would have been unwieldy at lower frequencies, the
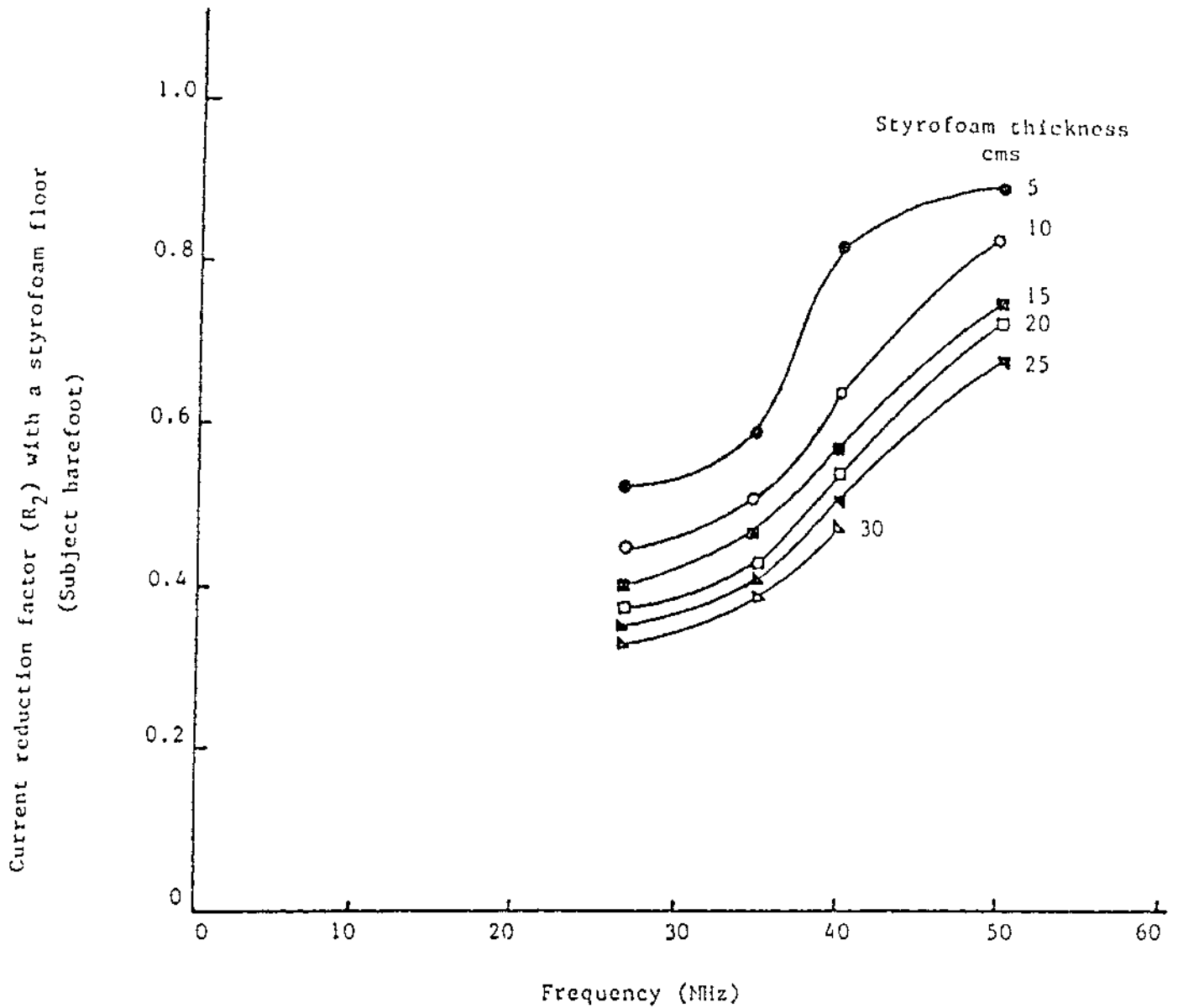
Figure 5. Current reduction factor (R_2) plotted against frequency for various styrofoam thicknesses. R_2 is the ratio of foot current with styrofoam separating subject from ground to current when subject is barefoot on ground.
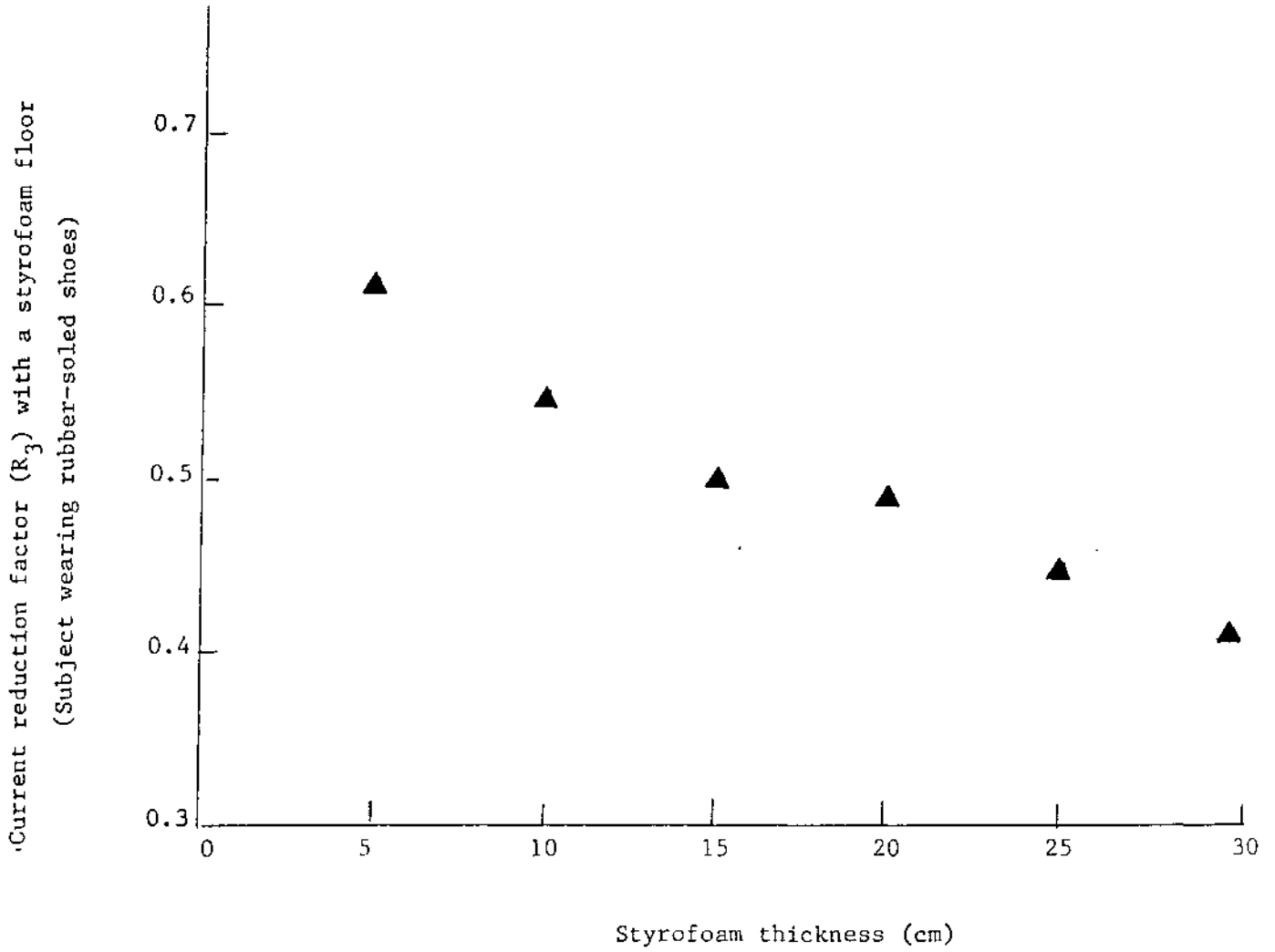
Figure 6. Current reduction factor (R_3) plotted as a function
of styrofoam floor thickness at $f = 27.12$ MHz. The
subject wore rubber-soled shoes. R_3 is the ratio of
foot current with styrofoam separating subject from
ground to current when subject is directly on ground.

experiments were done somewhat differently for frequencies of 1-25.5 MHz.
Similar to the experimental arrangement of Figure 3, the current in these
experiments passed through the human body on account of the subject holding a
rod electrode with one hand while standing on a 1.22 x 1.22 m aluminum
platform to which the ground terminal of the RF generator had been
connected. The current passing through the feet was measured by means of the
21 x 32 cm bilayer current sensor described earlier (Section II). The foot
current reduction factor with and without the copper bypass straps is shown in
Figure 7 for various frequencies. Reduction in current is fairly substantial
at lower frequencies and rises to a value of about 0.4-0.5 at the higher
frequencies. This is to be expected since the straps are likely to present an
equivalent inductance reducing their efficacy at higher frequencies. Also, as
expected, the narrower 3 cm straps result in currents passing through the feet
that are somewhat larger than those for broader 6 cm straps, particularly at
higher frequencies. It is interesting to note, however, that even at the high
frequencies, use of the grounding straps will reduce the ankle-section SARs by
a factor of almost four to six.

B. Use of Metal-Coated Insulating Gloves to Reduce Contact Hazards

We have investigated the use of metal-coated gloves to spread the RF
current to a wider area, thereby reducing the current density. Since the
sensations of perception and pain are related to the current density, it was
argued that this should help in reducing the contact hazards in the work-
place. Experiments have been performed using a kitchen rubber glove (average
thickness = 0.3 mm) that was covered with two copper tapes (each 6 cm wide, 30
cm long, 0.8 mm thick) to allow conduction of current to regions of the
forearm past the wrist. Since the effective conduction cross section of the
wrist is the smallest for the arm, which therefore results in the highest SARs
in this section, it was argued that larger RF currents may then be passed to
the forearm without heat or pain experienced by the subject. Similar to the
experiments in Section V, the subject held a cylindrical brass rod electrode
(diameter = 1.5 cm, length = 14 cm) while the second electrode was provided by
means of a copper band around the upper arm. Currents for perception at vari-
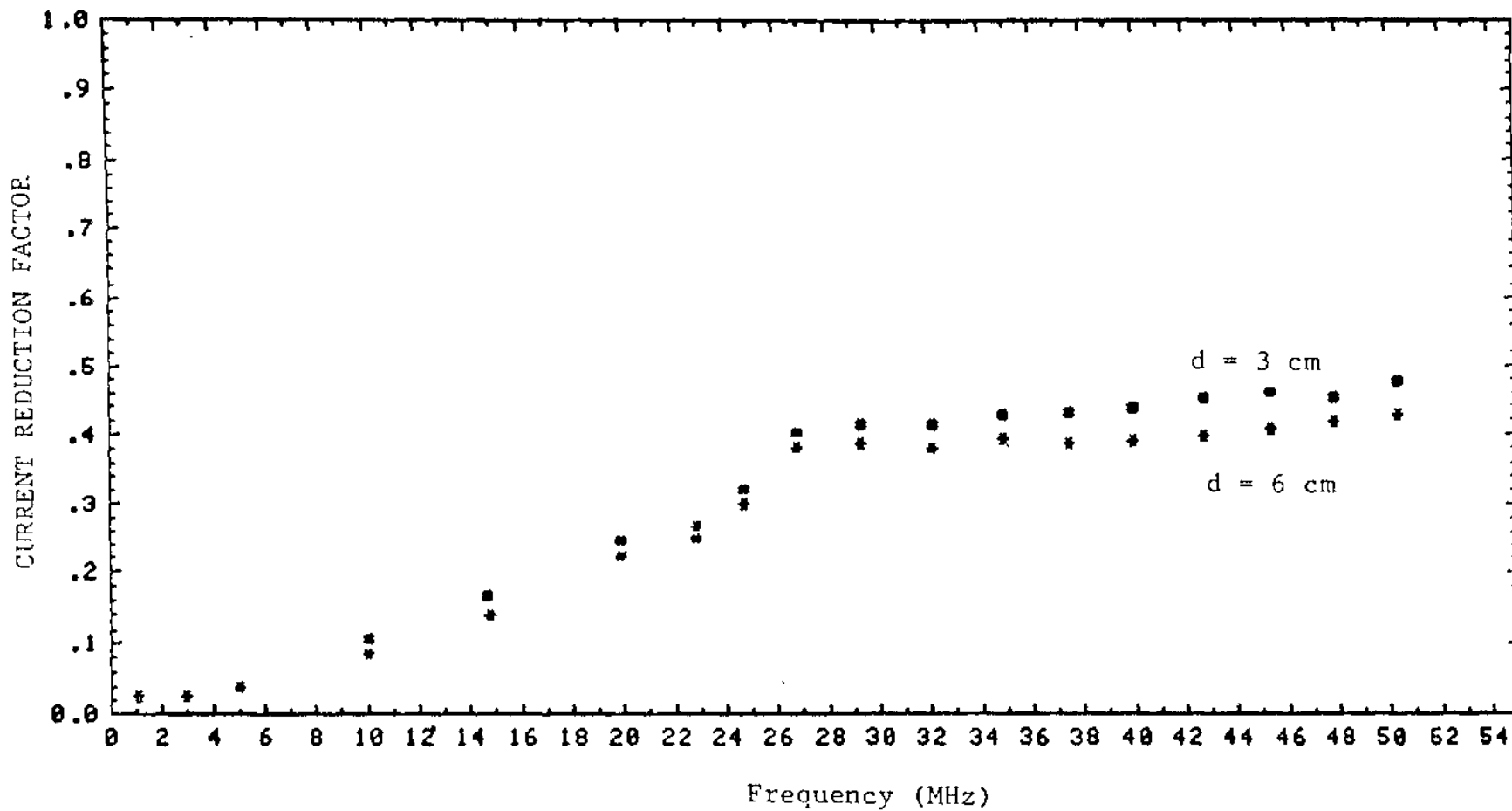
Figure 7. Foot current reduction factor with the metallic bypass straps to reduce high SARs in the ankle region. d is the width of the metallic strap.

ous frequencies are shown in Figure 8 for the subject without gloves and with conducting gloves. The sections where the perceptions occur are also indicated for the two curves in Figure 8. As expected, a somewhat larger current is needed to cause threshold of perception with the use of metal-coated insulating gloves. Unfortunately, however, the increase in current threshold is by a factor less than 2. As also observed earlier [5], the sensation is one of tingling or pricking at lower frequencies and one of heat for frequencies higher than 100 kHz. Whereas the data in the past [5] were obtained only for frequencies up to 3 MHz, it is interesting to note that the threshold current for perception is relatively independent of frequency even at the higher frequencies to frequencies as high as 40 MHz. This was to be expected since the perception phenomenon at these frequencies is thermal in nature and is, therefore, dependent only on SAR. The reason for only slight increase in the threshold current for perception with the use of the conducting gloves is that high SARs are now caused at the elbow section. The elbow section is also fairly bony and hence presents a relatively small conduction cross section as well. It is obvious that a longer glove that would carry the RF current past this section may help in increasing the threshold for perception current even higher.

IX. FOOT CURRENTS AND PEAK SARs PROJECTED
FOR ANSI C95-1982 GUIDE [1] ON E-FIELDS

From the ANSI C95.1-1982 guide, rms E-fields are given by the following:

$$E = 614 \text{ V/m} \quad \text{for} \quad 0.3 \leqslant f_{MHz} \leqslant 3.0$$

$$E = \frac{1842}{f_{MHz}} \text{ V/m} \quad \text{for} \quad 3.0 \leqslant f_{MHz} \leqslant 30$$

$$E = 61.4 \text{ V/m} \quad \text{for} \quad 30.0 \leqslant f_{MHz} \leqslant 300 \qquad (4)$$

We can use Eqs. 1 and 2 to calculate the foot currents induced in a human of height h = 1.75 m subjected to ANSI C95.1-1982 suggested E-fields. These are plotted in Figure 9. For frequencies to 10 MHz, currents fairly similar to those in Figure 9 have also been projected by Hill and Walsh [11]. We project
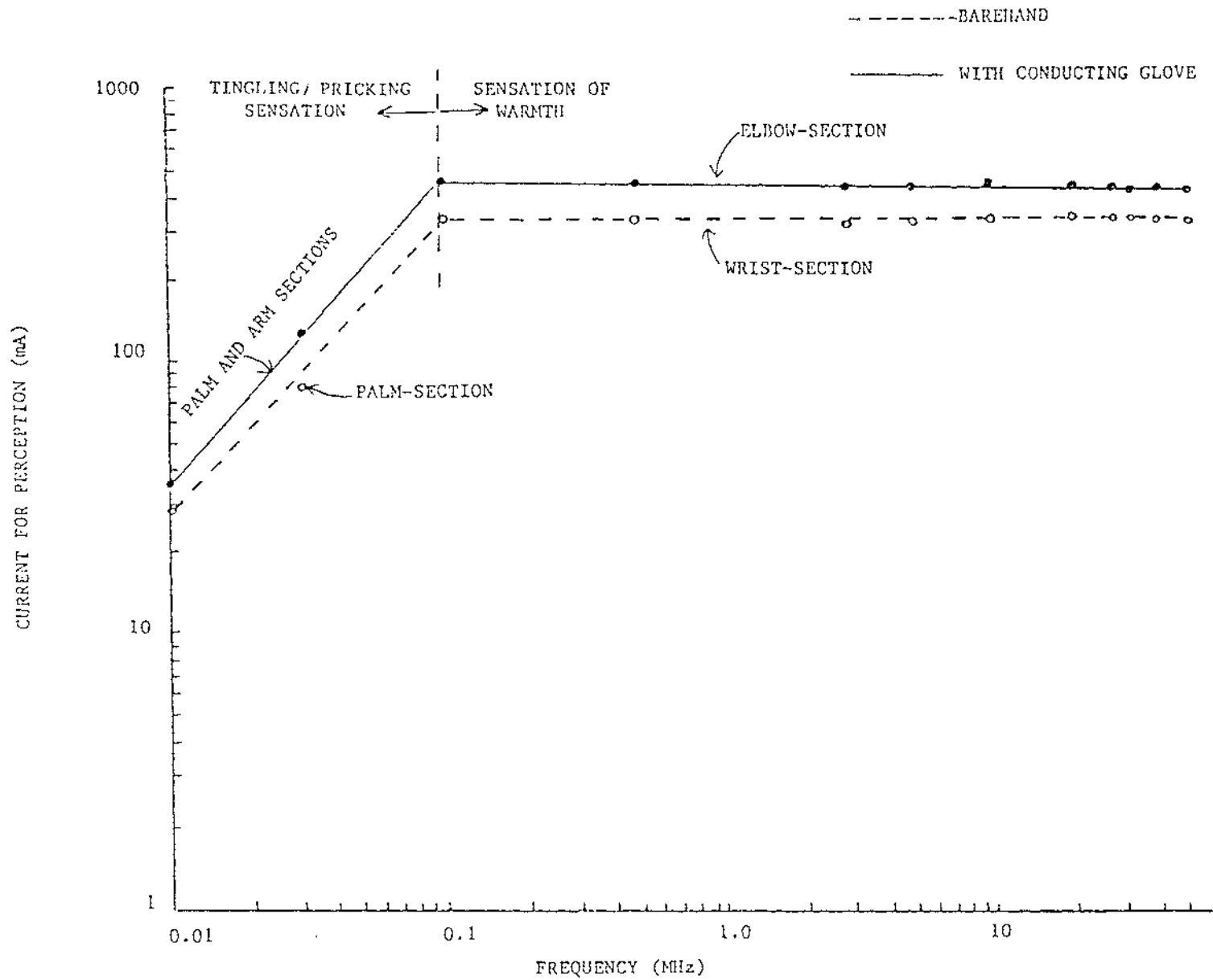
Figure 8. Current for perception without gloves and with conducting gloves. The sections where the perceptions occur are also indicated.
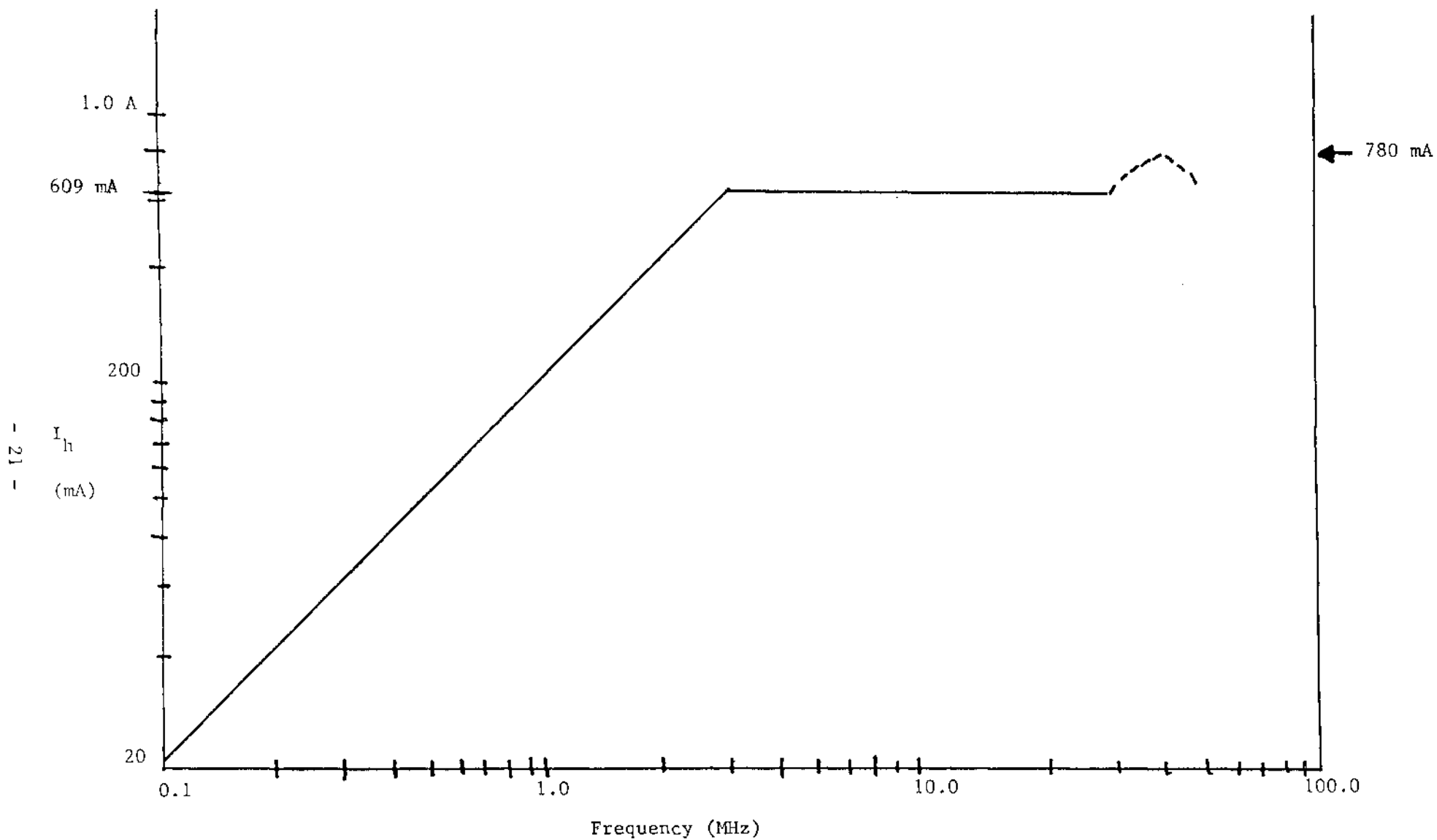
Figure 9. Foot current induced in an adult male (h = 1.75 m) subjected to fields recommended in the ANSI-1982 RF safety guide.

a current on the order of 780 mA for $E = 61.4$ V/m (1 mW/cm^2) for a frequency of 40 MHz with a value increasing or decreasing as h^2 for taller and shorter individuals. From reference 4 it should be noted that currents fairly comparable to those shown in Figure 9 will also be set up in the other sections of the body as well.

A. SARs in the Cross Section of the Ankle

The anatomical data for the cross section through the ankle have been used to estimate the effective cross-sectional area for the flow of the RF currents [4]. The effective cross-sectional area A_e is estimated by the equation

$$A_e = \frac{A_c \sigma_c + A_1 \sigma_1 + A_m \sigma_m}{\sigma_c} \tag{5}$$

where A_c, A_1, and A_m are the physical areas of the high-water-content and low-water-content tissues, and of the region containing red marrow, of conductivities σ_c, σ_1, and σ_m, respectively. The areas A_c, A_1, and A_m estimated for the anatomical cross section of the ankle [4] are, respectively, 4.7, 27.2, and 8.1 cm^2. Taking $\sigma_c = 0.6$ S/m, $\sigma_1 = 0.03$ S/m, and $\sigma_m = 0.26$ S/m for the frequency band 3-30 MHz [16], an effective area of 9.5 cm^2 is calculated for the cross section through the ankle for a human adult even though the physical cross section is on the order of 40 cm^2.

To estimate SARs in the various tissue types, we proceed as follows. The total current $I_h/2$ in each of the legs is assumed to be distributed as the inverse of the impedances Z_i. For the i-th tissue of area A_i, where the individual areas may refer to the aforementioned physical areas of the high-water-content and low-water-content tissues and of the region containing red marrow

$$Z_i = \frac{\ell}{\left(\sigma_i + j\omega\varepsilon_i\right) A_i} \tag{6}$$

$$I_i = \frac{I_h \frac{1}{Z_i}}{2 \sum\limits_i \frac{1}{Z_i}} = \frac{I_h \left(\sigma_i + j\omega\varepsilon_i\right) A_i}{2 \sum\limits_i \left(\sigma_i + j\omega\varepsilon_i\right) A_i} \tag{7}$$

$$E_i = \frac{J_i}{\sigma_i + j\omega\varepsilon_i} = \frac{I_h/2}{\sum\limits_i \left(\sigma_i + j\omega\varepsilon_i\right) A_i} \tag{8}$$

$$SAR\bigg|_i = \frac{\sigma_i E_i E_i^*}{\rho_i} = \frac{\left|I_h/2\right|^2 \sigma_i}{\rho_i \sum\limits_i \left(\sigma_i^2 + \omega^2 \varepsilon_i^2\right) A_i^2} \tag{9}$$

where σ_i and ε_i are the conductivity and permittivity of the i-th tissue at frequency ω in radians/s

ℓ is the length of the section of the leg

$J_i = I_i/A_i$ is the current density per unit area in the i-th tissue

ρ_i = mass density of the i-th tissue.

From Eq. 9, it is clear that the highest SAR occurs in high-water-content tissues with the highest conductivity. For these tissues a mass density of 10^3 kg/m^3 is assumed.

For E-fields recommended in the ANSI C95.1-1982 RF safety guide, the high-water-content (wet-) tissue SARs for the ankle section are calculated by using the currents I_h from Figure 9 and the values of the conductivities σ_c from reference 16. These are shown in Figure 10. A fairly large ankle-section SAR of 222 W/kg is projected for a standing adult of height h = 1.75 m at a frequency of 40 MHz. This is, of course, considerably in excess of the ANSI C95.1-1982 guideline of 8 W/kg for any 1 g of tissue.

Since the current is somewhat lower for a subject wearing shoes, the numbers in Figure 10 must be multiplied by the square of the corresponding current reduction factors from Figure 2.

B. Scaling to Other Heights; Five- and Ten-Year-Old Children

From Eq. 1, it is seen that the induced current is proportional to h^2 and is consequently smaller for shorter individuals. Since the cross-
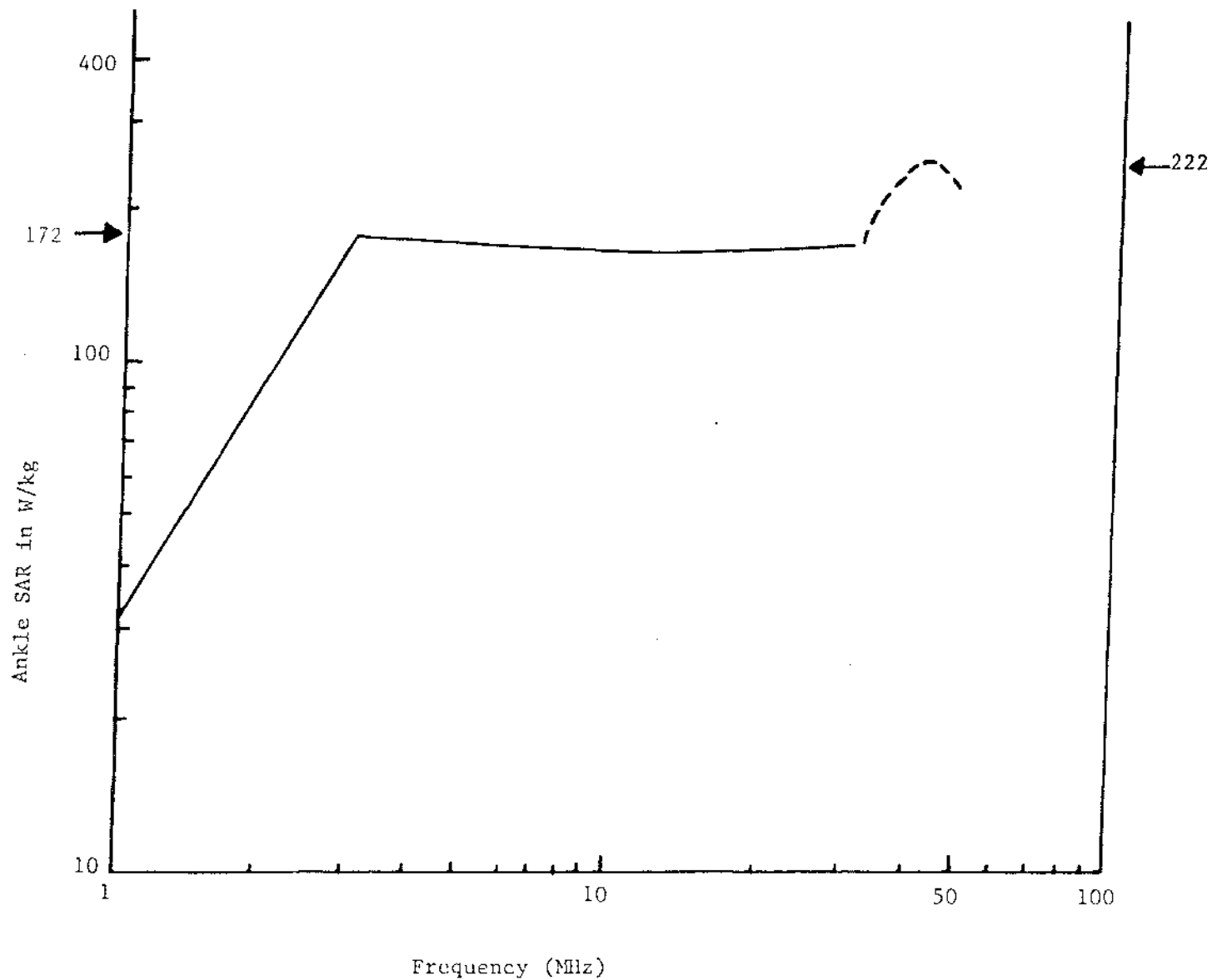
Figure 10.   Ankle-section high-water-content tissue SAR for
adult male (h = 1.75 m) for electric fields recom-
mended in the ANSI-1982 RF safety guide.

sectional dimensions of the body are to a first-order of approximation also proportional to (weight)$^{2/3}$ or h^2, the current density J, and hence the ankle-section SAR (proportional to J^2) may not be very different at a specific frequency from one height to another. From electromagnetic scaling concepts, the frequency corresponding to maximum ankle-section current or wet-tissue SAR would, however, increase as 1/h, to being on the order of 46.7 MHz for a 1.5 m-tall adult, 50.7 MHz for a ten-year-old child (h = 1.38 m), and 62.5 MHz for a five-year-old child (h = 1.12 m), as against 40 MHz for a 1.75 m-tall adult human. Since the current increases as f, the maximum SARs projected at the new peak-SAR frequencies would be considerably higher. Linearly interpolating between the values given at 40.68 and 100 MHz [16], we have taken somewhat larger conductivities σ_c of the wet tissues at the higher frequencies and have used the values 0.693, 0.73, and 0.77 S/m at 40 and 46.3, and at 50.7 and 62.5 MHz, respectively. The highest ankle-section wet-tissue SARs projected for ten- and five-year-old children for 1 mW/cm^2 incident plane waves $\left(E_{inc} = 61.4 \text{ V/m} \right)$ are estimated to be 328 and 462 W/kg, respectively (see Table 4).

X. CONTACT HAZARDS IN THE FREQUENCY BAND 10 kHz – 3 MHz

Our previous work [5,17,18] has pointed to a potential for shock and burn upon contact with large ungrounded metallic objects such as automobiles, vans, fences, etc., for incident electric fields considerably lower than the ANSI and ACGIH suggested E-fields of 614 V/m for frequencies lower than 3 MHz. Experimental data have been obtained [5,18] for 367 human subjects for the body impedance and threshold currents needed to produce sensations of perception and pain for the 10 kHz – 3 MHz band. Even though the measurements were made for adults of ages between 18-70 (197 male and 170 female subjects), scaling relationships have been developed to project the results for ten-year-old children. The details of these measurements are given in the report [18] based on these studies. Highlights of the results have been published as reference 5. Important graphs based on this study are reproduced here as Figures 11-15.

The procedure used to calculate the incident electric fields for thresholds of perception and pain upon contact with ungrounded metallic objects is as follows [17]. The human being represented by a series equivalent

TABLE 4. INDUCED CURRENTS AND ANKLE-SECTION WET-TISSUE SARs FOR THE ANSI C95.1-1982 RECOMMENDED E-FIELD OF 61.4 V/m [1]

	Height	Frequency	I_h[†]	Ankle-section Wet-tissue SAR[*]
	m	MHz	mA	W/kg
Average adult	1.75	40.0	780	222
Adult	1.5	46.7	669	294
10-year-old child	1.38	50.7	615	328
5-year-old child	1.12	62.5	499	462

[†] For subjects wearing shoes, the currents are somewhat lower (see Figure 2). This would result in correspondingly lower SARs.

[*] We have assumed a conductivity of 0.639 S/m for the high-water-content tissues at 40 and 46.7 MHz [16]. Somewhat larger conductivities of 0.73 and 0.77 S/m are taken at 50.7 and 62.5 MHz, respectively. The corresponding dielectric constants taken are 97.3 for 40 and 46.7 MHz and 92.9 and 87.4 for 50.7 and 62.5 MHz, respectively.

circuit of resistance R_h and reactance $-jX_h$ may be considered to be in parallel with the equivalent circuit of the large metallic object (see the Norton equivalent circuit of Figure 16). Assuming that the leakage resistance to ground of the metallic object is very large, the equivalent circuit of the object is purely capacitive, given by C_{og}.

The current induced in a human being in contact with the object is then given by
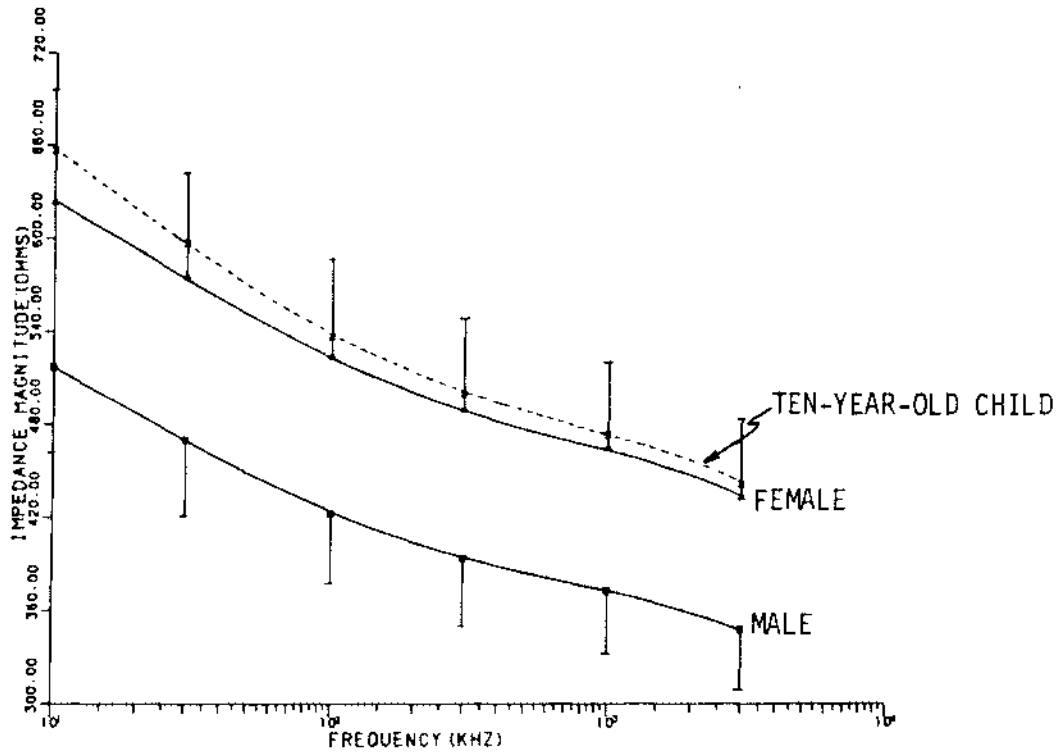
(a) MAGNITUDE
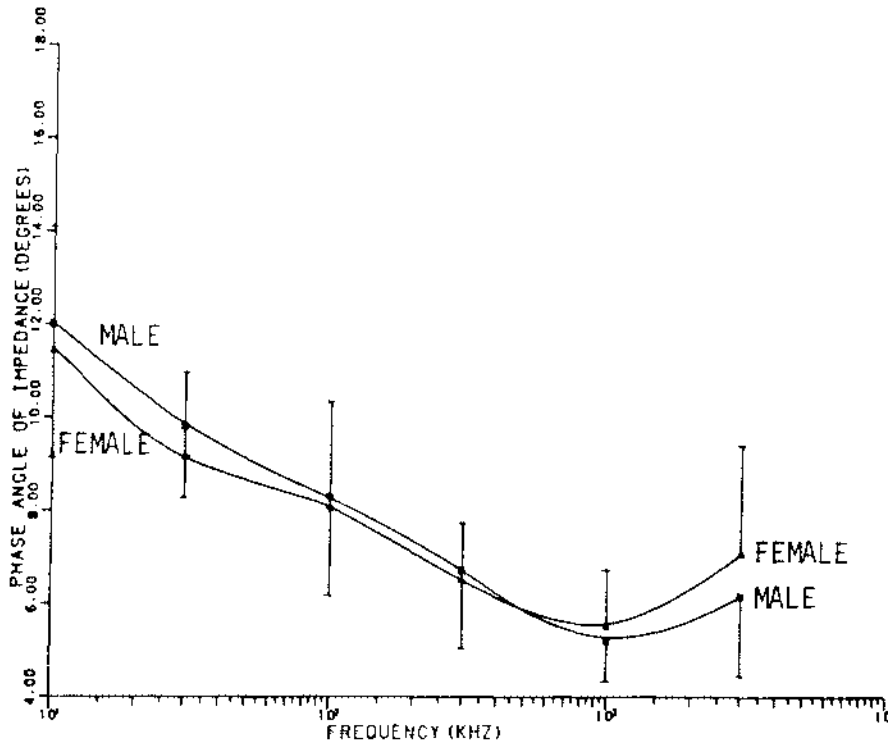
(b) PHASE

Figure 11. Average body impedance of adult males (N = 197), adult females (N = 170), and ten-year-old children (dashed line) for grasping contact with a brass rod of diameter 1.5 cm and length 14 cm.
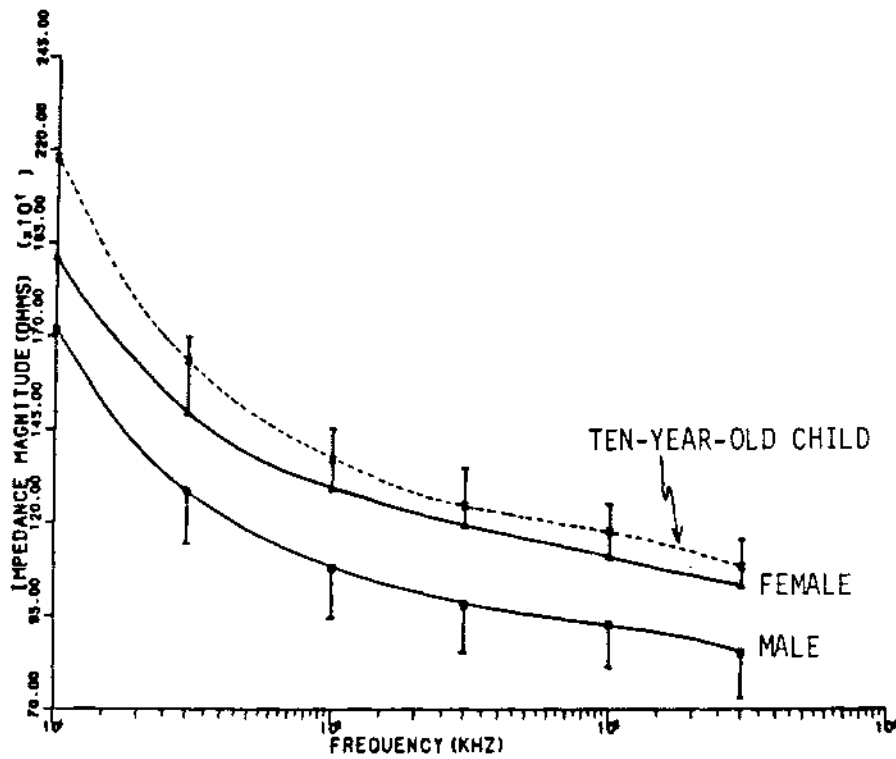
(a) MAGNITUDE
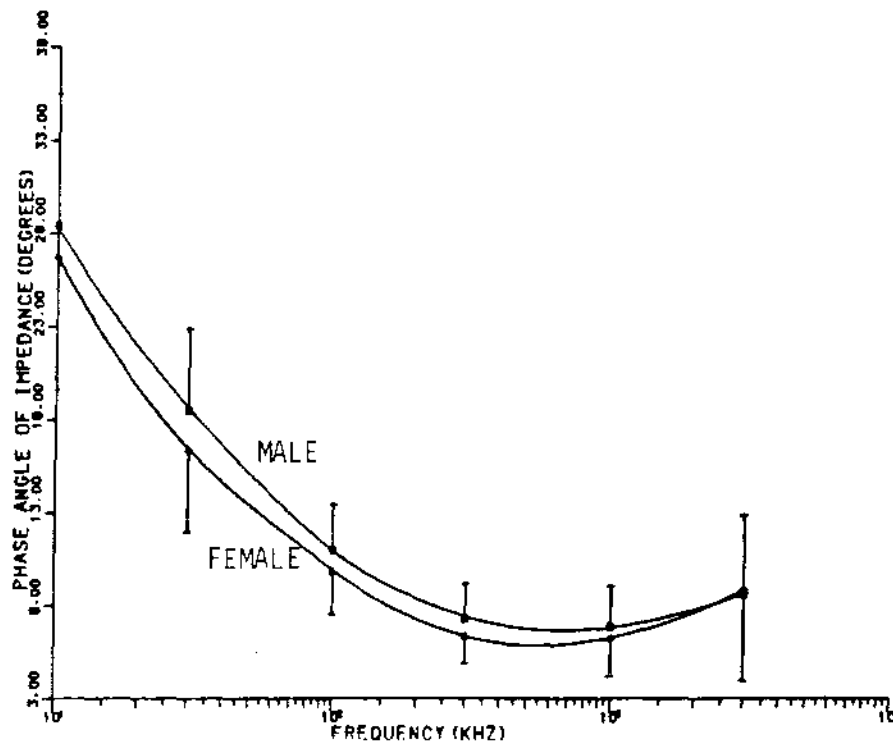
(b) PHASE

Figure 12. Average body impedance of adult males (N = 197), adult females (N = 170), and ten-year-old children (dashed line) for finger contact (plate of area 144 mm²).

Figure 13. Average threshold current for perception, finger contact for adult males (N = 197), adult females (N = 170), and ten-year-old children. Contact area = 25 mm².
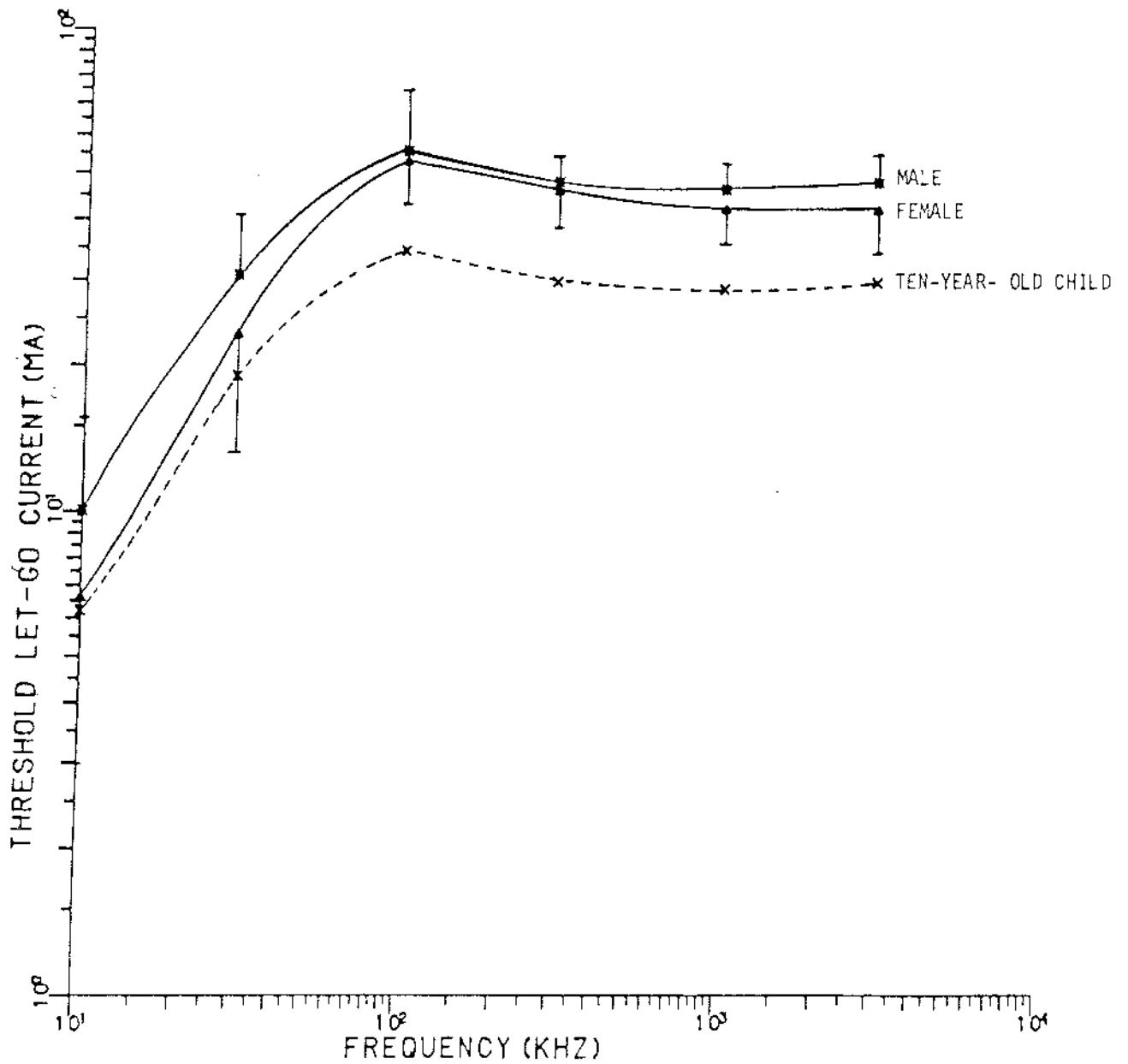
Figure 14. Average threshold current for pain, finger contact, for adult
males (N = 197), adult females (N = 170), and ten-year-old
children. Contact area = 25 mm^2.
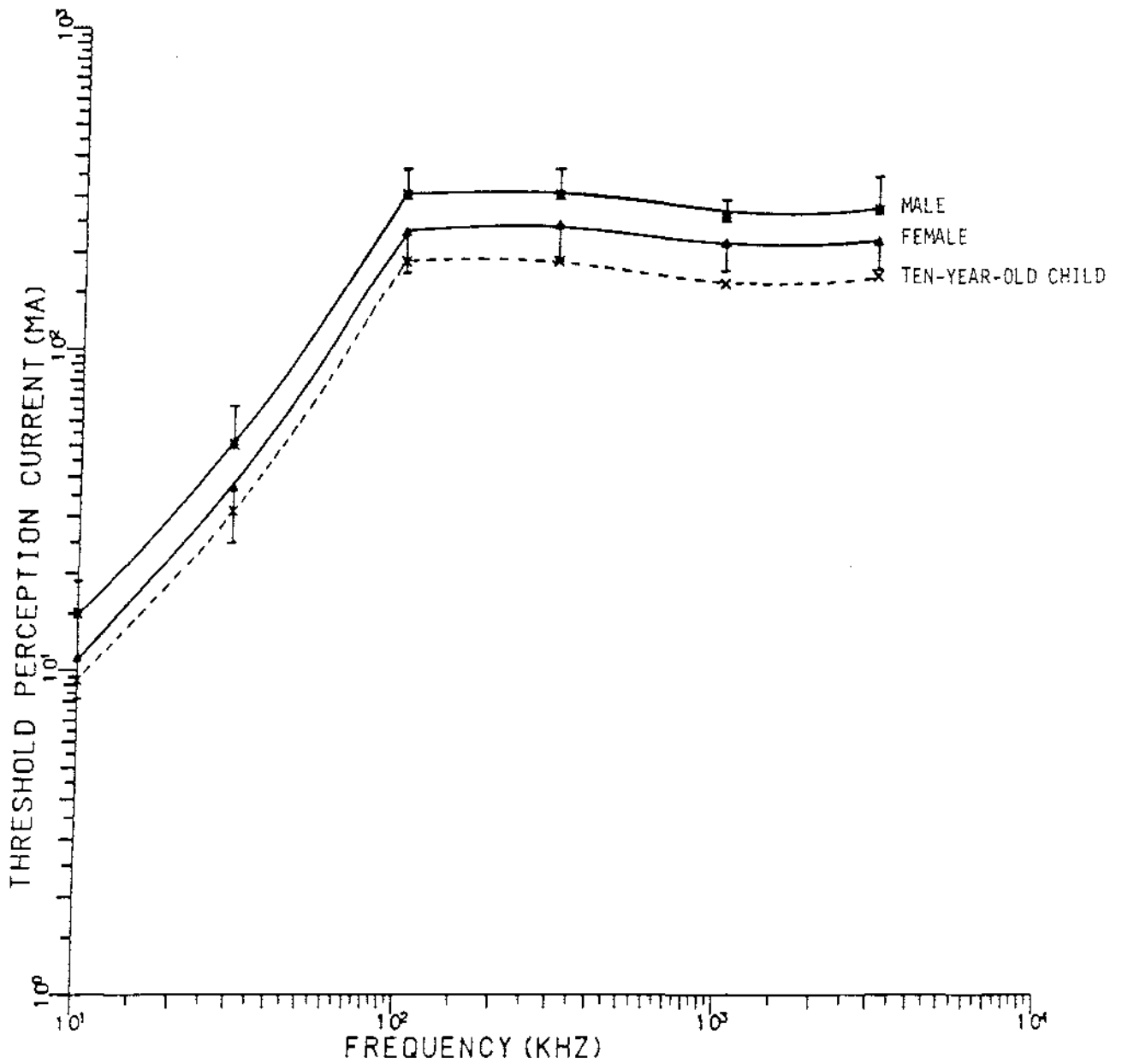
Figure 15. Average threshold current for perception, grasping contact, for adult males (N = 197), adult females (N = 170), and ten-year-old children.
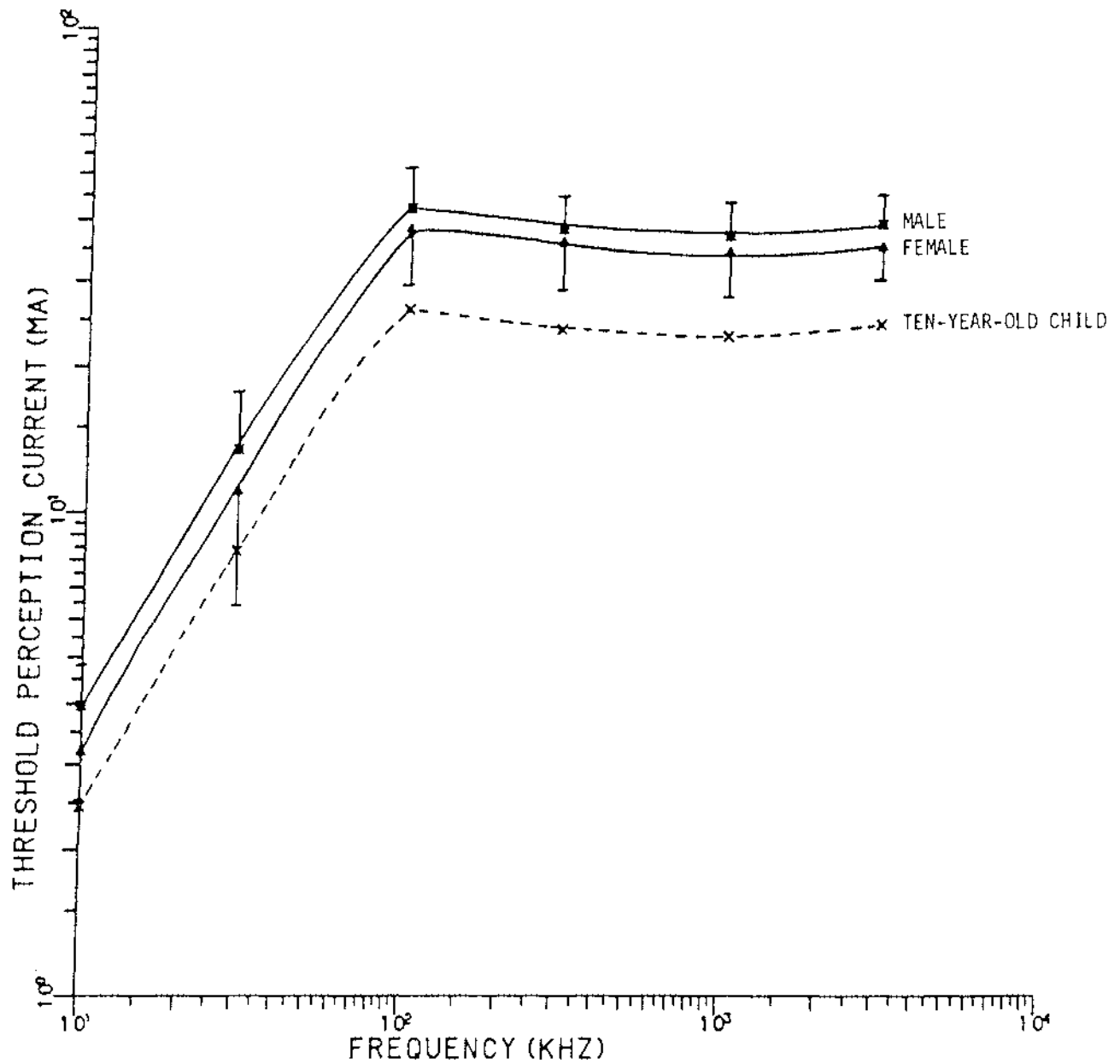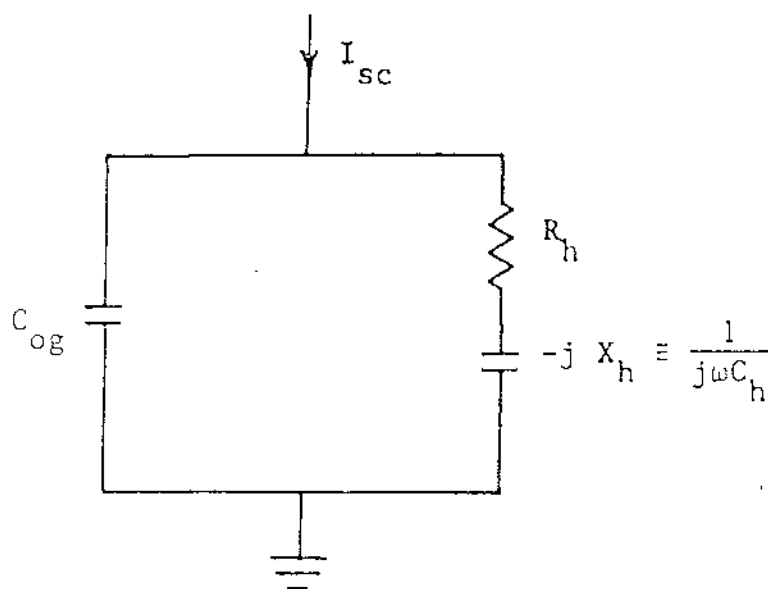
Figure 16. Norton equivalent circuit for a human being in conductive contact with a large metallic object. I_{sc} = short-circuit current induced in the metallic object.

$$I_h = I_{sc} \left| \frac{\dfrac{-j}{\omega \, C_{og}}}{R_h - jX_h - \dfrac{j}{\omega \, C_{og}}} \right| \qquad (10)$$

where I_{sc} = magnitude of the short-circuit current flowing through the vehicle

= $j\omega\varepsilon_o S_{eff} E$

ω = $2\pi f$, f = frequency

ε_o = permittivity of free space = 8.854×10^{-12} F/m

E = electric field incident on the vehicle (V/m)

S_{eff} = effective area of the vehicle tabulated for some of the vehicles in Table 5

R_h, X_h = resistance, reactance of the human being in contact with the vehicle (Ohms)

C_{og} = capacitance-to-ground of the vehicle (tabulated for some of the vehicles in Table 5) (F).

From measurements of the magnitudes of the short-circuit current $\left|I_{sc}\right|$ (= $\omega\varepsilon_o S_{eff} E$) and the open-circuit voltage of the ungrounded object

$$\left|V_{oc}\right| = \frac{I_{sc}}{\omega \, C_{og}} ,$$

one can calculate the effective area S_{eff} and its height h. The corresponding values for some vehicles are given in Table 5.

The average values of body impedance and threshold currents (Figures 11-15) have been used to calculate the threshold E-fields for perception and pain when a human being is in grasping or finger contact with various vehicles, for which the pertinent properties are given in Table 5. The magnitude of the threshold E-field is given by Eq. 11

$$\left| E \right| = \frac{C_{og}}{\varepsilon_o \, S_{eff}} \, I_h \left| R_h - j \left(X_h + \frac{1}{\omega \, C_{og}} \right) \right| \qquad (11)$$

TABLE 5. CAPACITANCE-TO-GROUND, EFFECTIVE AREA, AND EFFECTIVE HEIGHT OF VARIOUS VEHICLES IN QUASI-STATIC (LOW FREQUENCY) FIELDS

Vehicle	Capacitance-to-ground C_{og} pF	Effective area S_{eff} m^2	Effective height h m
Compact car [19]	800	26.4	0.292
GMC van [*]	1045	58.6	0.5
School bus [20,21]	2650	116.8	0.4

[*] measured by us at a local broadcast station at 700 kHz.

The average threshold E-fields for 197 male subjects and 170 female subjects and the scaled values for 10-year-old children are plotted versus frequency in Figures 17-22 [5,18]. It can be seen that for several cases the values of the E-field are below the ANSI C95.1-1982 guideline of E = 614 V/m for f < 3 MHz.

From Eq. 11 we can calculate the current that will flow through the human body upon grasping a vehicle in an incident field of 614 V/m. We calculate that a current of 854 mA will flow through the human hand holding an automobile van $\left(C_{og} = 1045 \text{ pF from Table 5} \right)$ parked in the ANSI-recommended electric field of 614 V/m at a frequency of 3 MHz. Following a procedure similar to that of Section IX (Eq. 5), we can estimate an effective cross-sectional area of the human wrist by apportioning the tissues into one of three categories -- the high-, the medium-, and the low-conductivity tissues, respectively. An effective cross-sectional area A_e of 11.1 cm^2 is thus calculated from the anatomical cross section of the wrist [6]. The wet-tissue SAR may be estimated from the equation

$$J^2 / \sigma_c \rho = I^2 / A_e^2 \, \sigma_c \rho \qquad (12)$$

where ρ is the mass-density of the tissue, taken to be 10^3 kg/m^3 for the high-water-content tissues.
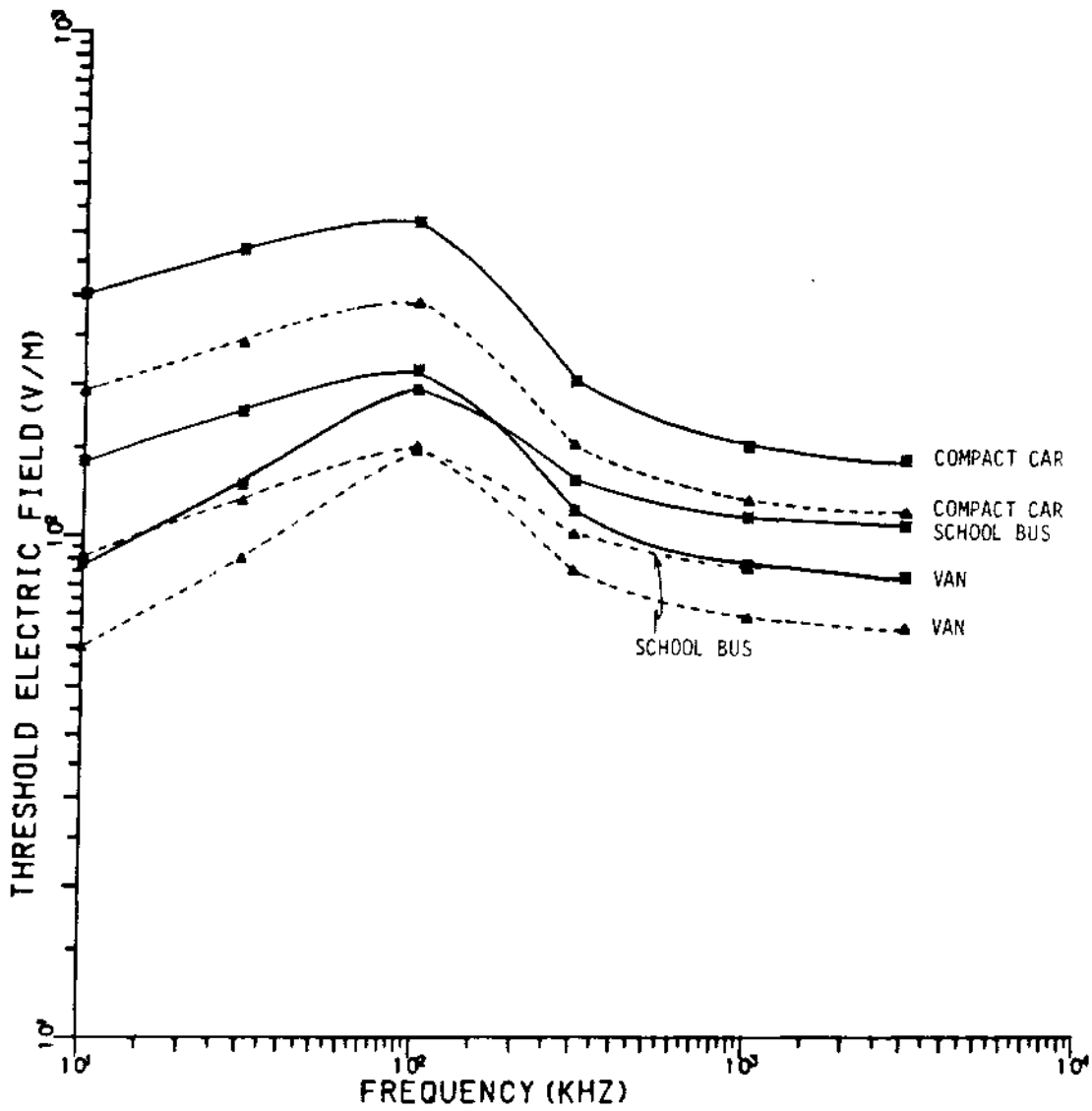
Figure 17. Average threshold electric field for perception for grounded adult
males (solid lines) and ten-year-old children (dashed lines) in
finger contact with various vehicles. Contact area = 25 mm^2.
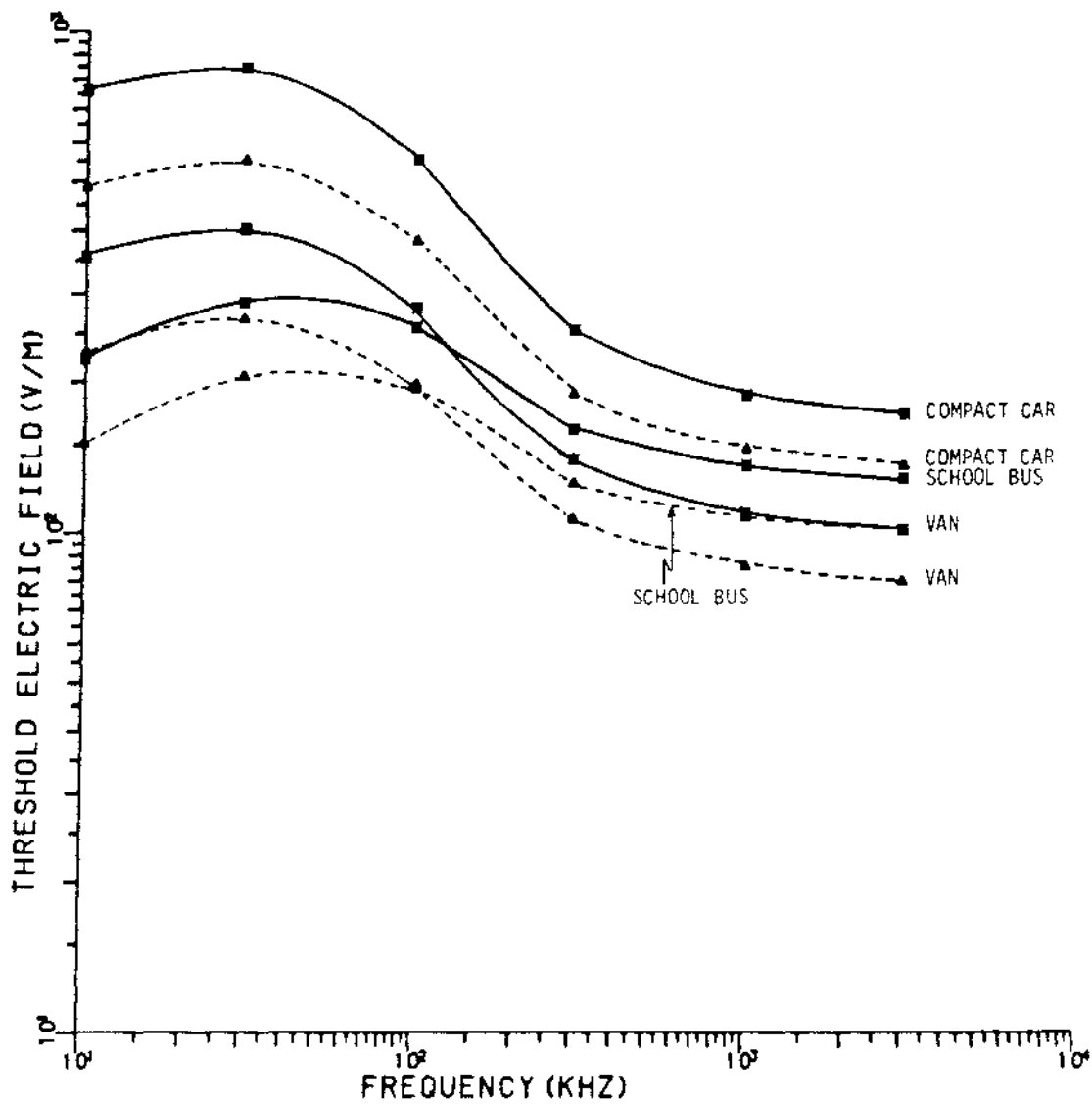
Figure 18. Average threshold electric field for pain for grounded adult males (solid lines) and ten-year-old children (dashed lines) in finger contact with various vehicles. Contact area = 25 mm^2.
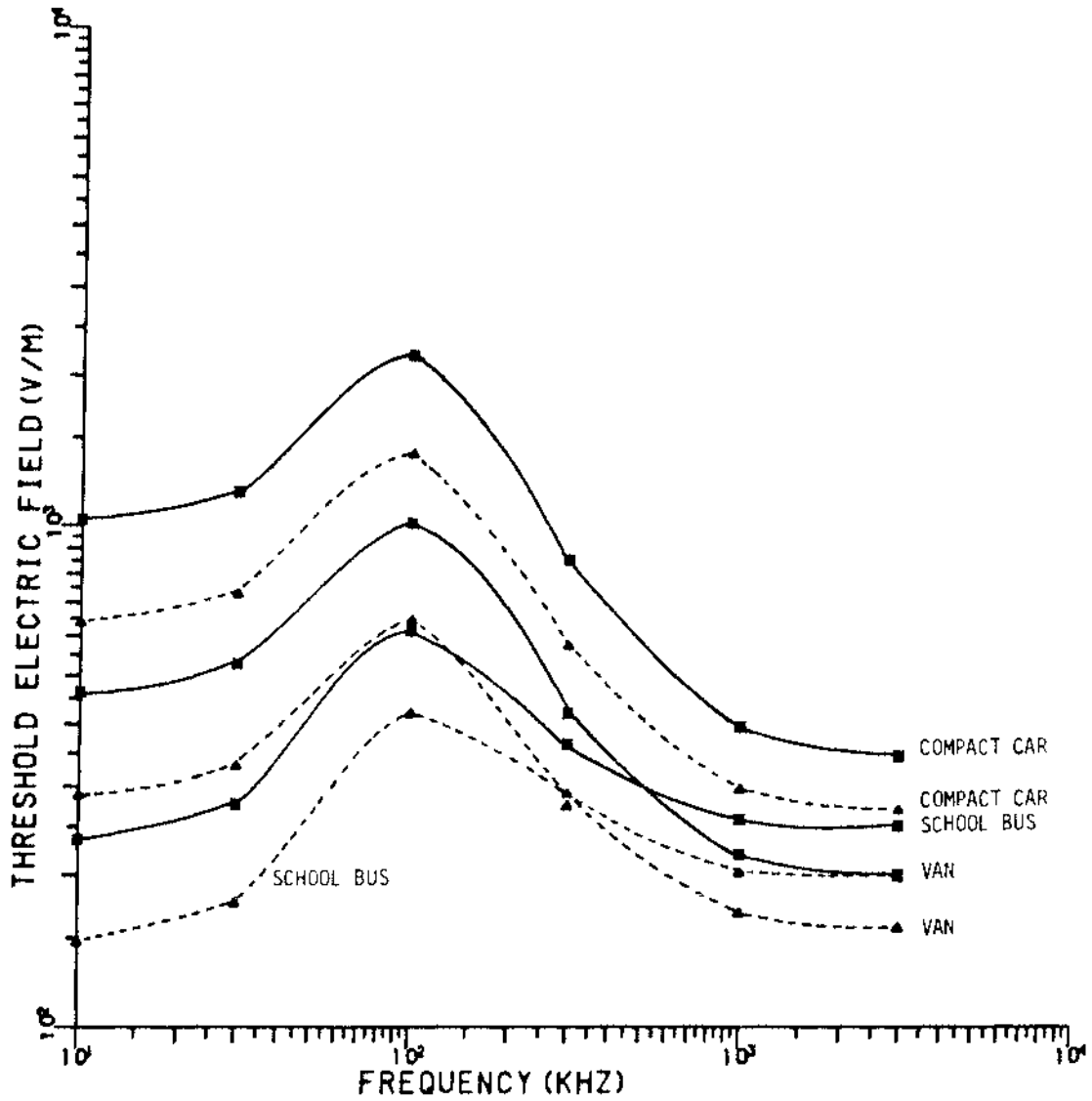
Figure 19. Average threshold electric field for perception for grounded adult males (solid lines) and ten-year-old children (dashed lines) in grasping contact with various vehicles.
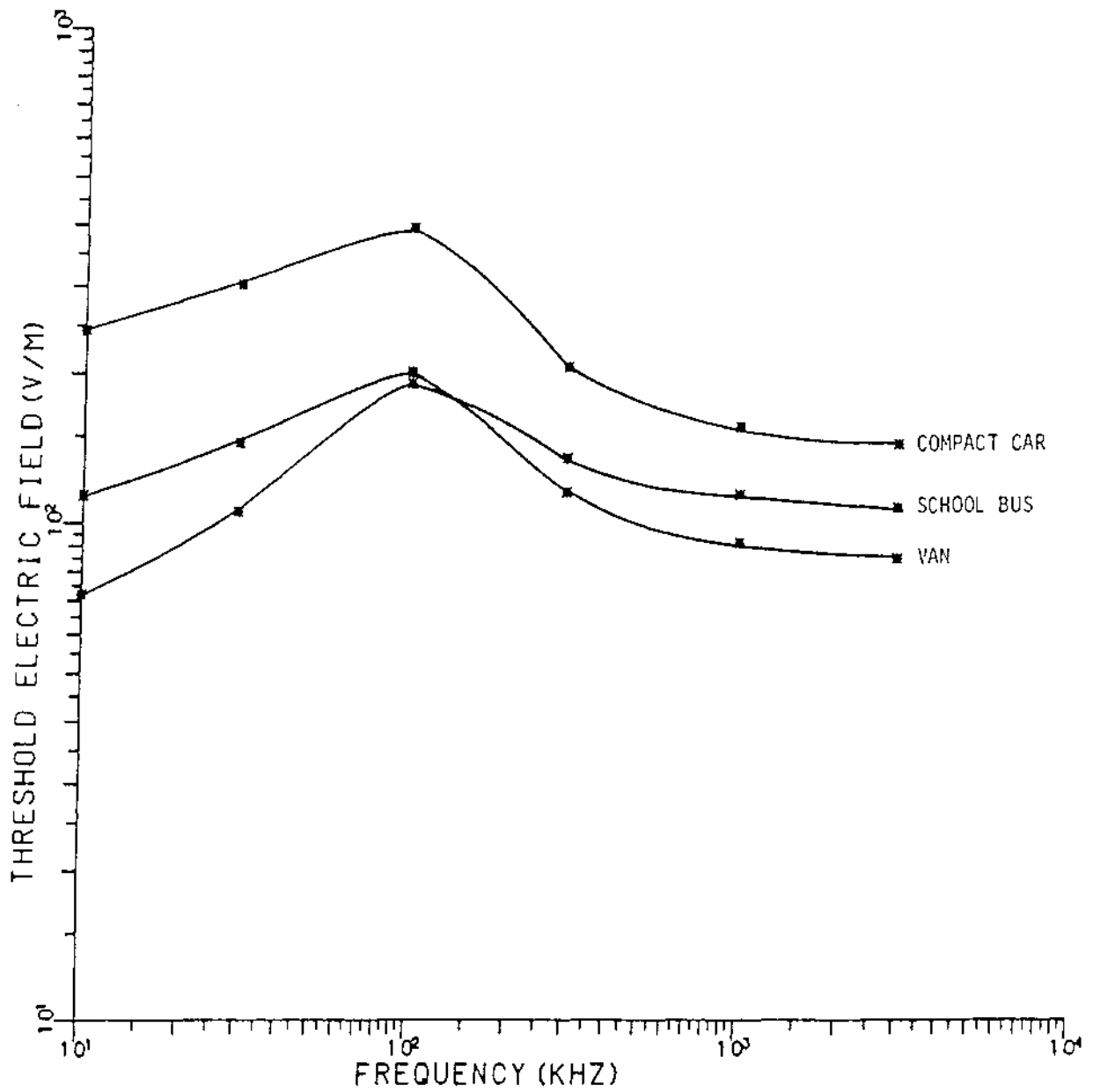
Figure 20. Average threshold electric field for perception for grounded adult
females in finger contact with various vehicles. Contact area =
25 mm^2.
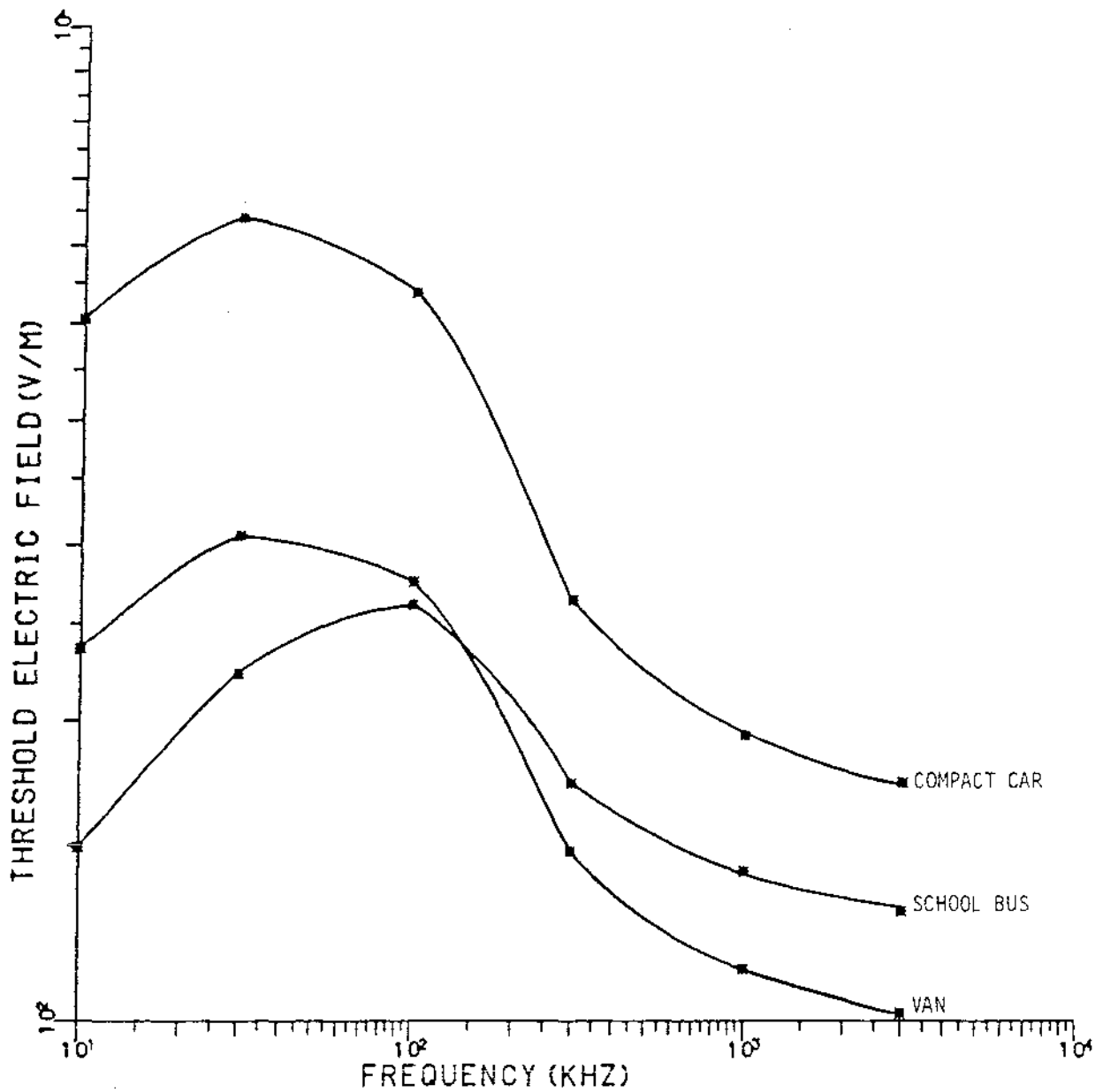
Figure 21. Average threshold electric field for pain for grounded adult females in finger contact with various vehicles. Contact area = 25 mm².
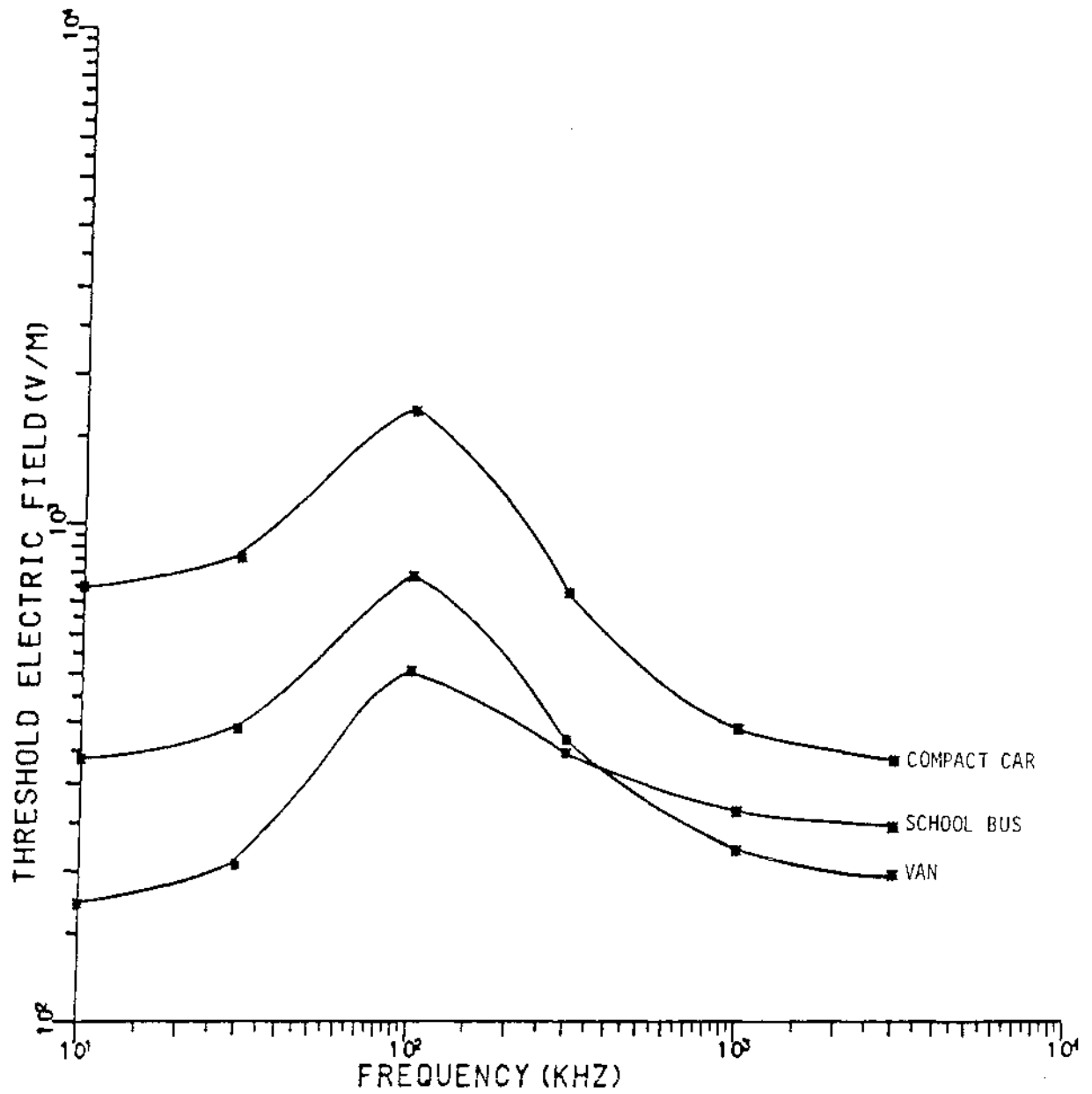
Figure 22. Average threshold electric field for perception for grounded adult females in grasping contact with various vehicles.

XI. THERMAL IMPLICATIONS OF HIGH RF CURRENTS IN THE BODY EXTREMITIES

As aforementioned, substantial RF currents may flow through the human legs or through the hand and wrist upon contact with large metallic objects for E-fields recommended by the ANSI C95.1-1982 RF safety guideline. These currents will result in high wet-tissue SARs in the body extremities such as the ankle and wrist sections. A study was conducted to determine the thermal implications of high RF currents in the ankle and wrist sections. The data generated as a result of this study have been submitted for possible publication to IEEE Transactions on Biomedical Engineering. The summary of the results is given in the following.

Surface temperature elevation of the wrist and the ankle sections were measured for a healthy human subject at room temperature (22-25° C) for a variety of RF currents and associated wet-tissue SARs for the frequency band 1-50 MHz. Rates of surface temperature increase in °C/min are given by the best-fit relationships: 0.0045 x SAR in W/kg for the ankle section and 0.0048 x SAR for the wrist section, the latter being involved for conditions of contact with ungrounded bodies like cars, trucks, fences, etc. Since wet-tissue ankle-section SARs on the order of 172-222 W/kg (see Figure 10) and wrist-section SARs as high as 1316[*] W/kg have previously been projected for E-fields recommended in the ANSI C95.1-1982 safety guide, fairly high rates of surface temperature increase are therefore anticipated. The deeper tissue temperatures may be even higher.

XII. COUPLING OF RF MAGNETIC FIELD TO THE HUMAN BODY

To obtain the SARs due to RF magnetic fields, we have developed a three-dimensional, 36,776-cell inhomogeneous model of man. This model is based on the anatomic cross sections of the human body [6] where each of the available sectional diagrams with spacings typically on the order of 23 to 27 mm were overlaid with a fine square mesh (Δ = 6.35 mm) and one of 14 tissue types

---

[*] Calculated for the projected current of 854 mA at 3 MHZ flowing through a wrist effective cross-sectional area of 11.1 cm^2.

representative of the predominant tissue in a given square was entered in the data base. The various tissues and the respective electrical properties [24] assumed for calculations at 30 MHz are given in Table 6. Thus the data associated with a particular layer consisted of three numbers for each square cell in the mesh: x and y positions relative to some anatomical reference point in this layer and an integer indicating which tissue the cell contained. The data were entered for each of the layers of the body for which the anatomical diagrams were available. Since these layers are somewhat variable in separations, a new set of equispaced layers with spacings of 6.35 mm were defined.

TABLE 6. TISSUE DIELECTRIC PROPERTIES AT 30 MHz

Tissue Type	Properties at 30 MHz	
	σ, S/m	ε_r
air	0.0	1.0
muscle	0.75	103.0
fat, bone	0.04	29.0
blood	0.30	100.0
intestine	0.30	60.0
cartilage	0.04	29.0
liver	0.52	130.0
kidney	0.80	200.0
pancreas	0.70	200.0
spleen	0.70	200.0
lung tissue*	0.50	100.0
heart	0.65	200.0
nerve, brain	0.46	150.0
skin	0.75	103.0
eye	0.46	150.0

* We used 33% lung tissue and 67% air for the lung properties.

This step was necessary since a regular grid network simplifies the computer software. The data were then redefined in a global (model) coordinate system, and this required an x-y shift for each of the original layers in order that the anatomical reference point for each layer would conform to the vertical contour of the body. The percentages of the tissues in a particular cubical cell of the final regularly spaced model ($\Delta = 6.35$ mm) were computed by using a linear interpolation of the original data. This process resulted in a data base of cell positions and percentages of 14 different tissue types of Table 1 for approximately 320,000 cells for torso alone. In order to reduce the number of cells for the present studies, a somewhat coarser model was needed. We have, therefore, volume-averaged the data for cells of dimensions 1.31 x 1.31 x 1.31 cm getting thereby the tissue percentages for each of the larger cells. The previously described impedance method [7] has been used for calculating the SARs due to an RF magnetic field at 30 MHz. A brief description of the impedance method is given in the following.

A. The Impedance Method

In this method applicable for the human body problem for quasi-static frequencies to about 40 MHz [22], the biological body is represented by a network of impedances whose values are obtained from the complex conductivities $\sigma + j\omega\varepsilon$ of the various regions of the body. To obtain the impedance network for the present calculations, the tissue percentages for each of the 36,776 cells are used to obtain the average electrical properties (σ, ε) for the individual cells. These are then used to obtain the various impedances from the expression

$$z_m^{i,j,k} = \frac{1/\Delta}{\sigma^{i,j,k} + j \omega \varepsilon^{i,j,k}} \tag{13}$$

where i, j, k indicates the cell index; m is the direction which can be x, y, or z; and $\sigma_m^{i,j,k}$ and $\varepsilon_m^{i,j,k}$ are the electrical properties of the i, j, k-th cell in the m-th direction. Even though isotropic electrical properties have been used for the present study, it should be recognized that directional

averaging of the electrical properties done at the stage of going from smaller to larger cells would have resulted in anisotropic properties for the cells -- a feature that is likely to be important in the VLF band of frequencies.

The effect of the RF magnetic field H is to set up emfs in the impedance loops of the model given from Faraday's law of induction by $j\omega \mu_o \vec{H}_n \Delta^2$ where $\vec{H}_n$ is the magnetic field normal to the plane of the loop of area Δ^2. The coupled equations for the various loops of the impedance network form a sparse linear system which may be solved efficiently for the unknown loop currents using successive overrelaxation [23]. A relaxation factor of 1.3 was found to be satisfactory for this problem. Once the loop currents are known, the currents which flow through the various elements of the impedance network are obtained by taking differences in currents for the loops that are common to that impedance element. The SAR for a given cell can then be computed from the expansion

$$SAR_{i,j,k} = \frac{1/2}{d_m \Delta^3} \text{Real} \left[\rho_x^{i,j,k} \left| J_x \right|^2 + \rho_y^{i,j,k} \left| J_y \right|^2 + \rho_z^{i,j,k} \left| J_z \right|^2 \right]$$

(14)

where $\rho_m^{i,j,k}$ is the complex resistivity of the cell, given by

$$\rho_m^{i,j,k} = \frac{1}{\sigma_m^{i,j,k} + j \omega \epsilon_m^{i,j,k}}$$

(15)

$\vec{J}$ is the current density for the cell and d_m is the average mass density of the tissues in the cell. For the present calculations, a mass density of 10^3 kg/m^3 has been assumed for all the cells of the body.

B. The Calculated SARs

SARs have been calculated for a uniform RF magnetic field of 1 A/m that is linearly polarized from front to back of the body at a frequency of 30 MHz. This polarization was selected since it couples the most power to the body on an averaged basis [24]. From our calculations we obtain a whole-body-averaged SAR of 0.0314 W/kg with a peak value of 0.693 W/kg at location (11, 9) in layer no. 38 (see Figure 23 for the layer numbering for the model). The

Layer Numbering Scheme
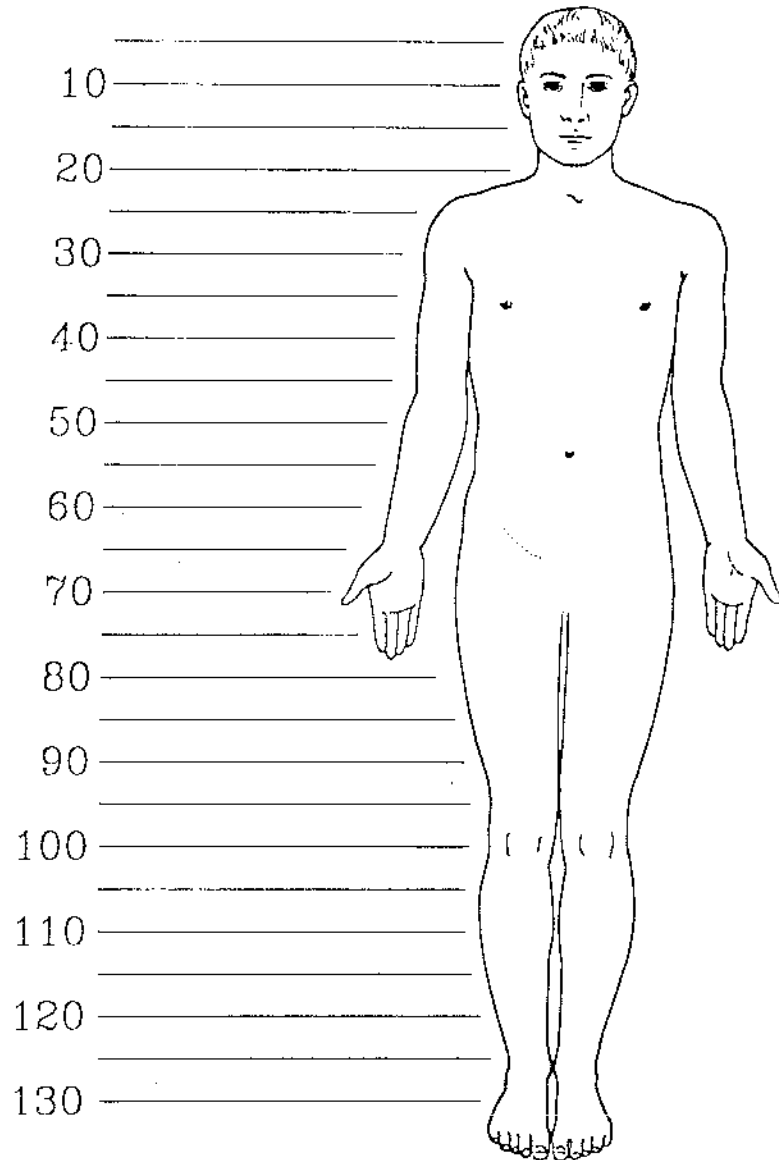
Figure 23. Layer numbering scheme used for the model of the human body. Each layer is 1.31 cm from its neighbors. Layer 1 is 0.655 cm from the top of the head.

whole-body-averaged SAR of 0.0314 W/kg for magnetic field alone appears to be reasonable as compared to the value of 0.0528 W/kg given in the dosimetry handbook [24] for a plane-wave irradiation of a homogeneous prolate spheroidal model of man at 30 MHz, H = 1 A/m.

The calculated homogeneous layer-averaged SARs for the human body are shown in Figure 24. Maximum layer-averaged SAR of 0.071 W/kg is calculated for layer no. 20 just below the neck (see Figure 23). The SAR distribution for layer no. 38 is shown in Figure 25. This is the section corresponding to the location of the peak SAR (693 mW/kg) in the body. In this figure it can also be noted that, as expected, the regions of highest current densities and SARs occur close to the surface, i.e., for largest distances from the center. From SAR one can calculate the local current density J from the relationship

$$ SAR = \frac{\sigma J^2}{d_m \left(\sigma^2 + \omega^2 \epsilon^2\right)} \tag{16} $$

We have scaled the SAR results obtained at 30 MHz to other frequencies in the band 0.1 to 100 MHz to obtain an estimate of the whole-body-averaged and peak SARs, and the peak current densities. The results are given in Table 7. In scaling the results up and down the frequency range, the induced currents are assumed to scale as f from Faraday's law of induction and SARs from Eq. 16 as $f^2 \cdot \sigma/\left(\sigma^2 + \omega^2\epsilon^2\right)$. The values of ($\sigma$, ϵ) corresponding to wet tissues [16] are also given in Table 7 for scaling from the calculated values at 30 MHz to other frequencies.

XIII. RECOMMENDATIONS FOR A RADIO-FREQUENCY PROTECTION GUIDE

A. For Occupational Exposures

The proposed radio-frequency protection guide (RFPG) is given in Table 8. We have used the information available in references 1 and 2 for the recommendations at higher radio frequencies. The proposed RFPG is plotted in Figure 26. Since higher E-fields proposed in Table 8 for the band 0.01-30 MHz, if these are vertical, would result in high RF induced currents and a

S. A. R. Average by Layer
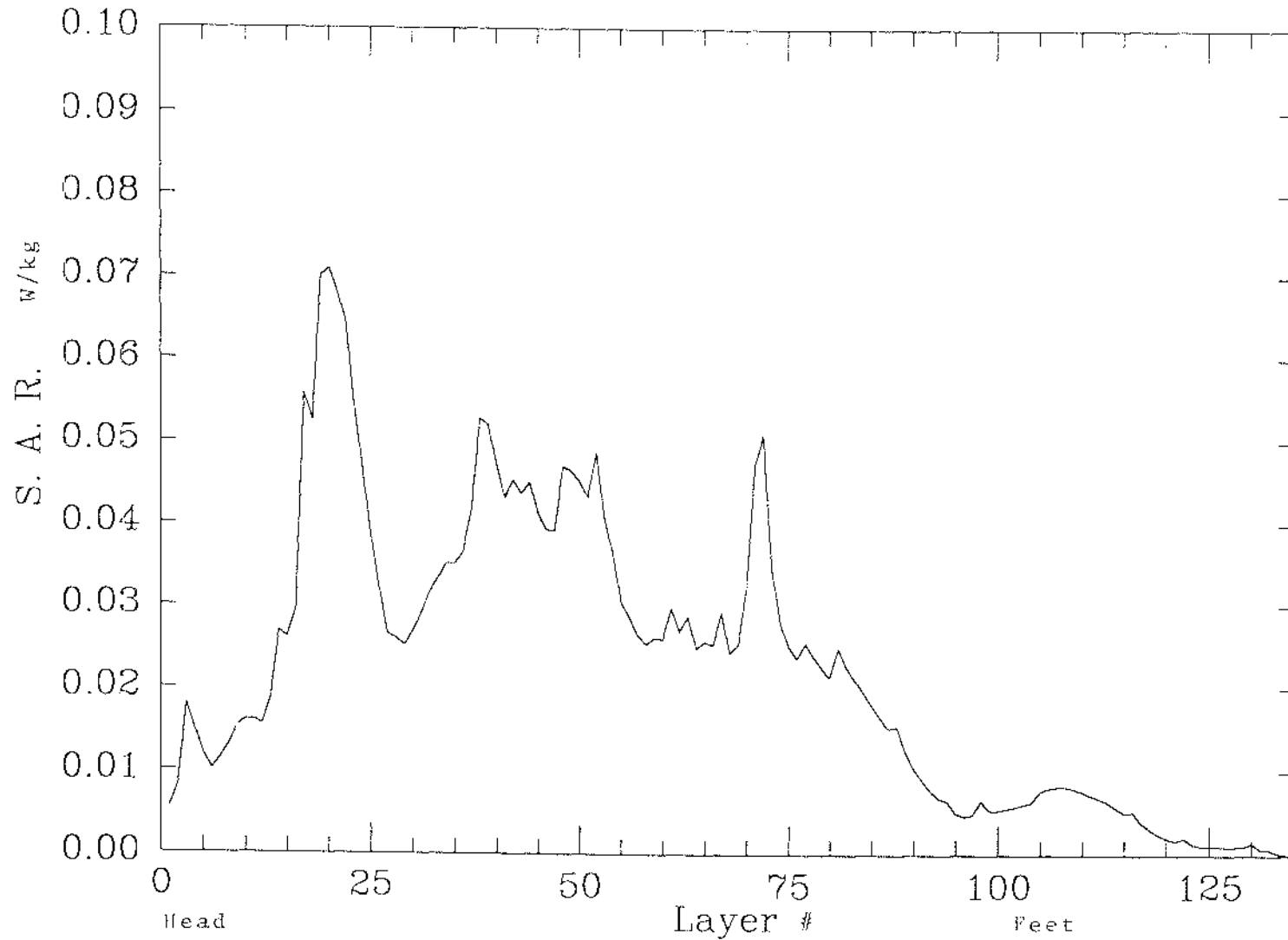
Figure 24. The layer-averaged SAR for a uniform RF magnetic field of 1 A/m at 30 MHz. The magnetic field is linearly polarized from front to back of the body. Layer numbers for the body are defined in Figure 23.

Layer 38   Average S. A. R.:0.527E-01   W/kg

```
24 | 0  0  0  0  0  0  0  0   0  0  0  0   0  0  0   0  0  0   0  0  0   0  0  0   0  0  0  0  0  0  0  0  0  0  0  0  0  0  0  0  0  0  0  0  0
23 | 0  0  0  0  0  0  0  0   0  0  0  0   0  0  0   0  0  0   0  0  0   0  0  0   0  0  0  0  0  0  0  0  0  0  0  0  0  0  0  0  0  0  0  0  0
22 | 0  0  0  0  0  0  0  0   0  0  0  0   0  0  0   0  0  0   0  0  0   0  0  0   0  0  0  0  0  0  0  0  0  0  0  0  0  0  0  0  0  0  0  0  0
21 | 0  0  0  0  0  0  0  0   0  0  0  0   0  0  0   0  0  0   2  4  2   2  2  2   1  2  4  4  3  0  0  0  0  0  0  0  0  0  0  0  0  0  0  0  0
20 | 0  0  0  0  0  0  0  0   0  0  0  0   0  0  0   0  4  6  12 17 13   9  3  4  10  6 19 20 11  6  5  0  0  0  0  0  0  0  0  0  0  0  0  0  0
19 | 0  0  0  0  0  0  0  0   0  0  0  0   0  0  0   8 21 29 42 24 13   7  4  4   4  8 16 26 40 81 29 13  9  0  0  0  0  0  0  0  0  0  0  0  0
18 | 0  0  0  0  0  0  0  0   0  0  0  0   0 12 35  49 51 36 24 16  8   4  3  4   8 16 27 36 45 79 85 24 10  0  0  0  0  0  0  0  0  0  0  0  0
17 | 0  0  0  0  0  0  0  0   0  0  0  0  11 37 58  85 50 39 22 16  7   3  1  2   6 12 23 38 60 88 113 83 22 0  0  0  0  0  0  0  0  0  0  0  0
16 | 0  0  0  0  0  0  0  0   0  0  0  0  24 131 98 63 40 32 23 14  8   3  1  1   4 10 18 34 51 76 116 126 96 13 0 0  0  0  0  0  0  0  0  0  0
15 | 0  0  0  0  0  0  0  0   0  0  0  0  42 120 94 55 38 29 24 13  8   3  0  0   3  7 16 26 44 67 98 140 143 50 0 0  0  0  0  0  0  0  0  0  0
14 | 0  0  0  0  0  1  0  0   0  0  0 18  46 88 59 52 40 27 21 14  8    4  1  0   2  5 12 24 38 60 87 132 172 54 10 0  0  0  3  1  0  0  0  0
13 | 0  0  0  0  4  3  2  0   2  1  0 49  73 158 56 42 37 30 19 16  7   4  1  0   1  3  9 18 33 53 79 122 168 85 83 30 5 3  3  8 11  4  0  0  0
12 | 0  0  0  5  9 12  4  3   9  8 95 91 124 76 46 76 26 39 23 16  8    3  1  0   0  2  7 15 28 46 72 113 153 125 370 108 34 11 9 23 27 19 3 0 0
11 | 0  0  0  8 27 19  5  3  19 46 398 196 151 88 105 66 32 23 11 7    4  5  1   1  0  1  4 12 24 41 69 102 159 90 546 337 84 18 12 28 53 34 10 0 0
10 | 0  0  0 17 32 18  7  6  28 211 432 381 153 104 88 78 44 60 27 11  5  2  1   1  1  0  3 10 21 37 59 95 151 118 618 261 90 20 18 28 57 39 15 0 0
 9 | 0  0  0 13 38 20 15  6  33 159 693 361 220 134 102 235 89 44 20 11 4  2  1  2  1  0  2  8 18 32 53 94 150 142 396 160 63 24 25 48 57 43 13 0 0
 8 | 0  0  0  6 24 22 13 12  30 74 283 186 141 157 103 83 65 65 31  8   2  2  1   2  1  0  1  6 17 27 48 96 157 86 344 80 47 28 26 44 51 18 6 0 0
 7 | 0  0  0  0  7 13 15  9  13  8 36 44 101 201 88 185 58 40 26 12    4  2  2   2  1  0  2  5 14 25 48 92 162 72 103 33 19 19 29 32 13 9 0 0 0
 6 | 0  0  0  0  3  4  5  3   2  1  0  0  50 200 190 95 119 40 39 18   8  6  2   3  3  1  2  5 15 28 50 105 114 42 24  0  3  5 10  7  7  0  0  0
 5 | 0  0  0  0  0  0  0  0   0  0  0  0  21 93 157 117 97 86 36 30 16 7 15  6   4  2  4  8 16 42 52 55 28 14  0  0  0  0  0  0  0  0  0  0  0
 4 | 0  0  0  0  0  0  0  0   0  0  0  0   0 25 55 54 56 55 37 29 19 10 10  7   6  3  3  4  9 10 14 12  3  0  0  0  0  0  0  0  0  0  0  0  0
 3 | 0  0  0  0  0  0  0  0   0  0  0  0   0  0  0  0 10 22 14 10  7   5  5  4   2  1  1  1  2  0  0  0  0  0  0  0  0  0  0  0  0  0  0  0  0
 2 | 0  0  0  0  0  0  0  0   0  0  0  0   0  0  0  0  0  0  0  0  0   0  0  0   0  0  0  0  0  0  0  0  0  0  0  0  0  0  0  0  0  0  0  0  0
 1 | 0  0  0  0  0  0  0  0   0  0  0  0   0  0  0  0  0  0  0  0  0   0  0  0   0  0  0  0  0  0  0  0  0  0  0  0  0  0  0  0  0  0  0  0  0
   ------------------------------------------------------------------------------------------------------------------------------------------
     1  2  3  4  5  6  7  8   9 10 11 12  13 14 15 16 17 18 19 20 21 22 23 24  25 26 27 28 29 30 31 32 33 34 35 36 37 38 39 40 41 42 43 44 45
```

Figure 25.   SARs in mW/kg for layer no. 38.   Note the position of the peak SAR of 693 mW/kg.   Radiation parameters are the same as in Figure 24.

TABLE 7. WHOLE-BODY-AVERAGED AND PEAK SARs SCALED FROM THE VALUES CALCULATED AT 30 MHz FOR AN ANATOMICALLY-REALISTIC MODEL OF A HUMAN BEING. A MAGNETIC FIELD OF 1 A/m ORIENTED FROM FRONT TO BACK OF THE BODY IS ASSUMED TO OBTAIN HIGHEST POSSIBLE SARs.

f_{MHz}	Wet tissue			Whole-body-averaged SAR W/kg	Peak Current Density mA/cm^2	Peak SAR W/kg
	σ S/m	$\dfrac{\varepsilon}{\varepsilon_o}$	$\dfrac{\sigma}{\sigma^2 + \omega^2 \varepsilon^2}$			
0.1	0.4	25000	2.231	5.22×10^{-7}	0.0072	11.5×10^{-6}
0.3	0.4	---	2.10 *	4.42×10^{-6}	0.022	9.75×10^{-5}
1.0	0.48	2000	1.977	4.62×10^{-5}	0.072	10.2×10^{-4}
3.0	0.5	---	1.761*	3.71×10^{-4}	0.216	8.19×10^{-3}
10.0	0.625	160	1.568	3.67×10^{-3}	0.72	0.081
30.0	0.612	113	1.492	0.0314	2.16	0.693
100.0	0.89	71.7	0.936	0.219	7.20	4.83

* Obtained by logarithmic interpolation.

TABLE 8. OCCUPATIONAL EXPOSURE RADIO-FREQUENCY PROTECTION GUIDES

Frequency Range (MHz)	E V/m	H A/m	Plane-Wave Equivalent Power Density (mW/cm^2)
0.01 - 0.1	* 614	163	---
0.1 - 3.0	* 614	16.3/f	---
3 - 30	* 1842/f	16.3/f	---
30 - 100	61.4	16.3/f	---
100 - 300	61.4	0.163	1.0
300 - 3000	$61.4 \, (f/300)^{1/2}$	$0.163 \, (f/300)^{1/2}$	f/300
3000 - 300,000	194	0.5	10.0

Note: f = frequency in MHz. E and H are the magnitudes of electric and magnetic fields, respectively.

* The personnel access areas should be restricted to limit induced RF currents as defined in the following.

potential for shock and burns for contact with ungrounded metallic bodies, the personnel access areas should be limited in the following manner:

1. For free-standing individuals (no contact with metallic bodies), RF current induced in the human body should be less than or equal to 100 mA as measured through both feet or 50 mA as measured through each of the feet. For a frequency of less than 100 kHz, the allowable induced current should be reduced as follows:

$$I = 1.0 \, f_{kHz} \qquad mA \qquad\qquad (17)$$

through both feet or one-half as much through each of the feet.
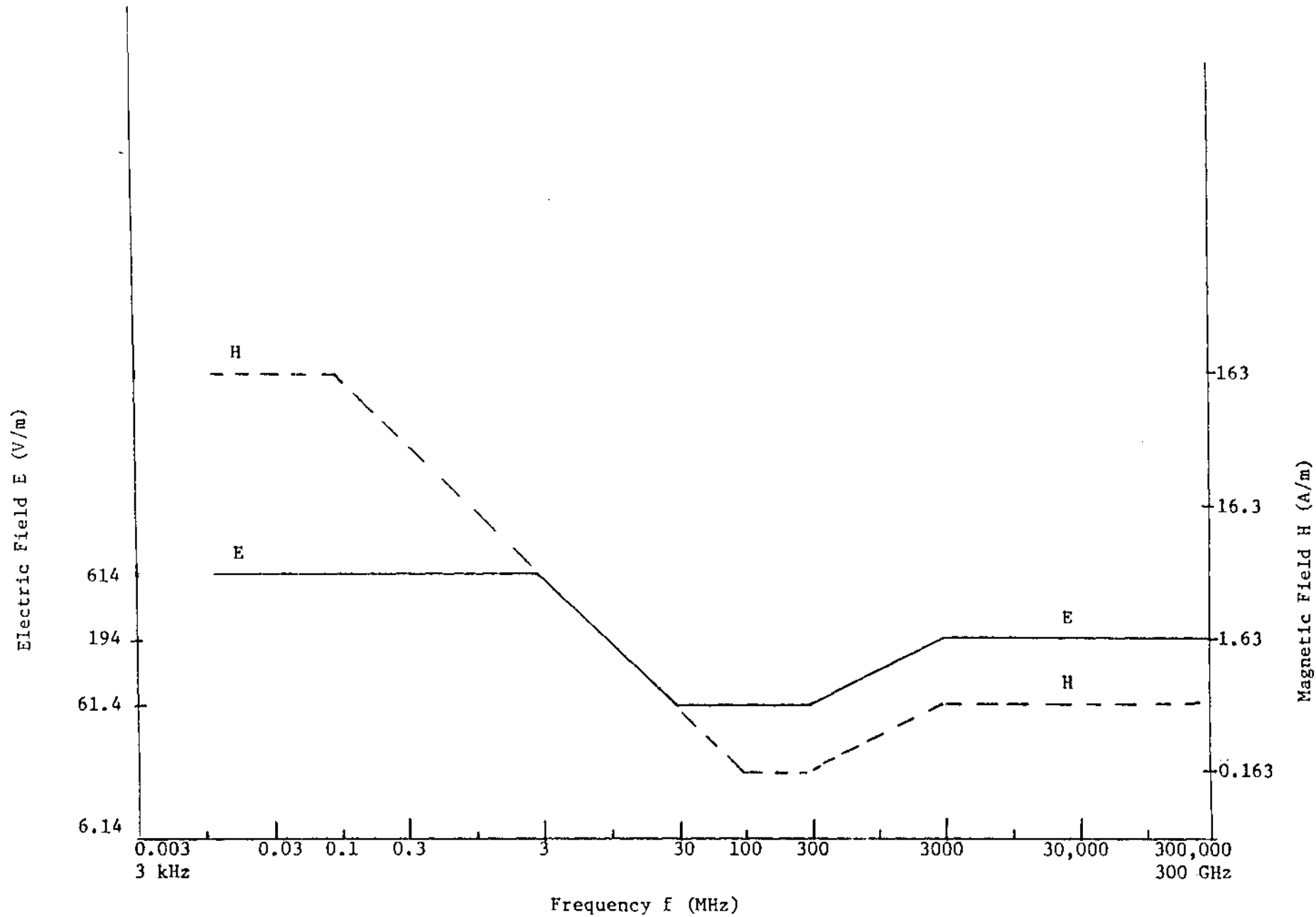
Figure 26. A proposed radio-frequency protection guide for occupational exposures.

The above limitations on RF induced currents are suggested to ensure that the ankle-section SARs for frequencies higher than 0.1 MHz will be no more than 5.8-10.7 W/kg for adults of heights 1.75-1.5 m. For frequencies lower than 100 kHz, the current densities in the ankle section will be slightly lower than those needed for stimulating thresholds for the nerve/muscle system [25].

For vertically-polarized electric fields, the above limitation on current would restrict the magnitude of the E-field to less than (300/f) V/m for frequencies in excess of 0.1 MHz (Section II).

2. For conditions of contact with metallic bodies, maximum RF current through an impedance equivalent to that of the human body for conditions of grasping contact (see Fig. 11), as measured with a contact current meter shall not exceed the following values

$$I = 0.5 \ f_{kHz} \qquad mA$$
$$\text{for} \qquad 10 \leqslant f < 100 \ kHz \qquad (18)$$

$$= 50 \ mA$$
$$\text{for} \qquad f > 0.1 \ MHz \qquad (19)$$

The current limits given by Eqs. 18 and 19 would help ensure that the current experienced by a human being upon contacting these metallic bodies would be less than that needed for perception or pain at each of the frequencies (Section X).

Steps such as grounding and use of safety equipment that result in reduced currents would obviously allow existence of higher fields without exceeding the above limits for conditions of contact with metallic bodies.

Significantly higher RF magnetic fields are recommended in the proposed RFPG of Table 8. For the frequency band 0.1-100 MHz, the RF magnetic field guideline is

$$H = \frac{16.3}{f} \quad A/m \tag{20}$$

For magnetic fields given by Eq. 20, the peak and whole-body-averaged SARs can be scaled from Table 7. These are given in Table 9 along with the peak internal current densities. A magnetic field orientation from front to back of the body is assumed for these calculations. This orientation was selected because of its strongest coupling to the human body.

TABLE 9. WHOLE-BODY-AVERAGED AND PEAK SARs FOR AN ANATOMICALLY-REALISTIC MODEL OF A HUMAN BEING FOR RF MAGNETIC FIELDS GIVEN BY EQ. 20. A MAGNETIC FIELD ORIENTATION FROM FRONT TO BACK OF THE BODY IS ASSUMED TO OBTAIN HIGHEST POSSIBLE SARs.

f_{MHz}	H A/m	Whole-body-Averaged SAR W/kg	Peak Current Density mA/cm^2	Peak SAR W/kg
0.1	163*	0.014	1.17	0.31
0.3	54.3	0.013	1.17	0.29
1.0	16.3	0.012	1.17	0.27
3.0	5.43	0.011	1.17	0.24
10.0	1.63	0.010	1.17	0.22
30.0	0.54	0.009	1.17	0.20
100.0	0.16	0.006	1.17	0.13

* A magnetic field of 163 A/m corresponds to a magnetic flux of 2.05 gauss in the gaussian system of units.

For frequencies less than 0.1 MHz, an RF magnetic field of 163 A/m implies a peak current density ≤ 0.0117 f_{kHz} mA/cm^2 where the frequency f_{kHz} is in kHz, which is considerably lower than the threshold of perception of currents at these frequencies (see Figure 13).

B. For General Public

The proposed RFPG for the general public is given in Table 10 and is plotted in Figure 27.

TABLE 10. RADIO-FREQUENCY PROTECTION GUIDES FOR GENERAL POPULATION

Frequency Range MHz	E V/m	H A/m	Plane-wave Equivalent Power Density mW/cm^2
0.01 – 0.1	(a) 61.4*	163	---
0.1 – 1.0	(a) 61.4*	16.3/f	---
1.0 – 3.9	(a) 61.4†	16.3/f	---
3.9 – 30	(b) 240/f†	16.3/f	---
30 – 100	(c) 8†	16.3/f	---
100 – 5,900	0.8f$^{1/2\dagger}$	0.163	---
5,900 – 300,000	61.4	0.163	(d) 1.0

The frequency f is in MHz. E and H are the magnitudes of electric and magnetic fields, respectively. Explanation for (a)-(d) is given below.

* spatially-averaged over a volume corresponding to that of an automobile.
$\dagger$ spatially-averaged over a volume corresponding to that of a human being.

(a) The electric field E suggested for these frequency bands is lower than the threshold of perception of commonly encountered metallic bodies such as a car, a van, etc. It is, however, close to the threshold of perception for finger contact of a school bus by a child (see Figure 17).

(b) For the E-field suggested here, the current induced in a free-standing (no contact with metallic bodies) human being is less than or equal to 100 mA (one leg current = 50 mA), which is consistent with the access area limitation for occupational exposures.

(c) An incident electric field of 8 V/m implies the following for maximum induced currents and ankle-section SARs.
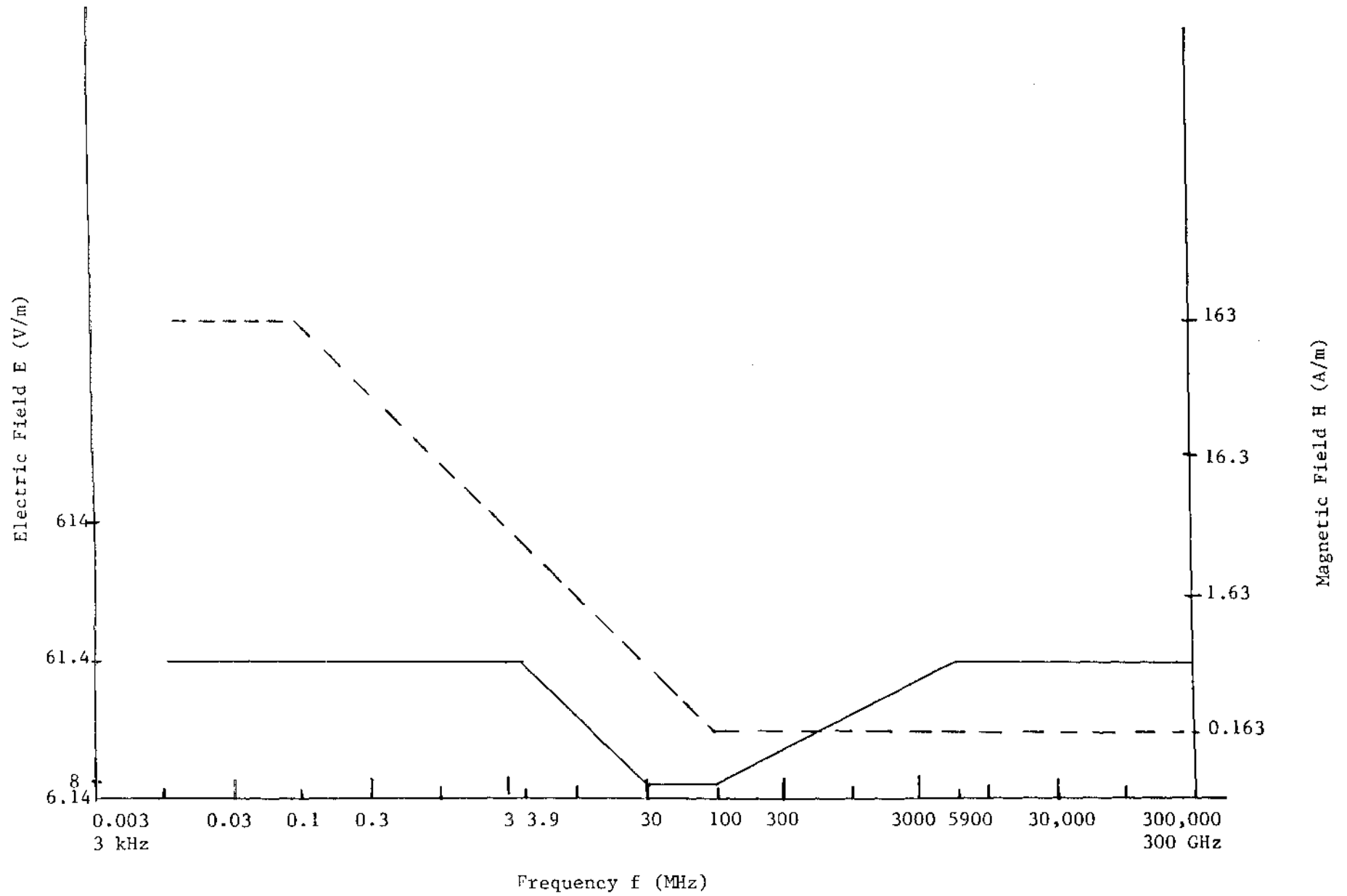
Figure 27. Radio-frequency protection guide for the general population.

TABLE 11. INDUCED CURRENTS AND ANKLE-SECTION SARs FOR AN INCIDENT E-FIELD OF 8 V/m (SCALED FROM TABLE 4).

	Height m	Frequency MHz	I_h mA	Ankle-section SAR[*] W/kg
Average adult	1.75	40.0	101.6	3.8
Adult	1.5	46.7	87.2	5.0
10-year-old child	1.38	50.7	80.1	5.6
5-year-old child	1.12	62.5	65.0	7.8

[*] We have assumed a conductivity of 0.693 S/m for the high-water-content tissues at 40 and 46.7 MHz [16]. Somewhat larger conductivities of 0.73 and 0.77 S/m are taken at 50.7 and 62.5 MHz, respectively. The corresponding dielectric constants taken are 97.3 for 40 and 46.7 MHz and 92.9 and 87.4 for 50.7 and 62.5 MHz, respectively.

(d) At higher frequencies, a power density of 1 mW/cm^2 is suggested to prevent threshold of perception of warmth [26]. Also the suggested power density of 1 mW/cm^2 is consistent with the recently proposed NCRP guideline for the general population.

The knowledge on the coupling of spatially nonuniform electromagnetic fields to the human body is grossly inadequate though some initial work along these lines was previously done in our laboratory [4,8]. It is recommended that the E-fields for the frequency band 0.01-100 MHz be considerably lowered because of the RF induced currents and the potential for contact hazards. It is felt, however, that a volume averaging of the E-fields may be quite appropriate. For noncontact situations where the concern is primarily that of RF induced currents for the frequency band 1-100 MHz, an incident E-field spatially-averaged over the volume of the human body should not exceed the values given in Table 10. For the lower frequencies the concern is primarily that of contact hazards due to instantaneous flow of large currents upon touching ungrounded metallic bodies. An incident E-field spatially-averaged

over a volume corresponding to that of an automobile should not exceed the values suggested for the frequency band 0.01-1.0 MHz.

Very little information is presently available on the relationship of biological effects with the peak values of pulsed fields. It is suggested, therefore, that the instantaneous peak values of the E- and H-fields not exceed 100 times the limits given in Tables 8 and 10 at the corresponding frequencies [3]. Similar to the ANSI guideline [1] for intermittent exposures, the fields time-averaged over any 6-minute period should not exceed the limits given in Tables 8 and 10.

In situations where simultaneous exposure occurs from a number of sources at different frequencies, the exposure should be measured at each frequency and expressed as a fraction of the E and H limits at the corresponding frequencies (from Table 8 or 10, whichever is appropriate). The sum of the squares of these fractions should not exceed unity.

XIV. COMPARISON OF THE RECOMMENDED RFPGs WITH STANDARDS AT OTHER FREQUENCIES

From Eq. 18, the suggested limit on the contact current is 1.5 mA at 3 kHz. This may be compared with the National Electric Safety Code [27] which specifies a maximum leakage current of 0.5 mA from portable electrical tools and household appliances and 0.75 mA for permanently fixed appliances. Recognizing that the threshold current for perception at 3 kHz is approximately 3 times higher than that at 60 Hz [28], a suggested contact current of 1.5 mA is not out of line with the leakage current of 0.5-0.75 mA specified in the National Electric Safety Code.

For higher RF frequencies, the suggested guideline of 10 mW/cm^2 for occupational exposures is in agreement with the occupational standard for infrared radiation, while a reduced guideline of 1 mW/cm^2 (see Table 10) is consistent with the recently proposed NCRP guideline for the general population.

XV. SOME AREAS RECOMMENDED FOR FURTHER WORK

As aforementioned, the knowledge on the coupling of spatially nonuniform electromagnetic fields to the human body is grossly inadequate. Recognizing

this inadequacy, we have, in the past, examined the coupling of cosinusoidally varying E-fields in the VHF band to a 180-cell inhomogeneous block model of man and have obtained an empirical equation that gives the reduced SAR vis a vis that for uniform or plane-wave exposures [4,8]. Because of the tremendous advances in the field since this early work, additional work, both experimental and theoretical, could and should be undertaken to examine the issue in greater detail and to obtain a valid way of interpreting the spatially variable fields that are the norm in real-life situations. New numerically-efficient procedures based on a high-resolution (40,000 cells) anatomically-realistic model of man have recently been developed [29-31] that may be useful for these studies.

Since the proposed RFPGs rely upon the limits of currents through the body for contact as well as free-field (no large metal objects) conditions, portable instrumentation is needed to validate that the limiting currents are not exceeded. We have fabricated a 1/8"-thick bilayer current sensor in the form of a shoe insert. The current induced in the body passes through this sensor to the ground. An RF diode is used to rectify this current which is then displayed on a digital display. Either instantaneous or six-minute-averaged current can be displayed from this portable, operator-mounted unit. With further work and detailed testing, this unit could be perfected for applications in this area. The detailed testing must also include the measurements of induced currents for spatially nonuniform fields both in the context of occupational as well as general population exposures. Such measurements are needed to validate the concept of volume-averaging of the fields and to examine if the greatly reduced E-fields suggested for the general population are justified. An RF current meter with an impedance corresponding to the average impedance for the humans under grasping contact conditions (see Figure 11) could similarly be used to validate the proposed concept of volume-averaging of E-fields for contact situations. Such a meter could eventually be used to ascertain that the proposed current limits under contact conditions are not exceeded.

To be consistent on the SAR basis, significantly higher RF magnetic fields have been suggested in the proposed RFPGs for the occupational as well as general population exposures. Some recent, albeit unconfirmed, reports

have alluded to the biological effects of low RF magnetic fields. Further work is definitely in order to examine the validity of the claimed biological effects due to RF magnetic fields. Last, but not least, one needs to study the biological effects of exposure to RF currents of the proposed current densities in the VLF to VHF range of frequencies. Implicit in the current-limited guidelines of Tables 8 and 10 are current densities at the extremities as high as 5.3-8.4 mA/cm^2. It may be appropriate to study the effects of RF currents on blood, bone marrow, and other relevant biological media.

REFERENCES

1. ANSI C95.1-1982. American National Standard — safety levels with respect to human exposure to radio-frequency electromagnetic fields, 300 kHz to 100 GHz. IEEE, New York.

2. ACGIH. Threshold limit values for physical agents. American conference of governmental industrial hygienists, Cincinnati, Ohio (1981).

3. IRPA. Interim guidelines on limits of exposure to radio-frequency electromagnetic fields in the frequency range from 100 kHz to 300 GHz. Health Physics 46:975-984 (1984).

4. Gandhi, O. P., J. Y. Chen, and A. Riazi. Currents induced in a human being for plane-wave exposure conditions 0-50 MHz and for rf sealers. IEEE Trans Biomed Eng BME-33:757-767 (1986).

5. Chatterjee, I., D. Wu, and O. P. Gandhi. Human body impedance and threshold currents for perception and for contact hazard analysis in the VLF-MF band. IEEE Trans Biomed Eng BME-33:486-494 (1986).

6. Eycleshymer, A. C., and D. M. Shoemaker. A cross-section anatomy. New York:D. Appleton Co., 1911.

7. Gandhi, O. P., J. F. DeFord, and H. Kanai. Impedance method for calculation of power deposition patterns in magnetically induced hyperthermia. IEEE Trans Biomed Eng BME-31:644-651 (1984).

8. Chatterjee, I., M. J. Hagmann, and O. P. Gandhi. An empirical relationship for electromagnetic absorption in man for near-field exposure conditions. IEEE Trans Microwave Theory Tech MTT-29:1235-1238 (1981).

9. Gandhi, O. P., I. Chatterjee, D. Wu, and Y. G. Gu. Likelihood of high rates of energy deposition in the human legs at the ANSI-recommended 3-30 MHz rf safety levels. Proc IEEE 73:1145-1147 (1985).

10. Deno, D. W. Currents induced in the human body by high voltage transmission line electric field – measurement and calculation of distribution and dose. IEEE Trans Power Apparatus and Systems PAS-96:1517-1527 (1977).

11. Hill, D. A., and J. W. Walsh. Radio-frequency current through the feet of a grounded human. IEEE Trans Electromagnetic Compatibility EMC-27:18-23 (1985).

12. Tell, R., E. D. Mantiply, C. H. Durney, and H. Massoudi. Electric and magnetic field intensities and associated induced body currents in close proximity to 50 KW AM standard broadcast station. To be published in IEEE Trans Broad.

13. Guy, A. W., and C. K. Chou. Hazard analysis: very low frequency through medium frequency range. Final report USAF SAM contract F33615-78-D-0617 Task 0065 (February 1982).

14. Gronhaug, K. L., and O. Busmundrud, Antenna effect of the human body of EMP (in Norwegian). Rep. FFI/NOTAT-82/3013, Norwegian Defense Research Establishment, P.O. Box 25-N-2007, Kjeller, Norway.

15. Gandhi, O. P., E. L. Hunt, and J. A. D'Andrea. Deposition of electromagnetic energy in animals and in models of man with and without grounding and reflective effects. Radio Science 12 (6S):39-47 (November/December 1977).

16. Johnson, C. C., and A. W. Guy. Nonionizing electromagnetic wave effects in biological materials and systems. Proc IEEE 60:692-718 (1972).

17. Gandhi, O. P., and I. Chatterjee. Radio-frequency hazards in the VLF to MF band. Proc IEEE 70:1462-1464 (1982).

18. Gandhi, O. P., I. Chatterjee, D. Wu, J. A. D'Andrea, and K. Sakamoto. Very low frequency (VLF) hazard study. Final report on contract no. F33615-83-C-0613, submitted to USAF School of Aerospace Medicine, Erooks Air Force Base, Texas 78235 (March 1985).

19. Deno, D. W. Calculating electrostatic effects of overhead transmission lines. IEEE Trans Power Apparatus and Systems PAS-93:1458-1471 (1974).

20. Deno, D. W., and L. E. Zaffanella. Electrostatic and electromagnetic effects of ultra-high voltage transmission lines. Report prepared for Electric Power Research Institute, Palo Alto, CA (June 1978).

21. Reilly, J. P. An approach to the realistic case analysis of electric field induction from AC transmission lines. Presented at the 3rd Int Symp High Voltage Engineering, Milan, Italy (August 1979).

22. DeFord, J. F., and O. P. Gandhi. Calculation of three-dimensional patterns for rf hyperthermia. To be published.

23. Ralston, A., and P. Rabinowitz. A first course in numerical analysis. New York:McGraw-Hill Book Company, 232-238 (1978).

24. Durney, C. H., et al. Radio-frequency radiation dosimetry handbook (2nd edition). US Air Force School of Aerospace Medicine SAM-TR-78-22 (1978).

25. Bernhardt, J. H. Evaluation of human exposures to low frequency fields. AGARD lecture series no. 138, The impact of proposed radio-frequency radiation standards on military operations:8-1 to 8-18, available from NATO Advisory Group for Aerospace Research and Development (AGARD), 7 Rue Ancelle 92200 Neuilly Sur Seine, France.

26. Gandhi, O. P., and A. Riazi. Absorption of millimeter waves by human beings and its biological implications. IEEE Trans Microwave Theory Tech MTT-34:228-235 (1986).

27. National Electrical Safety Code, 1977 Edition, ANSI C2, published by the Institute of Electrical and Electronics Engineers, Inc., New York.

28. Dalziel, C. F., and T. H. Mansfield. Effect of frequency on perception currents. AIEE Trans:1162-1168 (1950).

29. Gandhi, O. P., and J. F. DeFord. Calculation of EM power deposition for operator exposure to rf induction heaters. IEEE Trans Electomagnetic Compatibility EMC-29 (1987).

30. Sullivan, D. M., D. T. Borup, and O. P. Gandhi. Use of the finite-difference time-domain method in calculating EM absorption in human tissues. IEEE Trans Biomed Eng BME-34:148-157 (1987).

31. Sullivan, D. M., O. P. Gandhi, and A. Taflove. Use of the finite-difference time-domain method in calculating EM absorption in man models. IEEE Trans Biomed Eng BME-34 (1987).

APPENDIX A

THERMAL IMPLICATIONS OF HIGH SARs IN THE BODY EXTREMITIES
AT THE ANSI RECOMMENDED MF-VHF SAFETY LEVELS[*][§]

Jin-Yuan Chen and Om P. Gandhi
Department of Electrical Engineering
University of Utah
Salt Lake City, Utah 84112

Abstract

Surface temperature elevation of the wrist- and the ankle-sections
were measured for a healthy human subject at room temperature (22-25° C)
for a variety of RF currents and SARs in the frequency band 1-50 MHz.
The observed highest rates of temperature increase in °C/min are given
by the best-fit relationships: 0.0045 x SAR in W/kg for the ankle-
section and 0.0048 x SAR for the wrist-section, the latter being
involved for conditions of contact with ungrounded bodies like cars,
trucks, fences, etc. Since ankle-section SARs on the order of 182-243
W/kg and wrist-section SARs as high as 1045 W/kg have previously been
projected for the E-fields recommended in the ANSI C95.1-1982 safety
guide, fairly high rates of temperature increase are therefore
anticipated.

LIST OF TABLE AND FIGURE CAPTIONS

THERMAL IMPLICATIONS OF HIGH SARs IN THE BODY EXTREMITIES
AT THE ANSI RECOMMENDED MF-VHF SAFETY LEVELS

Introduction

The radio-frequency radiation (RFR) standards suggested [1,2] by
the American National Standards Institute (ANSI), the American Confer-
ence of Governmental Industrial Hygienists (ACGIH) and, more recently,
by standards-setting groups elsewhere (Canada, IRPA, Australia, etc.),
have relied on the knowledge of whole-body-average specific absorption
rate (SAR). This knowledge has led to recommendations that the allowed
power density can be increased in proportion to the square of the fre-
quency from 1 mW/cm^2 (E = 61.4 V/m) for frequencies below 30 MHz.
Recognizing that if the exposure limits were allowed to increase without
limit at lower frequencies, potential hazards could exist for shock and
burn, an upper bound of 100 mW/cm^2 (E = 614 V/m) has been recommended
for the region 0.3-3.0 MHz.

We have shown [3,4] that vertically polarized incident plane waves
are capable of inducing fairly significant RF currents in a human being
standing on a ground plane. Foot currents on the order of 627 mA with a
value peaking at 780 mA at 40 MHz have been projected for a 1.75 m tall
barefoot human being for the electric fields recommended in the ANSI
C95.1-1982 RF Safety Guide. There is only a marginal reduction in these
currents with the use of footwear particularly at the VHF frequencies
[4]. As these currents flow through the small cross section, highly
bony regions like the ankle section, fairly high current densities
result, with an SAR in high-water-content tissues estimated to be on the

order of 182 W/kg for the frequency band 3-30 MHz, increasing to a still higher value of 243 W/kg for E = 61.4 V/m (1 mW/cm^2) at 40 MHz. Using electromagnetic scaling concepts, the corresponding ankle-section SARs as high as 371 and 534 W/kg have been projected for ten- and five-year-old children, respectively, for f = 50.7 and 62.5 MHz. Fairly large RF currents flowing through the body have also been projected for a human in either touching or grasping contact with commonly encountered ungrounded bodies such as a car, a truck, a fence, etc. [5-7]. As an example, we estimate that a current of 879 mA will flow through the human hand holding an automobile van parked in the ANSI-recommended electric field of 614 V/m at a frequency of 3 MHz. This will produce an SAR in the high-water-content tissues of the wrist of about 1045 W/kg.

In this paper, the data are given on the surface temperature elevation of the ankle-section and the wrist for a healthy human subject at room temperature (22-25°C). Different rates of heating were observed for the various locations at the surface for both the ankle- and wrist-sections. Most of the data were, therefore, obtained for the locations where the highest rates of heating were observed; namely, at the front of the leg and at the inside of the wrist. Rates of heating for these points are given for a variety of RF currents and the concomitant estimated high-water-content tissue SARs in the frequency band 1-50 MHz. Best-fit relationships are obtained for the rates of temperature rise $\Delta T/\Delta t$ in °C/min. These are: $\Delta T/\Delta t = 0.0045$ x SAR for the ankle-section and $\Delta T/\Delta t = 0.0048$ x SAR for the wrist-section, where the SAR is in W/kg. Substantial rates of surface temperature increase are therefore implied for the SARs that have been projected for the ANSI-

recommended safety levels. It should be recognized that internal tissue temperatures may be still higher, leading one to question the safety of the so-called safety guideline.

Experimental Procedures and SAR Calculations

For ankle-section measurements, a copper tape (6 cm wide x 0.8 mm thick) was wrapped around the lower leg as one of the electrodes while the other electrode was provided by a wide area (1.2 x 2.4 m) aluminum sheet under the foot. The subject wore his normal shoe, which in this case was a rubber-soled shoe. The current passing through the foot was measured using a bilayer current sensor similar to the one described in our earlier paper [4]. This current sensor was made of a 6 mm-thick, 21 x 32 cm polyethylene sheet clad on both sides with copper. The current from the upper sheet on which the subject's foot was placed passed to the lower plate through a relatively noninductive carbon resistor (nominal value = 5 Ω) placed at the center of the bilayer sensor. The impedance Z of the resistor in this setting was measured and is given in Table 1 for each of the experimental frequencies. RF voltage V across the resistor was measured using a Fluke model 8060A digital multimeter (with model 85 RF high-frequency probe), and used to calculate the current $I = |V|/|Z|$. The currents thus obtained were compared with a direct measurement of RF current using Tektronix P 6042 current probe (0 - 50 MHz) together with a Tektronix 7603 oscilloscope. For these measurements a single-foot current sensor was fabricated and used. This also is a bilayer sensor of two copper sheets of dimensions 8 x 21 cm with a separating layer of 2.5 cm thick styrofoam. The current path

Table 1. Impedance Z of the current
sensor at various fre-
quencies.*

Frequencies MHz	Z Ohms
3.0	5.5 $\angle +5°$
5.0	5.5 $\angle +8°$
10.0	5.7 $\angle +14°$
27.12	6.85 $\angle +34°$
40.68	8.0 $\angle +43°$
50	8.9 $\angle +47°$

* Inductive component of the measured impedance is due primarily to the inductance of the coaxial connector (Amphenol 31-10) and of the connecting lead.

between the two plates was provided by means of a shorting copper conductor around which the probe P 6042 could be looped for current measurements. For frequencies to 40.68 MHz, the currents calculated using Fluke multimeter were within 5 percent of those obtained with Tektronix current probe. Because of the simplicity of the direct-reading Fluke multimeter, this instrument was used in all further experiments. The surface temperatures for the various locations of the ankle-section were measured using a semiconductor fiberoptic temperature probe [8] that was taped with a thin plastic tape at the respective locations to provide good contact with the body.

A similar procedure was followed for the wrist-section measure-

ments where the current passed from the copper armband, wrapped around the forearm just below the elbow, through the hand placed on the bilayer current sensor back to the RF power source. The power sources used to create the RF currents at the various frequencies were: 1. General Radio Type 1330-A bridge oscillator connected to a Krohn-Hite model BR7500 amplifier for power at 1 MHz; 2. A 100 W Kenwood model TS 4305 transreceiver (1.8-30 MHz) for frequencies between 3 and 27.12 MHz; and 3. MCL RF power generator model 15122 for 30 MHz and above.

To estimate SARs in the various tissue types, we proceed as follows. The total current I_t is assumed to be distributed as the inverse of the impedances Z_i. For the i-th tissue of area A_i,

$$Z_i = \frac{\ell}{(\sigma_i + j\omega\epsilon_i) A_i} \tag{1}$$

$$I_i = \frac{I_t \frac{1}{Z_i}}{\sum_i \frac{1}{Z_i}} = \frac{I_t (\sigma_i + j\omega\epsilon_i) A_i}{\sum_i (\sigma_i + j\omega\epsilon_i) A_i} \tag{2}$$

$$E_i = \frac{J_i}{\sigma_i + j\omega\epsilon_i} = \frac{I_t}{\sum_i (\sigma_i + j\omega\epsilon_i) A_i} \tag{3}$$

$$SAR\bigg|_i = \frac{\sigma_i E_i E_i^*}{\rho_i} = \frac{|I_t|^2 \sigma_i}{\rho_i \sum_i (\sigma_i^2 + \omega^2 \epsilon_i^2) A_i^2} \tag{4}$$

where σ_i and ϵ_i are the conductivity and permittivity of the
                    i-th tissue at frequency ω in radians/s

- 5 -

ℓ is the length of the section of the leg

$J_i = I_i/A_i$ is the current density per unit area in the i-th tissue

ρ_i = mass density of the i-th tissue.

From Eq. 4, it is clear that the highest SAR occurs in high-water-content tissues with the highest conductivity. For these tissues a mass density of 10^3 kg/m^3 is assumed. For the SAR calculations in this paper, we have looked at the anatomy of the ankle- and wrist cross-sections and have cataloged the tissues into one of three broad categories: 1. Area A_c, conductivity σ_c of the high-water-content, high-conductivity tissues like muscle, blood, skin, etc.; 2. Area A_m, conductivity σ_m of medium conductivity tissues like red marrow; and 3. Area A_ℓ, conductivity σ_ℓ of the low-water-content tissues like bone, fat, tendon, etc. The areas A_c, A_m, A_ℓ estimated from the anatomical cross section of the ankle [9] are, respectively, 11.75, 20.25 and 68 percent of the total cross-sectional area A_T. The corresponding subareas estimated from the anatomical diagram of the cross-section of the wrist [10] are: 31.2, 14.0 and 54.8 percent of the total cross-section for the high, medium, and low conductivity tissues, respectively. For the experimental subject, the total areas for the ankle- and wrist-sections were measured to be 40 and 23.7 cm^2, respectively. The conductivities σ_c, σ_m, and σ_ℓ, and the dielectric constants ϵ_c, ϵ_m, and ϵ_ℓ taken at the various frequencies are given in Table 2 [11,12].

Table 2. Conductivities for the various tissues
at different frequencies [11,12].

f_{MHz}	σ_c S/m	ε_c	σ_m S/m	ε_m	σ_ℓ S/m	ε_ℓ
1.0	0.4	2000	0.22	100	0.03	20
3.0	0.45	1600	0.22	74	0.03	20
5.0	0.50	1200	0.22	63	0.03	20
10.0	0.625	160	0.22	40	0.03	20
27.12	0.612	113	0.27	32	0.03	20
40.68	0.693	97.3	0.27	27	0.03	14.6
50.0	0.722	93	0.27	25	0.03	13.4

Surface Temperature Elevation of the Ankle-
and Wrist-Sections Due to RF Current Flow

It was recognized that surface temperature elevations along the circumference of the ankle- and wrist-sections may be nonuniform, both on account of the inhomogeneous SAR distribution as well as different thermal conductivities of the tissues. The skin over the ankle, for example, is not likely to get heated as fast on account of the low thermal conductivity bony region just underneath. Experiments were performed to obtain surface temperature elevations at four representative points each for the ankle- and wrist-sections. The data are shown in Figs. 1 and 2, respectively. For the ankle-section the rates of heating are fairly comparable for points 1 and 2 at the front and back
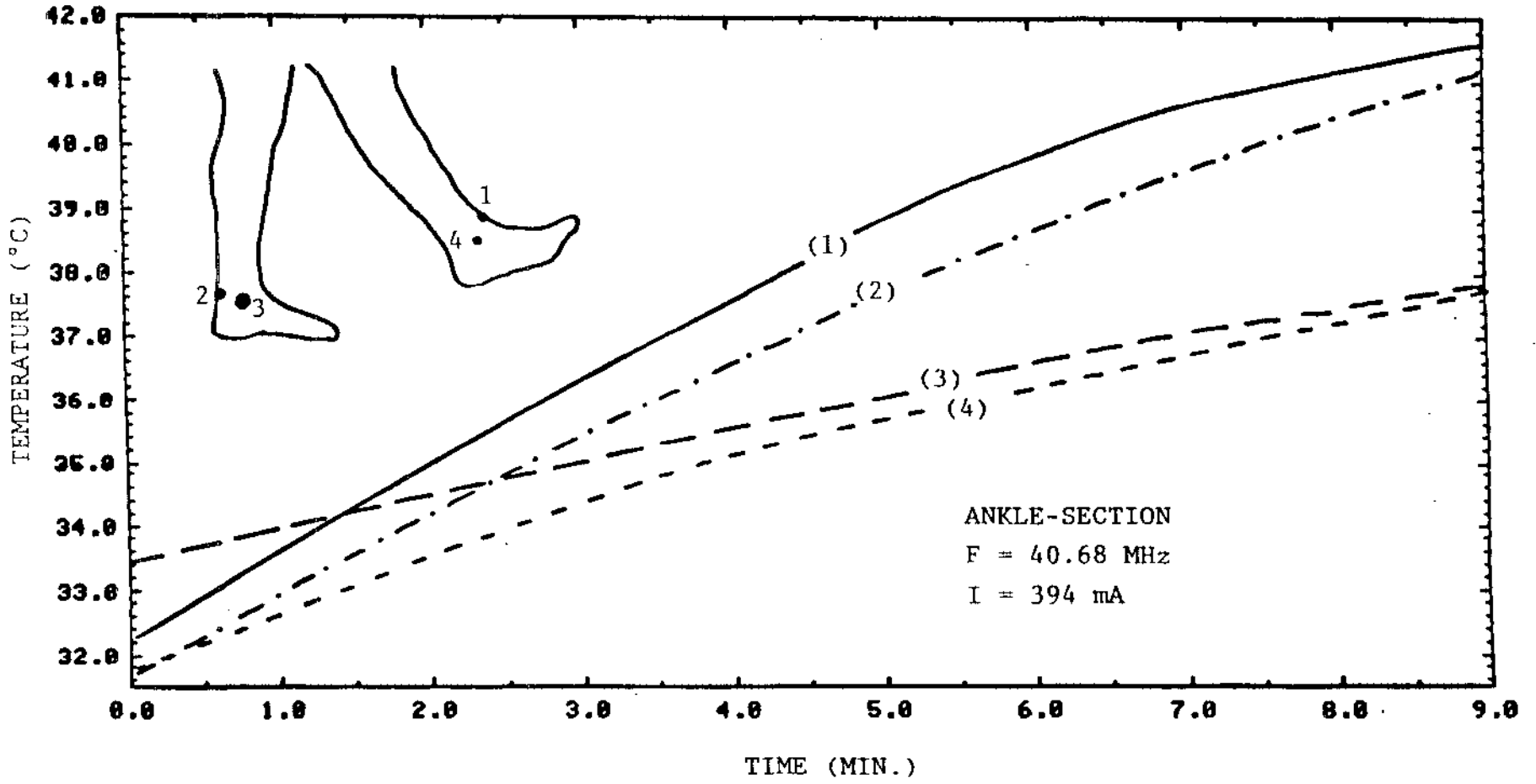
Fig. 1. Temperature of several locations at the surface of the ankle-section under condition of RF current through the leg. Estimated SAR in high-water-content tissues = 239 W/kg.
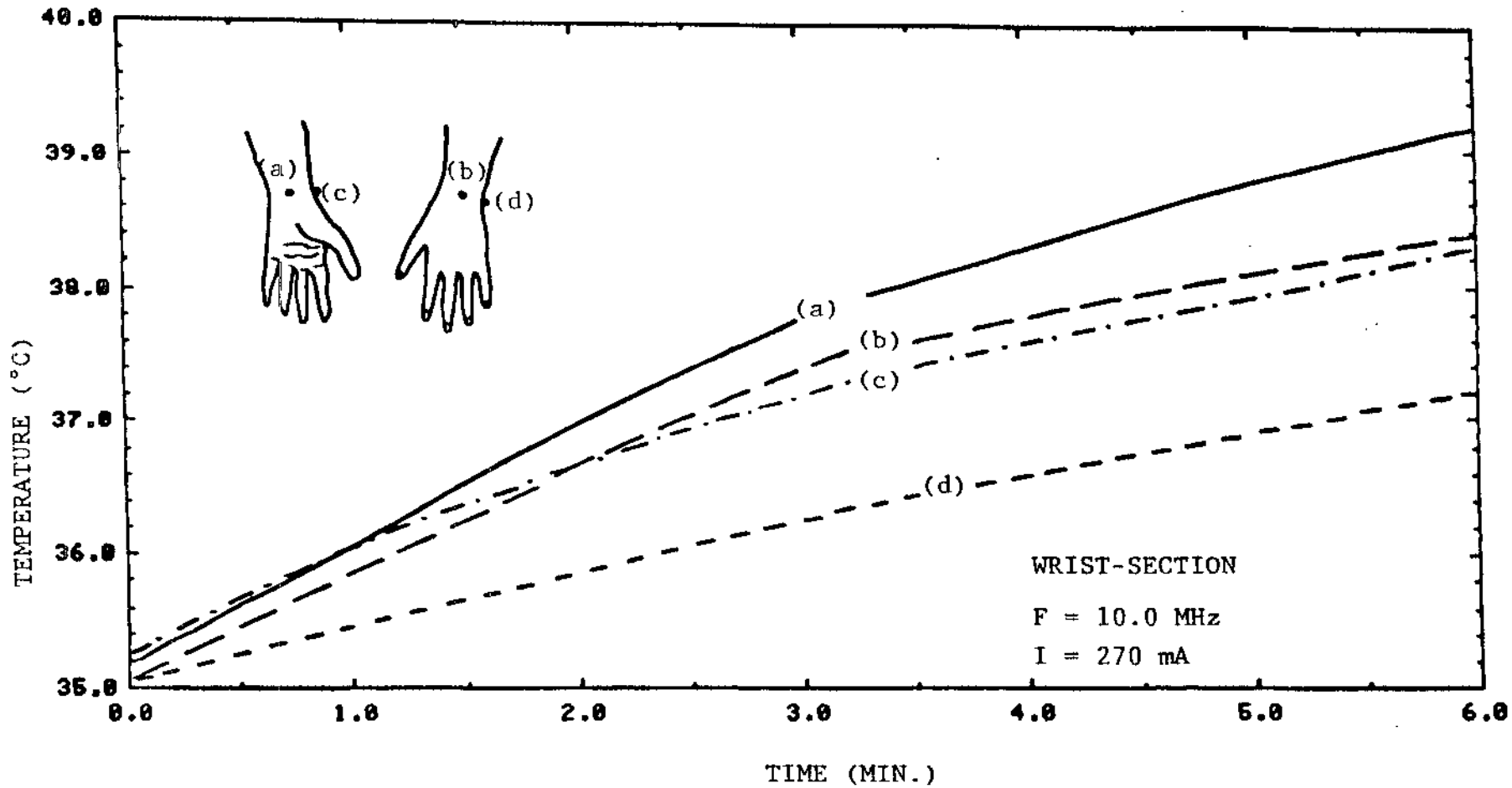
Fig. 2. Temperature of several locations at the surface of the wrist-section
under condition of RF current through the hand. Estimated SAR in
high-water-content tissues = 134 W/kg.

of the leg, respectively. As expected, considerably lower rates of heating are observed for points 3 and 4 on the skin above the bony regions of the ankles. To estimate the highest rates of heating, point 1 at the front of the leg was used for the remainder of the experiments in this study. An interesting point to note from Fig. 1 is that the temperature at point 1 rises to a "painful" surface temperature of 41.5°C after just nine minutes of exposure for a current that has been estimated through each of the human legs at the ANSI-recommended safety level of 1 mW/cm^2 at 40.68 MHz [4]. The response "painful" is likely to be due to higher deeper temperatures experienced under this condition. Since the purpose of our experiments was to study rates of heating rather than the thermoregulatory phenomenon, experiments were mostly discontinued once some tapering of the temperature rise had set in. In related numerical studies (to be published), we have modeled increased blood flow and sweating from the lower part of the human leg for current flow conditions similar to those of Fig. 1. The surface temperature was found to rise to a maximum of 42.6° C approximately 13 minutes after the onset of RF current. The temperatures decreased thereafter asymptotically approaching a steady-state surface temperature of 39.8° C.

The highest rate of heating for the wrist section (see Fig. 2) was obtained for point (a) on the inside of the wrist. This point was consequently used for all further experiments in this study.

Since it is difficult to set up high-power far-field irradiation facilities, particularly at lower RF frequencies, a question naturally arises whether temperature measurements based on a copper tape electrode exposure system are representative of the currents that are estimated

for plane-wave exposures. An important aspect of the latter exposures is that the current is induced over the entire body and propagates through the legs resulting in highly-concentrated current densities and hence large SARs in the ankle section. Consequently, a couple of experiments were performed using vertical monopole antennas as radiators at the higher RF frequencies 27.12 and 40.68 MHz where the radiator length L, which is typically a fraction of a wavelength (λ), can be quite reasonable. We used antennas of length 1.14 m or 0.103 λ and 1.54 m or 0.209 λ at the two respective frequencies. The radiator at 27.12 MHz was a base-loaded commercially available antenna used for CB radios while the antenna at 40.68 MHz consisted of a vertical length of wire selected for convenience of matching to the RF source. To satisfy the far-field condition $d > 2 (2L)^2/\lambda$, one need only be about 1 to 2 m away from the monopole above ground antennas of the two lengths that were used. The rates of temperature rise obtained using vertical monopole radiators are compared in Figs. 3 and 4 with those obtained using the copper tape as one of the electrodes. The agreement is quite good. Because of the convenience of using the copper tape as the current launching electrode particularly at MF frequencies, this procedure was used in all further experiments.

Some typical graphs on the surface temperature elevations for the points 1 and (a) of ankle- and wrist-sections, respectively, are given in Figs. 5-8 for a few representative RF currents that are indicated on respective figures. Also given in the individual captions are the SARs estimated for the high-conductivity, high-water-content tissues of the respective anatomic cross sections. Since in actuality these currents are induced as a result of exposure to electromagnetic fields [3,4], one
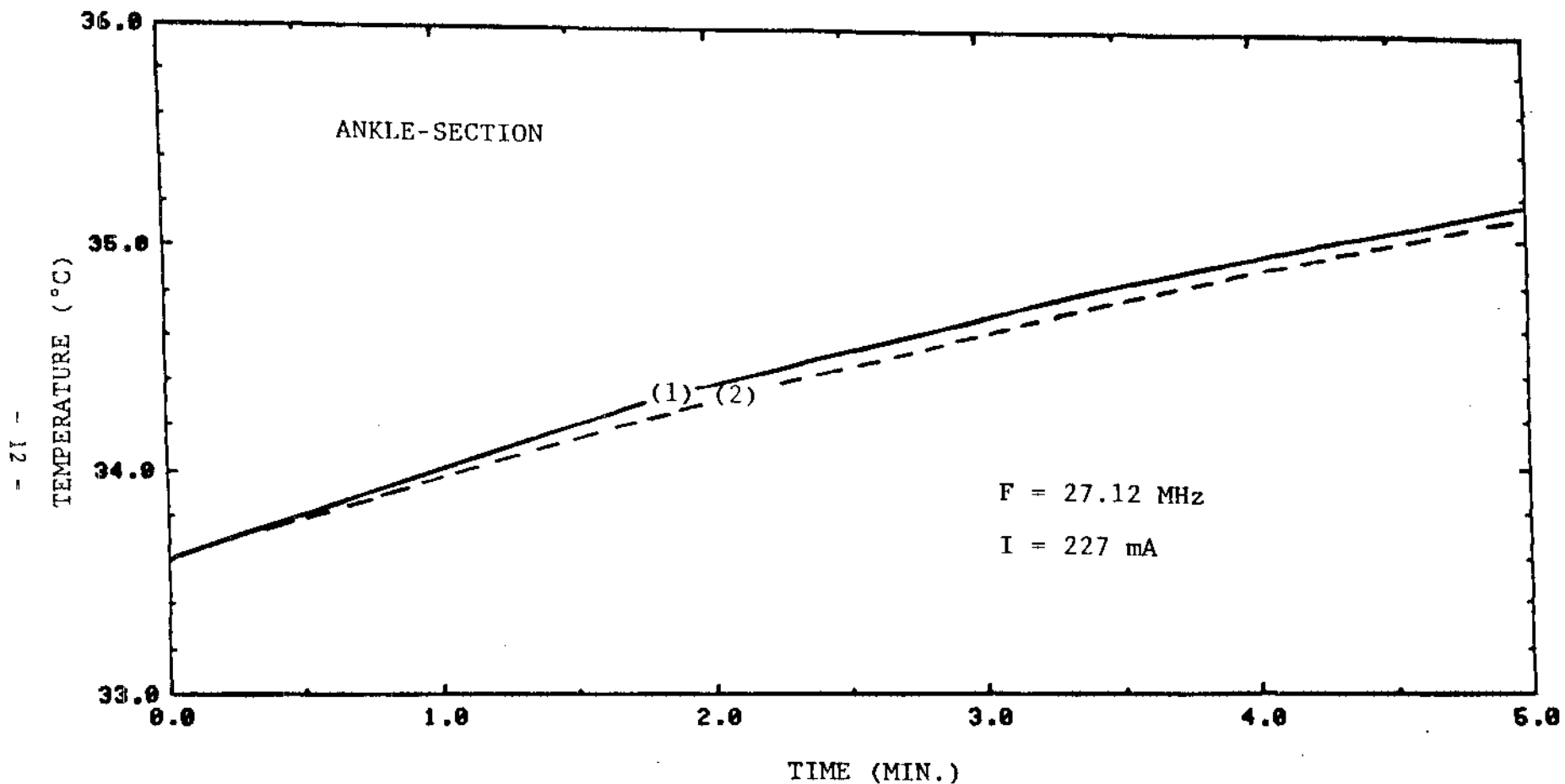
Fig. 3. Surface temperature at point 1 of the ankle-section under condition of RF current through the leg. Estimated SAR in high-water-content tissues = 81.4 W/kg. (1) Current induced by the EM fields due to a vertical monopole antenna of length L = 1.14 m. (2) Current produced by a copper tape wrapped around the leg.
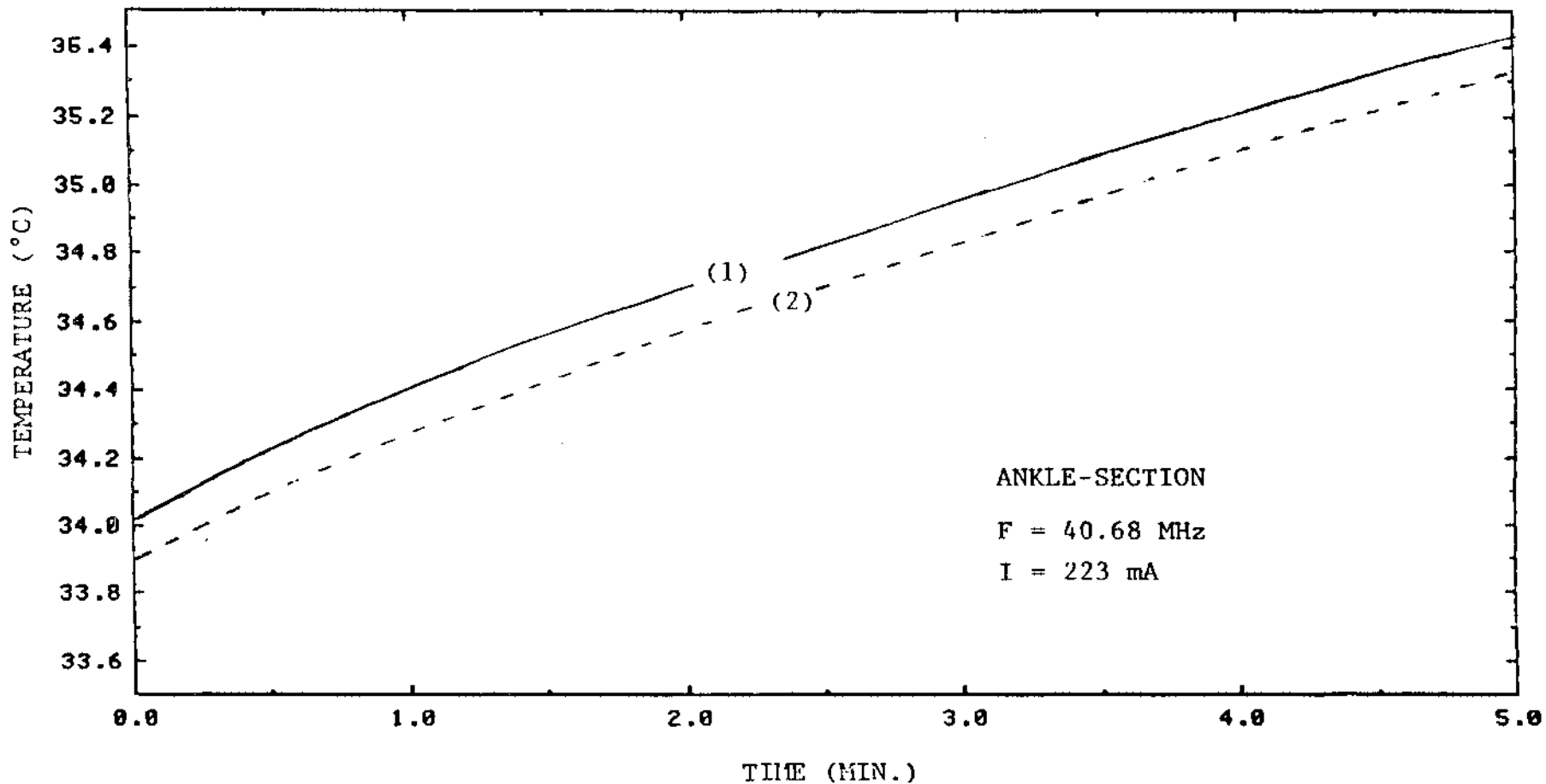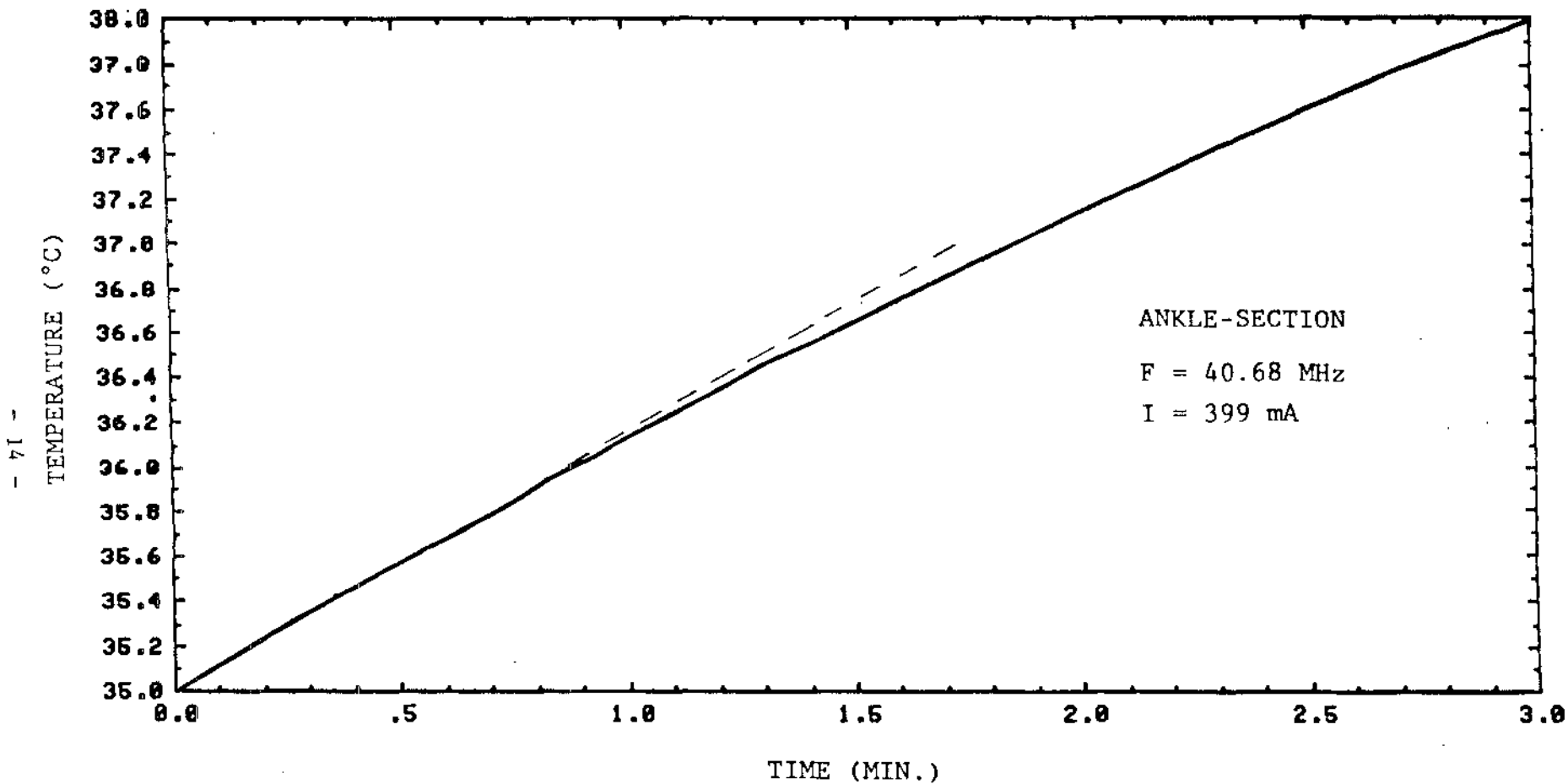
Fig. 4. Surface temperature at the point 1 of the ankle-section under condition of RF current through the leg. Estimated SAR in high-water-content tissues = 76.6 W/kg. (1) Current induced by the EM fields due to a vertical monopole antenna of length L = 1.54 m. (2) Current produced by a copper tape wrapped around the leg.
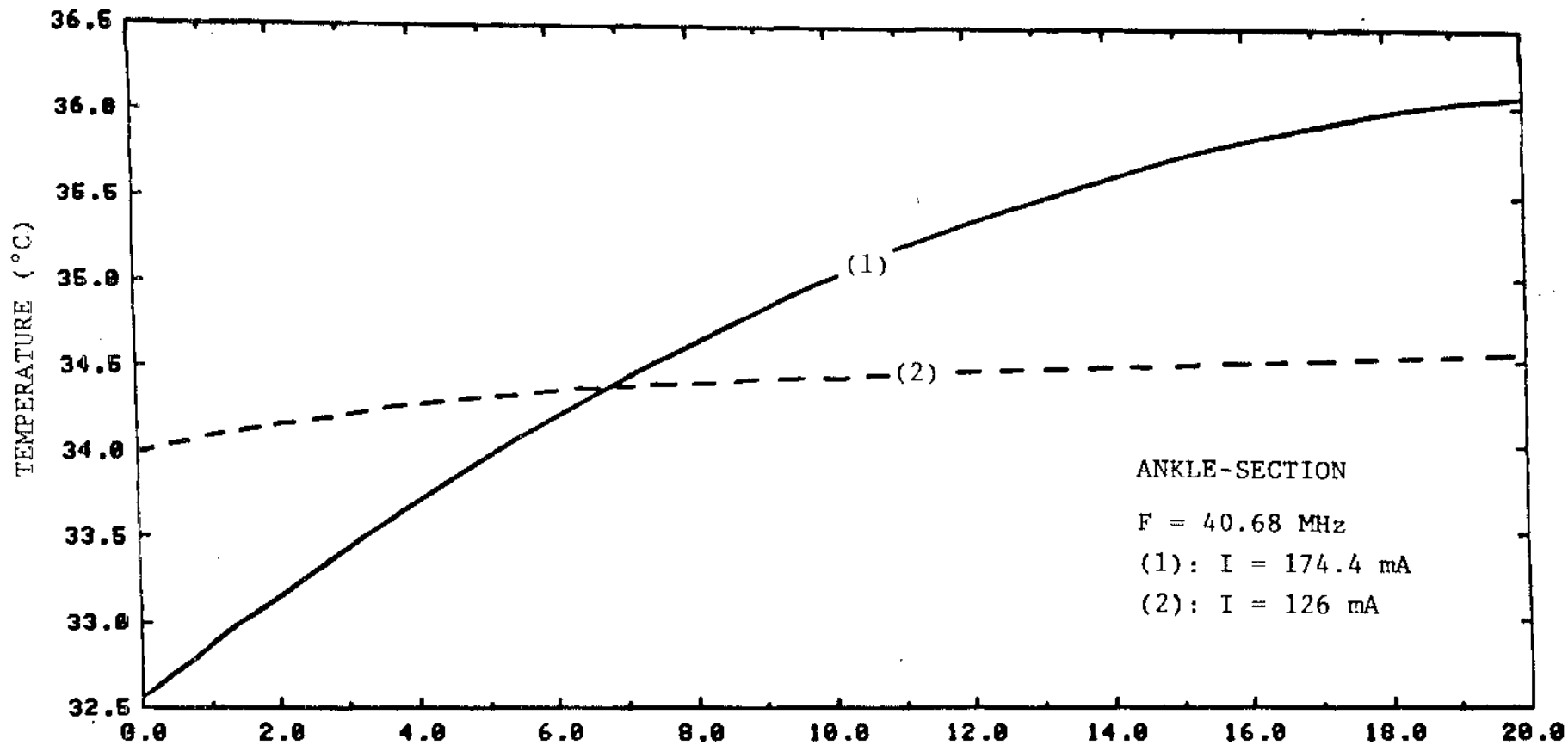
Fig. 5. Surface temperature at point 1 of the ankle-section under condition
of RF current through the leg. Initial rate of temperature rise =
1.15°C/min. Estimated SAR in high-water-content tissues = 245 W/kg.

Fig. 6. Surface temperature of point 1 of the ankle-section under conditions of RF current through the leg. Initial rates of temperature rise for the curves (1) and (2) are 0.29 and 0.09°C/min., respectively. The corresponding SARs estimated for the high-water-content tissues are 46 and 24 W/kg.
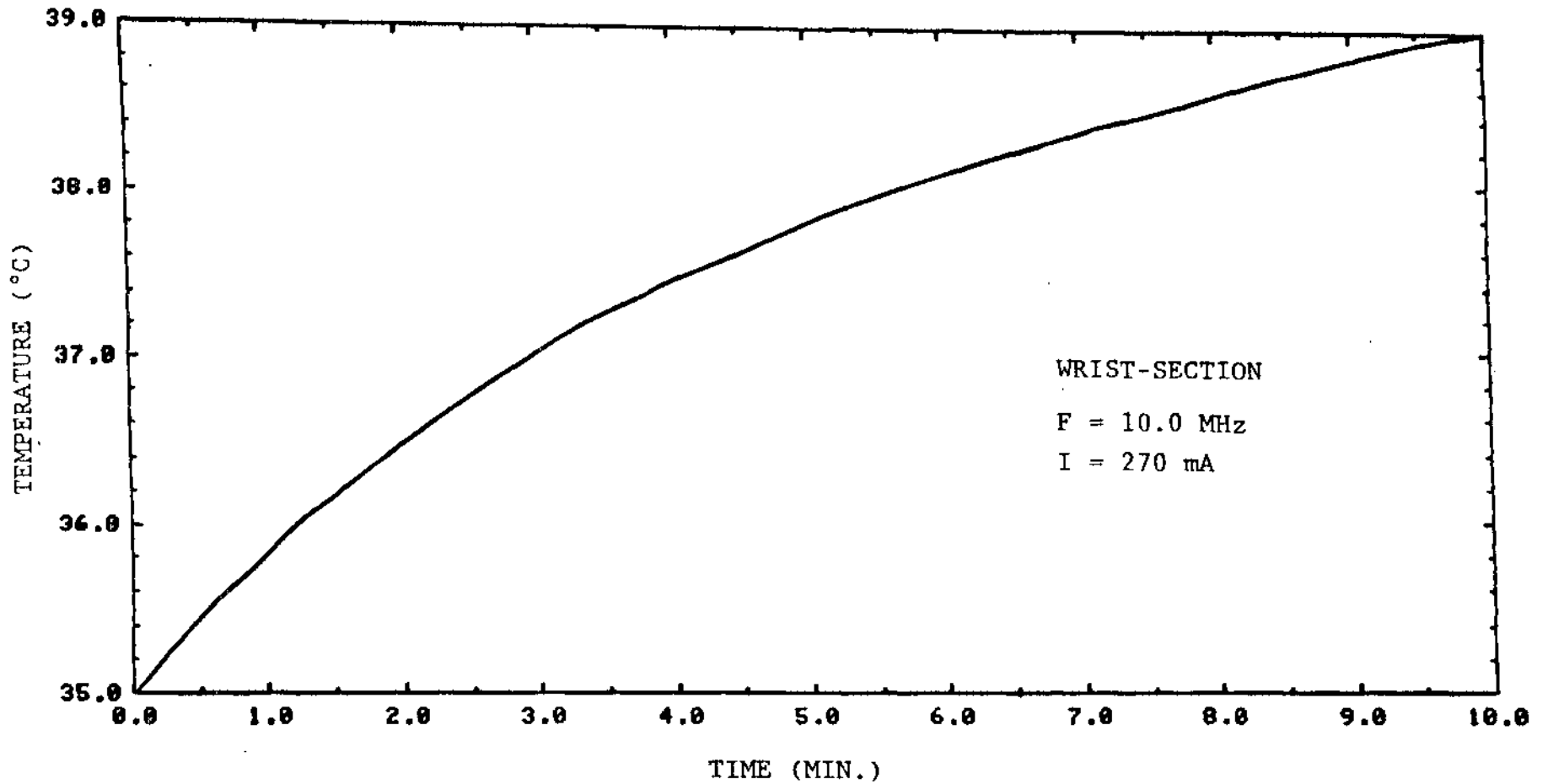
Fig. 7. Surface temperature at point (a) of the wrist under condition of RF current through the hand. Initial rate of temperature rise = 0.825°C/min. Estimated SAR in high-water-content tissues = 134 W/kg.
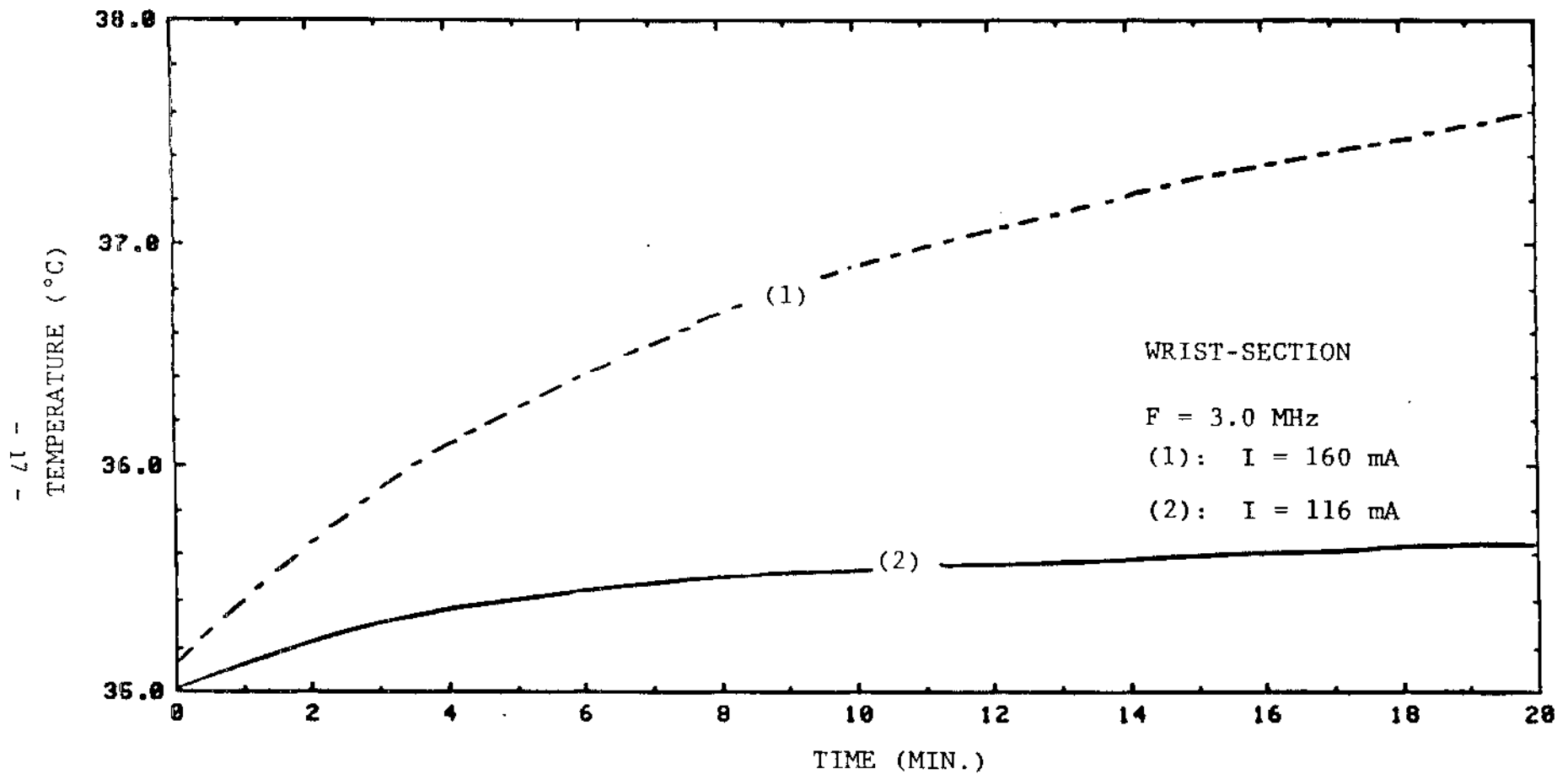
Fig. 8. Surface temperature at point (a) of wrist-section under conditions of RF current through the hand. Initial rates of temperature for rise curves (1) and (2) are 0.3 and 0.14°C/min., respectively. The corresponding SARs estimated for the high-water-content tissues are 47.6 and 25 W/kg, respectively.

can estimate the incident electric fields that it will take to induce the currents given in Figs. 5-8. The respective incident plane-wave E-fields are 62.8 V/m for Fig. 5 and 27.5 and 19.8 V/m for Fig. 6 and E-fields of 190 V/m, and 111.8 and 81 V/m incident on an automobile van for Figs. 7 and 8, respectively [5,7]. It may be recalled that high currents pass through the human wrist only upon contacting ungrounded metallic bodies; in this case grasping the handle of an automobile van. In Figs. 9 and 10 we have plotted the initial rates of heating for a large number of data that we have collected. Using the least-squares approximation to a straight line dependence, we have obtained empirical relationships for the highest rates of heating of the surface for ankle- and wrist-sections. These are:

$$\left.\frac{\Delta T}{\Delta t}\right|_{surface} = 0.0045 \times SAR \qquad °C/min \qquad (5)$$

for point 1 of the ankle-section, and,

$$\left.\frac{\Delta T}{\Delta t}\right|_{surface} = 0.0048 \times SAR \qquad °C/min \qquad (6)$$

for point (a) of the wrist-section, where the SAR is in W/kg and pertains to the high-water-content tissues in the respective cross sections.

It is interesting to note that fairly comparable rates of maximal heating have been obtained for both the ankle- and wrist-sections.
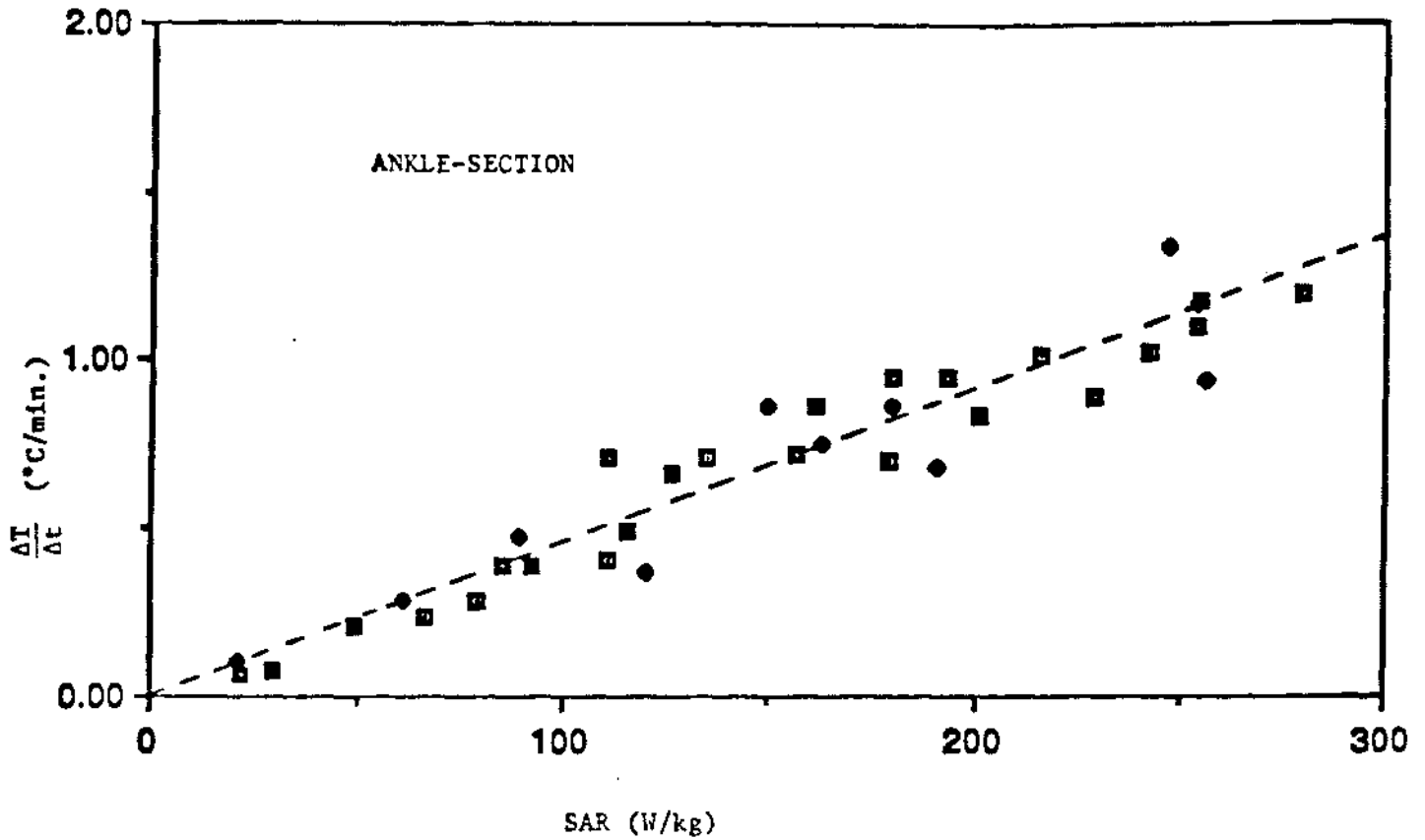
Fig. 9. Rate of temperature increase for point 1 of the
         ankle section as a function of SAR estimated
         from Eq. 4 for high-water-content tissues.

◪ 1.0, 3.0, and 5.0 MHz   ◆ 10.0 MHz

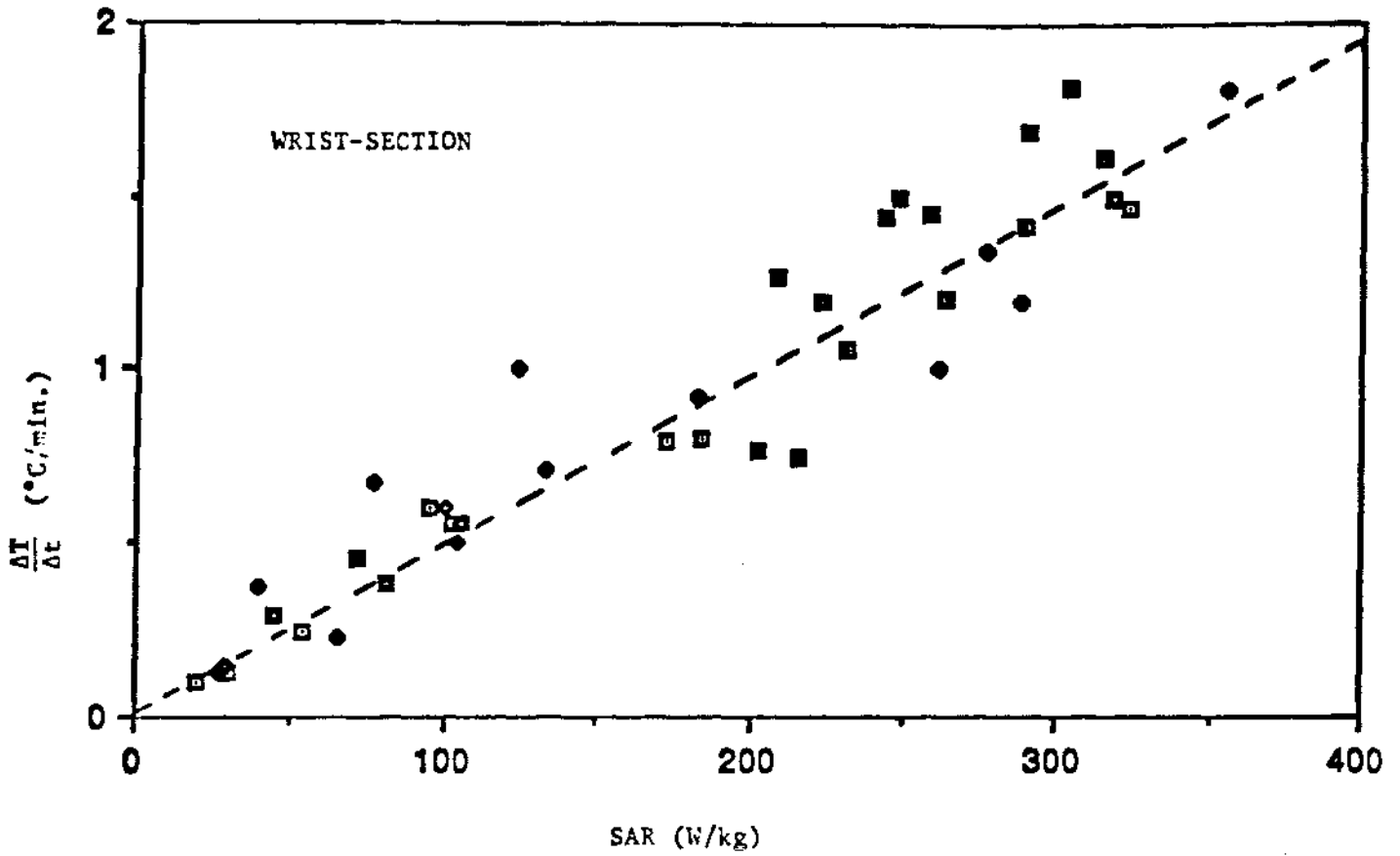◪ 27.12 MHz   ◼ 40.68 MHz

◆ 50.0 MHz

Fig. 10. Rate of temperature increase for point (a) of the
wrist as a function of SAR estimated from Eq. 4
for high-water-content tissues.

■ 1.0, 3.0, and 5.0 MHz   ◆ 10.0 MHz

■ 27.12 MHz   ■ 40.68 MHz

◆ 50.0 MHz

Conclusions

We have reported the surface temperature increases of the wrist- and ankle-section for a healthy human subject for a variety of RF currents for the frequency band 1-50 MHz. From the data given in this paper, substantial rates of surface heating are projected for the E-fields suggested in the ANSI C95.1-1982 RF Safety Guideline [1]. Since internal tissue temperatures may be even higher, one can question the safety of the so-called safety guidelines.

References

1. ANSI C95.1-1982, "American National Standard -- Safety Levels with Respect to Human Exposure to Radio-Frequency Electromagnetic Fields, 300 kHz to 100 GHz," printed by the Institute of Electrical and Electronics Engineers, Inc., 345 East 47th Street, New York, New York, 10017.

2. American Conference on Governmental Industrial Hygienists, "Threshold Values for 1983-1984," Cincinnati, Ohio.

3. O. P. Gandhi, I. Chatterjee, D. Wu, and Y. G. Gu, "Likelihood of High Rates of Energy Deposition in the Human Legs at the ANSI-Recommended 3-30 MHz RF Safety Levels," *Proceedings of the IEEE*, Vol. 73, pp. 1145-1147, 1985.

4. O. P. Gandhi, J. Y. Chen, and A. Riazi, "Currents Induced in a Human Being for Plane-Wave Exposure Conditions 0-50 MHz and for RF Sealers," *IEEE Transactions on Biomedical Engineering*, Vol. BME-33, pp. 757-767, August 1986.

5. O. P. Gandhi and I. Chatterjee, "Radio-Frequency Hazards in the VLF to MF Band," *Proceedings of the IEEE*, Vol. 70, pp. 1462-1464, 1982.

6. A. W. Guy and C. K. Chou, "Hazard Analysis: Very Low Frequency through Medium Frequency Range," Final Report, USAF SAM Contract F36615-78-D-0617, Task 0065, 1982.

7. I. Chatterjee, D. Wu, and O. P. Gandhi, "Human Body Impedance and Threshold Currents for Perception and Pain for Contact Hazard Analysis in the VLF-MF Band," *IEEE Transactions on Biomedical Engineering*, Vol. BME-33, pp. 486-494, May 1986.

8. D. A. Christensen, "A New Nonperturbing Temperature Probe Using Semiconductor Band Edge Shift," *Journal of Bioengineering*, Vol. 1, pp. 541-545, 1977.

9. D. J. Morton, R. C. Truex, and C. E. Kellner, *Manual of Human Cross-Section Anatomy*, Baltimore: Williams and Wilkins, 1941.

10. A. C. Eycleshymer and D. M. Shoemaker, *A Cross-Section Anatomy*, New York: Appleton Company, 1911.

11. C. C. Johnson and A. W. Guy, "Nonionizing Electromagnetic Wave Effects in Biological Materials and Systems," *Proceedings of the IEEE*, Vol. 60, pp. 692-718, 1972.

12. S. R. Smith and K. R. Foster, "Dielectric Properties of Low-Water-Content Tissues," *Physics in Biology and Medicine*, Vol. 30, pp. 965-973, 1985.